

AD-A173 312

THE COUPLED THREE DEGREE OF FREEDOM MOTION RESPONSE OF
A DRYDOCKED SUBMAR. (U) MASSACHUSETTS INST OF TECH
CAMBRIDGE DEPT OF OCEAN ENGINEERIN. D E SIGMAN JUN 86

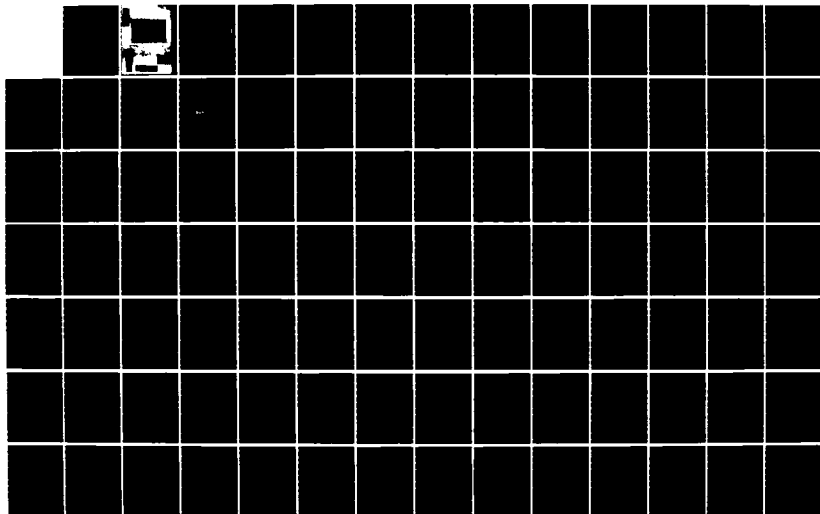
1/2

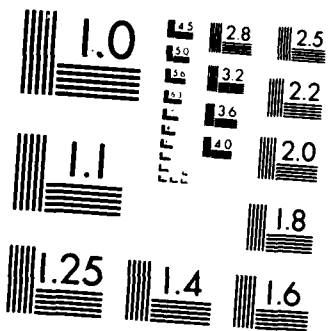
UNCLASSIFIED

N00228-85-G-3262

F/G 13/13

NL





MICROCOPY RESOLUTION TEST CHART
NATIONAL BUREAU OF STANDARDS 1963 A

DEPARTMENT OF OCEAN ENGINEERING

MASSACHUSETTS INSTITUTE OF TECHNOLOGY

CAMBRIDGE, MASSACHUSETTS 02139

**THE COUPLED THREE DEGREE OF FREEDOM MOTION RESPONSE OF
A DRYDOCKED SUBMARINE TO SEISMIC LOAD**

BY
DALE EDWARD SIGMAN
OCEAN ENGINEERING - COURSE XIII A
MECHANICAL ENGINEERING - COURSE II

JUNE 1986

THE COUPLED THREE DEGREE OF FREEDOM MOTION RESPONSE
OF A DRYDOCKED SUBMARINE TO SEISMIC LOAD

by

DALE EDWARD SIGMAN
B.S., Kansas University
(1980)

SUBMITTED TO THE DEPARTMENT OF OCEAN ENGINEERING AND
MECHANICAL ENGINEERING IN PARTIAL FULFILLMENT OF THE
REQUIREMENTS FOR THE DEGREES OF

OCEAN ENGINEER
and
MASTER OF SCIENCE IN MECHANICAL ENGINEERING

at the

MASSACHUSETTS INSTITUTE OF TECHNOLOGY

June 1986

© DALE E. SIGMAN, 1986

DTIC
ELECTE
OCT 21 1986

The author hereby grants to M.I.T. and to the U.S. Government
permission to reproduce and to distribute copies of this
thesis document in whole or in part.

Signature of Author Dale E. Sigman
Department of Ocean Engineering
May 1986

Certified by: Dale G. Karr
Professor Dale G. Karr
Thesis Supervisor

Certified by: J. Karl Hedrick
Professor J. Karl Hedrick
Thesis Reader

Accepted by: A. Douglas Carmichael
Professor A.D. Carmichael, Chairman
Ocean Engineering Department Graduate Committee

Accepted by: A.A. Sonin
Professor A.A. Sonin, Chairman
Mechanical Engineering Department Graduate Committee

This document has been approved
for public release and sale; its
distribution is unlimited.

THE COUPLED THREE DEGREE OF FREEDOM MOTION RESPONSE OF A
DRYDOCKED SUBMARINE TO SEISMIC LOAD

by

DALE EDWARD SIGMAN

Submitted to the Department of Ocean Engineering and
Mechanical Engineering in partial fulfillment of the
Requirements for the Degrees of Ocean Engineer and Master of
Science in Mechanical Engineering.

ABSTRACT

A mathematical model is developed to analyze the seismic response of a drydocked vessel in three degrees of freedom; vessel rotation about its keel and vessel horizontal and vertical translations relative to the drydock cradle. Data from eleven actual vessel-drydock systems and the time acceleration history of an earthquake are implemented to predict vessel three degree of freedom response during an earthquake. Vessel seismic response and the resultant drydock forces are compared to vessel-drydock system failure criteria to determine stability of the system during earthquakes. The three degree of freedom vessel response model is compared to a one and two degree of freedom vessel response models and a model in which seismic loading is simulated by a single static force. The three degree of freedom vessel motion is shown to be the most accurate method for analyzing vessel-drydock system failure criteria.

THESIS SUPERVISOR: Dale G. Karr, Ph.D.

TITLE: Assistant Professor of Ocean Engineering

NAVAL POSTGRADUATE SCHOOL
MONTEREY CA 93943-5000
N00288-85-G-3262

ACKNOWLEDGEMENTS

Several people played significant roles in carrying this work through to its presentation here. Professor Dale G. Karr and Frankie P. Law, graduate student, provided me with the confidence in my ability to take on such an effort. I am grateful for their detailed guidance and assistance that made this work possible. I am thankful to my friend Mary C. Kreuz for her skillful preparation of this thesis. Finally, to my wife and son, Janice and Troy, whose love and undying devotion lifted my spirits when I needed it most.

Accession For		
NTIS GR&I	<input checked="" type="checkbox"/>	
DTIC TAB	<input type="checkbox"/>	
Unannounced	<input type="checkbox"/>	
Justification		<i>form 50 per</i>
By		
Distribution/		
Availability Codes		
Avail and/or		
Dist Statement		
<i>A-1</i>		



TABLE OF CONTENTS

	<u>PAGE</u>
LIST OF FIGURES.	6
LIST OF TABLES	10
SECTION 1 INTRODUCTION.	11
1.1 Background.	11
1.2 Previous Work	11
1.3 Contributions of This Thesis.	12
1.4 Outline of This Thesis.	12
SECTION 2 THE VESSEL-DRYDOCK SYSTEM	16
2.1 General Description	16
2.2 System Components	16
SECTION 3 VESSEL-DRYDOCK SYSTEM FAILURE MECHANISMS.	19
3.1 Block Crushing.	19
3.2 Block Sliding	19
3.3 Block Overturning	21
3.4 Vessel Liftoff.	22
SECTION 4 MATHEMATICAL MODELS OF VESSEL-DRYDOCK SYSTEM.	27
4.1 The Quasi-static Method of Modelling Seismic Response.	27
4.1.1 Approach	27
4.1.2 Force Equations.	27
4.1.3 Vessel Response in Quasi-static Load Method	28
4.2 One Degree of Freedom: Rotational Response	29
4.2.1 Approach	29
4.2.2 One Degree of Freedom Equation of Motion Model	30
4.3 Two Degree of Freedom: Rotational and Horizontal Translation Response.	33
4.3.1 Approach	33
4.3.2 Two Degree of Freedom Equation of Motion Model	34
4.4 Three Degree of Freedom: Rotational, Horizontal, and Vertical Translation Response	38
4.4.1 Approach	38
4.4.2 Three Degree of Freedom Equation of Motion Model	39
SECTION 5 SYSTEM PARAMETERS	49
5.1 Vessel-Drydock System Parameters.	49
5.2 Block Parameters.	50
5.2.1 Vertical Stiffness K_v	50
5.2.2 Horizontal Stiffness K_h	52

TABLE OF CONTENTS (Cont.)

	<u>PAGE</u>
SECTION 6 VESSEL RESPONSE TO SEISMIC EXCITATION . .	60
6.1 Vessel Response: Modal Analysis.	61
6.2 Vessel Response: Fourth Order Runge-Kutta Numerical Analysis.	63
6.3 Vessel Response: Response Spectrum Analysis.	65
6.4 Vessel Response: Quasi-static Force Analysis.	69
SECTION 7 COMPUTER SOLUTIONS.	73
7.1 Modal Analysis Solution	73
7.1.1 Computer Program Development	73
7.1.2 Computer Program Input	75
7.1.3 Computer Program Testing	78
7.1.4 Computer Program Results	82
7.2 Fourth Order Runge-Kutta Solution	86
7.2.1 Computer Program Development	86
7.2.2 Computer Program Input	88
7.2.3 Computer Program Testing	88
7.2.4 Computer Program Results	89
7.3 Discussion of Computer Results.	94
SECTION 8 SUMMARY, CONCLUSIONS AND RECOMMENDATIONS FOR FURTHER STUDY	124
8.1 Summary	124
8.2 Conclusions	125
8.3 Recommendations for Further Study	126
REFERENCES	127
APPENDIX 1 Three Degree of Freedom Response Program Using Modal Analysis	128
APPENDIX 2 Three Degree of Freedom Response Program Using Fourth Order Runge-Kutta Numerical Analysis	139
APPENDIX 3 Modal Analysis of the Two and Three Degree of Freedom Systems.	149

LIST OF FIGURES

	<u>Page</u>
Figure 1.1 Acceleration Time History, El Centro Earthquake, 1946.	15
Figure 2.1 Vessel-Drydock System	18
Figure 3.1 Keel Pier Forces.	24
Figure 3.2 Side Pier Forces, General	24
Figure 3.3 Side Pier Forces, Block-Vessel Interface.	25
Figure 3.4 Block Tipping Forces.	26
Figure 4.1 Vessel-Drydock System with Applied Quasi-static Force.	44
Figure 4.2 Vessel-Drydock System Force Diagram with Applied Quasi-static Force.	44
Figure 4.3 Idealized One Degree of Freedom Vessel-Drydock System at Rest.	45
Figure 4.4. Idealized One Degree of Freedom Vessel-Drydock System, Excited	45
Figure 4.5 Dynamic Side Block Force.	46
Figure 4.6 Idealized Two Degree of Freedom Vessel-Drydock System at Rest.	47
Figure 4.7 Idealized Two Degree of Freedom Vessel-Drydock System, Excited	47
Figure 4.8 Idealized Three Degree of Freedom Vessel-Drydock System at Rest.	48
Figure 4.9 Idealized Three Degree of Freedom Vessel-Drydock System, Excited.	48
Figure 5.1 Standard Composite Block Stiffness Model.	58
Figure 5.2 Standard Timber Block Stiffness Model	58
Figure 5.3 Standard Block in Bending	59
Figure 5.4 Standard Block in Shear	59
Figure 6.1 Actual El Centro Earthquake Response Spectrum.	71

LIST OF FIGURES (Cont.)

	<u>Page</u>
Figure 6.2 Idealized El Centro Earthquake Response Spectrum, 5% Damping.	72
Figure 7.1 Sinusoidal Ground Acceleration.	99
Figure 7.2 Vessel Seismic Response in Rotation using Modal Analysis with Sinusoidal Ground Acceleration.	100
Figure 7.3 Side Pier Forces, with Softwood Cap Block	101
Figure 7.4 Vessel Seismic Response in Rotation for One Degree of Freedom Model using Modal Analysis.	102
Figure 7.5a Vessel Seismic Response in Relative Horizontal Translation for Two Degree of Freedom Model using Modal Analysis . .	103
Figure 7.5b Vessel Seismic Response in Rotation for Two Degree of Freedom Model using Modal Analysis.	104
Figure 7.6a Vessel Seismic Response in Relative Horizontal Translation for Three Degree of Freedom Model using Modal Analysis . .	105
Figure 7.6b Vessel Seismic Response in Relative Vertical Translation for Three Degree of Freedom Model using Modal Analysis. . . .	106
Figure 7.6c Vessel Seismic Response in Rotation for Three Degree of Freedom Model using Modal Analysis.	107
Figure 7.7 Vessel Seismic Response in Rotation using Runge-Kutta Numerical Analysis with Sinusoidal Ground Acceleration.	108
Figure 7.8 Vessel Seismic Response in Rotation for One Degree of Freedom Model using Runge-Kutta Analysis.	109
Figure 7.9a Vessel Seismic Response in Relative Horizontal Translation for Two Degree of Freedom using Runge-Kutta Analysis. . . .	110
Figure 7.9b Vessel Seismic Response in Rotation for Two-Degree of Freedom Model using Runge-Kutta Analysis.	111

LIST OF FIGURES (Cont.)

	<u>Page</u>
Figure 7.10a Vessel Seismic Response in Relative Horizontal Translation for Three Degree of Freedom Model using Runge-Kutta Analysis.	112
Figure 7.10b Vessel Seismic Response in Relative Vertical Translation for Three Degree of Freedom Model using Runge-Kutta Analysis.	113
Figure 7.10c Vessel Seismic Response in Rotation for Three Degree of Freedom Model using Runge-Kutta Analysis.	114
Figure 7.11 Vessel Seismic Response in Rotation for Non-Linear One Degree of Freedom Model using Runge-Kutta Analysis	115
Figure 7.12a Vessel Seismic Response in Relative Horizontal Translation for Non-linear Two Degree of Freedom Model using Runge-Kutta Analysis.	116
Figure 7.12b Vessel Seismic Response in Rotation for Non-linear Two Degree of Freedom Model using Runge-Kutta Analysis.	117
Figure 7.13a Vessel Seismic Response in Relative Horizontal Translation for Non-linear Three Degree of Freedom Model using Runge-Kutta Analysis.	118
Figure 7.13b Vessel Seismic Response in Relative Vertical Translation for Non-linear Three Degree of Freedom Model using Runge-Kutta Analysis.	119
Figure 7.13c Vessel Seismic Response in Rotation for Non-linear Three Degree of Freedom Model using Runge-Kutta Analysis.	120
Figure 7.14a Linearity Selection Criteria, 5% Damping, Beta = 0.1.	121
Figure 7.14b Linearity Selection Criteria, 5% Damping, Beta = 0.5.	121
Figure 7.14c Linearity Selection Criteria, 5% Damping, Beta = 1.0.	122

LIST OF FIGURES (Cont.)

	<u>Page</u>
Figure 7.14d Linearity Selection Criteria, 5% Damping, Beta = 5.0	122
Figure 7.14e Linearity Selection Criteria, 5% Damping, Beta = 10.0	123

LIST OF TABLES

	<u>Page</u>
Table 5.1 Vessel-Drydock Configurations.	49
Table 5.2 Key Vessel Parameters.	50
Table 5.3 Keel and Side Piers Cross-Sectional Area Analysis	55
Table 5.4 Total Keel and Side Pier Stiffness	57
Table 6.1 One Degree of Freedom Vessel-Drydock System Maximum Response Using Response Spectrum Analysis.	68
Table 6.2 System Response using Quasi-static Force Analysis.	70
Table 7.1 One Degree of Freedom Equation of Motion Response Comparison	84
Table 7.2 Three Degree of Freedom Equation of Motion Response Comparison	85
Table 7.3 One Degree of Freedom Equation of Motion Response.	91
Table 7.4 Two Degree of Freedom Equation of Motion Response.	92
Table 7.5 Three Degree of Freedom Equation of Motion Response.	93
Table A3.1 Three Degree of Freedom Vessel-Drydock System Natural Frequencies	158
Table A3.2 Three Degree of Freedom Vessel-Drydock System Damping Coefficients.	157
Table A3.3 Three Degree of Freedom Vessel-Drydock System Maximum Response using Response Spectrum Analysis.	158

1.0 INTRODUCTION

1.1. Background

In the design of a drydock for military vessels, an important factor is the environmental-generated forces that are found in the drydock cradle which supports the ship. Earthquakes and the wind are considered the two most significant environmental loading factors. This thesis explores the seismic loading aspect of the problem.

Regardless of its location, any U.S. Navy ship that is nuclear powered and in drydock is considered to be in a high seismic risk area. Currently the Navy defines a high seismic risk area as one in which earthquake forces be approximated by a steady horizontal force of 0.2 g times the vessel mass acting at the center of gravity. The drydock can be analyzed to see if it can withstand this quasi-static loading.

1.2 Previous Work

In 1981 B.V. Viscomi studied the seismic response of a drydocked submarine using a single degree of freedom model [14]. This analysis assumed that the vessel was allowed to rotate about the keel. Viscomi used the time history acceleration record of the North-South component of the 1946 El Centro, CA Earthquake, California Institute of Technology processing scheme. The vessel was analyzed for system failure (i.e. the vessel lifting off of a row of side blocks).

A thesis by C.F. Barker in 1985 [1] used a two degree of freedom model to study seismic response. Employing the 1946 El Centro Earthquake, Massachusetts Institute of Technology

standard processing scheme, Barker analyzed rotation about the keel plus horizontal relative translation between the vessel and the drydock cradle perpendicular to the vessel longitudinal axis. The two degree of freedom model permitted the analysis of drydock cradle failure: block sliding and tipping, which were not possible to analyze in Viscomi's one degree of freedom model, along with block liftoff.

1.3 Contributions of This Thesis

This thesis develops a three degree of freedom model of a vessel in drydock. Motion will be permitted in three directions: rotation about the keel and relative translations, horizontal and vertical, between the vessel and the drydock cradle. The three degree of freedom model will make possible the analysis of drydock cradle failure: additional block crushing forces due to vertical motion, which was not conceivable in the previous one and two degree of freedom models developed by Viscomi and Barker respectively, along with block sliding, tipping and liftoff.

The seismic input for the three degree of freedom model is the time acceleration history of the North-South component of the 1946 El Centro, CA Earthquake, Massachusetts Institute of Technology standard processing scheme. The MIT version of the El Centro Earthquake acceleration record is described in reference [9] , and is displayed graphically in Figure 1.1.

1.4 Outline of This Thesis

Section 2 of this thesis describes the vessel-drydock system for the reader and introduces terms which are used throughout the thesis. Section 3 describes the various

failure mechanisms found in the vessel-drydock system which can occur.

Section 4 examines the modelling of the vessel-drydock system under seismic loading. Section 4.1 describes the quasi-static loading method, and Section 4.2 develops the one degree of freedom equation of vessel motion model. Section 4.3 develops the two degree of freedom equations of vessel motion model. Finally, Section 4.4 develops the three degree of freedom equations of motion model.

Section 5 discusses the system parameters that are required for the mathematical model found in Section 4. Included in this Section is the modelling of block stiffness. Eleven typical vessel-drydock system configurations are studied to be implemented into Section 6.

Section 6 examines methods of evaluating the one, two and three degree of freedom models found in Section 4. Section 6.1 evaluates the linear equations of motion models using modal analysis method. Section 6.2 evaluates both linear and non-linear equations of motion models using a fourth-order Runge-Kutta numerical analysis scheme. Section 6.3 explains the response spectrum method of determining the maximum value of vessel seismic response. Section 6.4 determines system response using quasi-static force method.

Section 7 describes the development and testing of the one, two and three degree of freedom vessel motion computer programs, and contains the results for a seismic analysis of several actual vessel-drydock systems.

Section 8 summarizes the response predictions for several

actual vessel-drydock systems obtained with quasi-static, one degree of freedom, two degree of freedom and three degree of freedom analysis methods, and conclusions are drawn.

Appendix 1 is an example listing of the fourth-order Runge-Kutta computer program. Appendix 2 is an example listing of the modal analysis computer program. Finally, Appendix 3 describes the modal analysis of the two and three degree of freedom vessel-drydock systems and predicts maximum system response using the response spectrum method of analysis and modal participation factors.

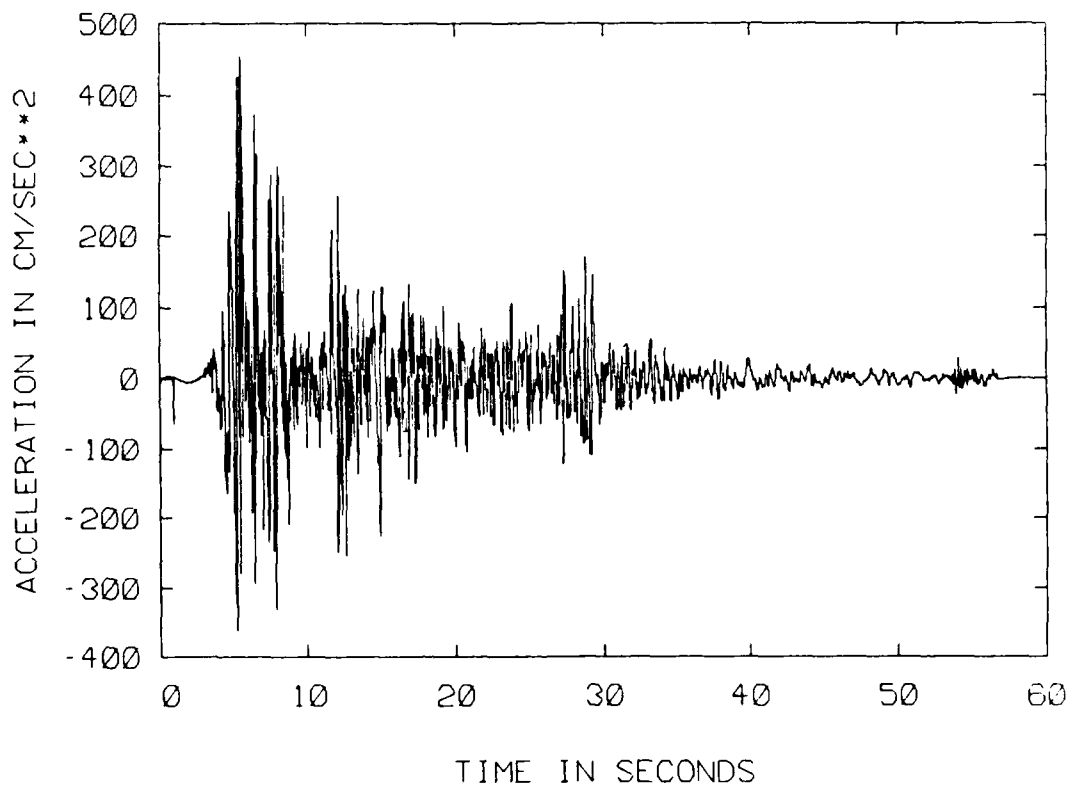


FIGURE 1.1
Acceleration Time History, El Centro Earthquake, 1946

2.0 THE VESSEL-DRYDOCK SYSTEM

2.1 General Description

In order to perform inspection, maintenance and repair on the outer hull of a ship, it is necessary to place the vessel in a drydock. A drydock is a concrete encasement built into the earth. At one end of the drydock is a flood gate to allow the entry and departure of the vessel. A cradle, formed by drydock blocks, is built upon the drydock floor in order to support the ship once the water is pumped out of the encasement. The drydock must be able to hold the weight of the vessel and cradle.

Due to the various hull configurations associated with the different classes of ships, the cradle component of the drydock-cradle-vessel system is varied to suit a particular docking situation. The cradle accomplishes the transfer of vessel weight to the drydock floor, provides stable support to the vessel and allows access to the vessel hull. This cradle is usually constructed of timber, concrete, or a timber-concrete composite.

2.2 System Component

The primary components of the drydock-cradle-vessel system are shown in Figure 2.1. This section defines terms, related to docking, used in this thesis to describe the system components.

1. Blocks - The units, consisting of timber, concrete, steel and other materials, which together make up the cradle.
2. Cradle - A framework of blocks which supports the vessel when the drydock is dewatered.
3. KG - The distance between the vessel baseline (ship's keel) to its vertical center of gravity.
4. Keel Blocks - The center blocks, directly beneath the vessel's keel.
5. Pier - A column built of blocks that extends from the ship hull to dock floor.
6. Side Blocks - The blocks located to the right and left of the keel blocks.
7. Ton - A long ton, 2240 lbs.
8. g- Acceleration of gravity, 32.2 ft/sec².

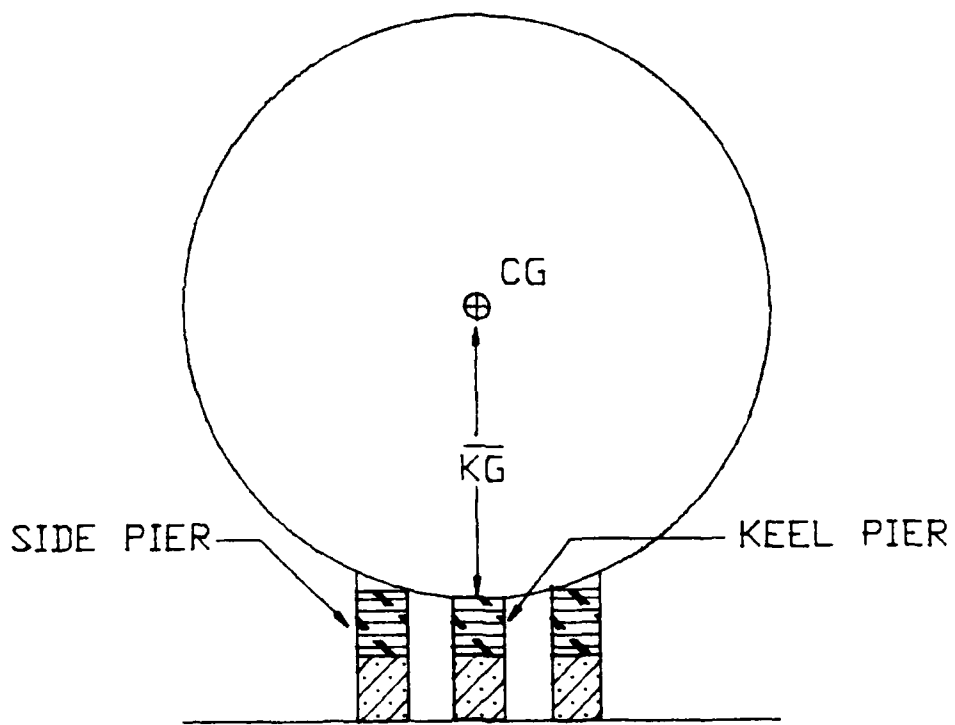


FIGURE 2.1
Vessel-Drydock System

3.0 VESSEL-DRYDOCK SYSTEM FAILURE MECHANISMS

There are four failure modes that the vessel-drydock system can exhibit: block crushing, block sliding, block overturning and block liftoff (i.e. the liftoff of vessel from a row of blocks).

3.1 Block Crushing⁶

A block can support compressive stresses linearly until the blocks' proportional limit is exceeded. The proportional limit is a material property of the block and is the maximum compressive stress at which stress is still linearly proportional to strain. If the compressive proportional limit is exceeded, the block is considered to have failed.

3.2 Block Sliding⁶

Due to friction at the interfaces between the blocks and the vessel and between blocks with other blocks, drydock blocks will have the tendency to resist sliding when subjected to vertical and horizontal loads. This is true when in the absence of mechanical fasteners.

First consider the blocks that form the keel pier. Figure 3.1 shows that the resistance of the keel pier to sliding is

$$H = \mu_1 V \quad (\text{block-block interface})$$

$$\text{and } H = \mu_2 V \quad (\text{vessel-block interface})$$

where

H = horizontal resisting force

μ_1 = coefficient of friction, block-block interface

μ_2 = coefficient of friction, block-vessel interface

V = vertical load on the blocks.

Failure of the keel pier due to sliding will occur when the ratio of horizontal force to the vertical force is greater than the lowest coefficient of friction found in the block. In other words, sliding occurs when

$$\frac{H}{V} > (\mu_1 \text{ or } \mu_2).$$

As with the keel piers, the resistance of the side piers to sliding will depend on the interface which offers the least resistance, the block-vessel interface or the block-block interface. However, this case is more complicated due to the complex geometry of the side pier as shown in Figure 3.2.

The block-vessel interface of the side pier is examined and shown in Figure 3.3. An arbitrary force F at some angle from vertical is applied to the face for the side block cap. At this interface, the horizontal and vertical block force reactions are:

$$\text{Normal Force} = H \sin\phi + V \cos\phi$$

$$\text{Tangential Force} = H \cos\phi - V \sin\phi$$

where

H = Horizontal Reaction

V = Vertical Reaction

ϕ = Block Inclination Angle.

Using the formula for horizontal sliding resistance, $H = \mu V$, previously introduced in the keel pier case and the above equations yields

$$H \cos\phi - V \sin\phi = \mu_2 (H \sin\phi + V \cos\phi).$$

Rearranging the above equation gives

$$\frac{H}{V} = \frac{\mu_2 \cos\phi + \sin\phi}{\cos\phi - \mu_2 \sin\phi}$$

or

$$\frac{H}{V} = \mu_2'$$

where

$$\mu_2' = \frac{\mu_2 \cos\phi + \sin\phi}{\cos\phi - \mu_2 \sin\phi} .$$

For the block-block interface of the side pier, sliding resistance is found by taking the vertical and horizontal components of the applied force, F , and using them in the formula $H = \mu_1 V$. Like in the keel pier, failure of the side pier due to sliding will occur when the following is satisfied

$$\frac{H}{V} > (\mu_1 \text{ or } \mu_2').$$

There is a critical angle α where no slippage occurs. Referring again to Figure 3.3, this angle can be calculated by comparing the maximum tangential force $F_t \text{ max}$ the interface can have without slipping and the corresponding normal force F_n . The following relationship holds

$$F_t \text{ max} = \mu F_n$$

Finally,

$$\alpha = \text{arc tan } \mu.$$

Since the applied force F acts in a straight line through all blocks to the ground, the angle α for each interface must be calculated. If force F is applied outside of these angles, slippage will occur.

3.3 Block Overturning¹¹

The third failure mechanism is the overturning of a block due to an applied force. The line of action of this force must fall within the middle one-third of the base of the block, as shown in Figure 3.4, or the block will tip over.

In order to show the region that the block will remain upright, the inclined force F must be broken into a transverse

component F_h and a vertical component F_v . Superposing the bending and axial stresses caused by F_h and F_v gives the resultant stress at any point in the block as

$$\sigma_x = -\frac{Ly}{I_z} F_h - \frac{F_v}{A}$$

where

L = block height

A = base area, here bh

I_z = base moment of inertia, here $bh^3/12$.

The minimum stress point on the bottom of the block occurs at point M (Figure 3.4), a distance $-h/2$ from the z axis. Hence,

$$(\sigma_x)_m = \frac{6L}{bh} F_h - \frac{F_v}{bh} .$$

When σ_{xm} at M is negative, compressive stress is present and the block is stable. When σ_{xm} at M is positive, tensile stress is present and the block will overturn since no fasteners hold block to the ground to develop tensile stress. The limit of block stability is when

$$(\sigma_x)_m = 0.$$

Thus, the following equation holds

$$F_h = \frac{h}{6L} F_v.$$

This condition exists when force F is applied at an angle such that the line of force lies within the one-third of the base of the block. If the line of force is outside this region, the block will tip.

3.4 Vessel Liftoff¹⁴

The fourth and final failure mode occurs when the vessel breaks contact with either the side or keel piers. This failure occurs when the dynamic deflection of a row of blocks is equal to, or exceeds the average static deflection of the

blocks. The static deflection of blocks is given by

$$\delta_s = \frac{W}{2K_{sv} + K_{kv}}$$

where

W = submarine weight

K_{sv} = side pier vertical stiffness

K_{kv} = keel pier vertical stiffness.

The dynamic deflection can be due to vertical displacement y , rotational displacement θ , or a combination of both.

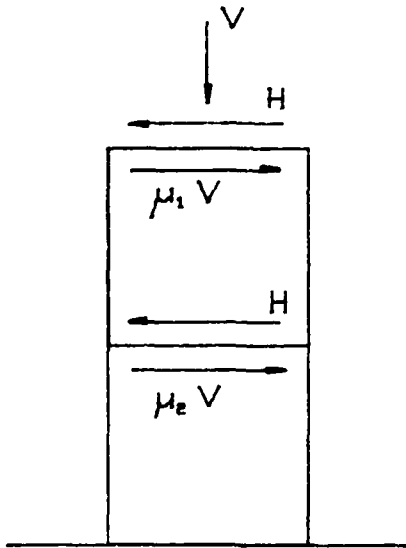


FIGURE 3.1
Keel Pier Forces

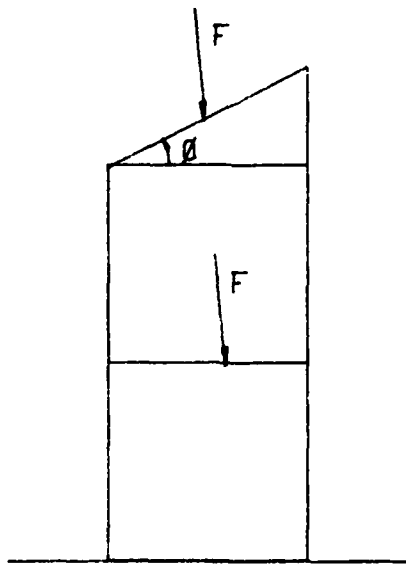


FIGURE 3.2
Side Pier Forces, General

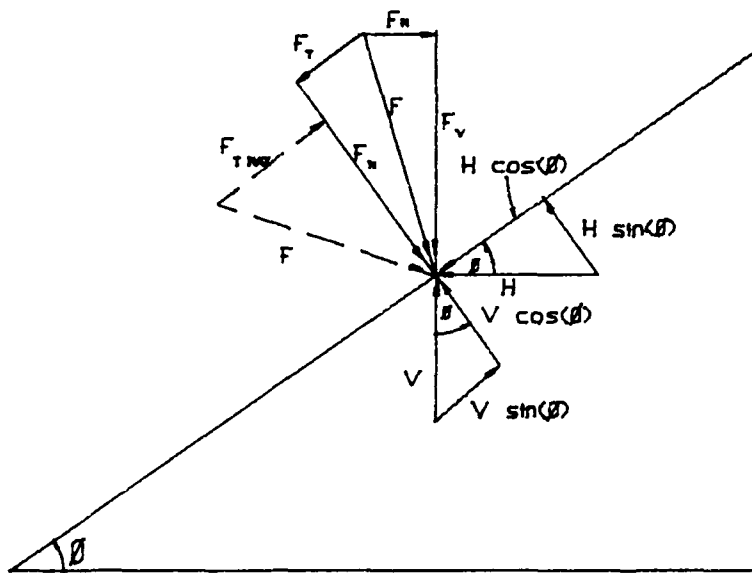


FIGURE 3.3
Side Pier Forces, Block-Vessel Interface.

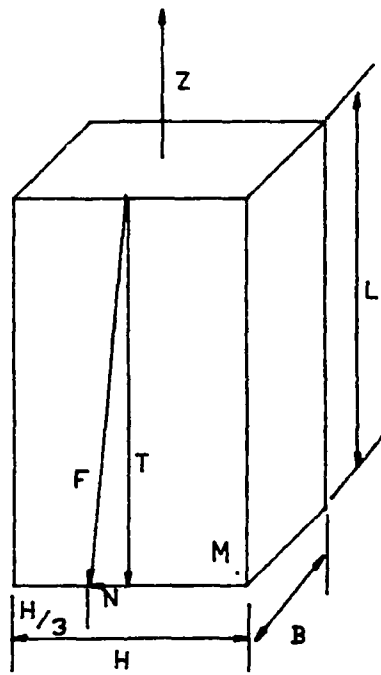


FIGURE 3.4
Block Tipping Forces

4.0 MATHEMATICAL MODELS OF VESSEL-DRYDOCK SYSTEM

This portion of the thesis discusses the modelling of the drydocked submarine subjected to a seismic load. Models will include a quasi-static method, one, two and three degree of freedom mathematical models. The models developed in this section will be analyzed in Section 6 and 7 to predict the vessel seismic response.

4.1 The Quasi-static Method of Modelling Seismic Response

4.1.1 Approach^{5,6}

Current U.S. Navy design method for submarine's seismic response will be examined in this section. The submarine is described as a rigid cylindrical body with its weight evenly dispersed longitudinally.

The quasi-static force method replaces the earthquake motions by a force corresponding to the vessel mass time 0.2 g. This force is horizontally applied to the submarine's center of gravity in the tranverse direction. The drydock blocking system is determined by the evaluation of the loads generated by the quasi-static force.

4.1.2 Force Equations

The application of the static force to the center of gravity of the submarine in drydock is represented in Figure 4.1. The seismic overturning moment, M_S , is defined as

$$M_S = (\Delta/g)(a)(\overline{KG})(2240) \text{ ft-lb}$$

where

Δ = vessel displacement in long tons

g = acceleration of gravity

a = vessel's center of gravity acceleration.

Current U.S. Navy design practice states that the acceleration of the submarine's center of gravity, a , should be set equal to 0.2 g. Hence

$$M_S = 448(\Delta)(\overline{KG}) \text{ ft-lb}$$

After determining the seismic overturning moment, the number of sideblocks required on one side of the vessel is

$$N = \frac{M_S}{A S_p L}$$

where

N = # of side blocks required in the row

A = contact area of a block in square inches

S_p = proportional limit of the block cap in lb/in²

L = distance between centerline of keel and side blocks, in feet, as shown in Figure 4.1.

4.1.3 Vessel Response in the Quasi-static Load Method

The application of a force applied at a vessel's center of gravity will generate reactionary side block forces in the vertical direction to oppose the seismic moment, as shown in Figure 4.2. Summation of moments about the keel yields the equation

$$\Sigma M = M_S - L(F_{Sr} + F_{Mr}) + L(F_{Sl} - F_{Ml}) = 0 \quad (4.1.1)$$

where

F_S = static pier forces (left and right)

F_M = pier forces due to the applied moment (left and right),

Due to symmetry in the vessel-drydock system, the applied moment resistive forces in the side blocks are equal

in magnitude but opposite in direction. Thus, Equation 4.1.1 simplifies to the form

$$M_S = 2L(F_m) \quad (4.1.2)$$

where $F_m = F_{ml} = F_{mr}$.

The force F_m is equal to the side pier compression displacement, δ_m , times its vertical stiffness, K_{VS} . This compression displacement can be expressed as

$$\delta_m = L \sin(\theta). \quad (4.1.3)$$

where θ = angle of vessel rotation about its keel.

Assuming the rotational angle is small, Equations 4.2.1 and 4.1.3 are combined to yield

$$\theta = \frac{M_S}{2L^2 K_{SV}} \quad (4.1.4)$$

4.2 One Degree of Freedom: Rotational Response

4.2.1 Approach

A one degree of freedom mathematical model of a submarine in drydock is developed in this section. The submarine is identified as a rigid cylindrical body with an even longitudinal weight distribution. The system damping and stiffness are provided by the drydock blocking arrangement. System excitation is due to seismic ground accelerations. Other assumptions are

- The keel and side piers remain vertical during the ground motions,
- no slippage between the block cradle and drydock, and
- the keel and side piers bases accelerate at the same rate as the drydock (ground).

The idealized model of the vessel-drydock system is shown

in Figure 4.3. In this system, vessel motion is restricted to rotation about the keel. The side piers are modelled as vertical due to typically small angles or inclination of the tops of the side piers. Only vertical displacements in the side piers are considered.

The one degree of freedom mathematical model predicts and analyzes vessel rotational response about its keel caused by seismic ground accelerations normal to the submarine's longitudinal axis. The resultant angle or rotation, expressed in radians, and side pier forces, generated by the rotation, are compared to applicable pier failure criteria found in Section 3, to see if the blocking arrangement will remain intact.

4.2.2 One Degree of Freedom Equation of Motion Model

For the one degree of freedom case, the keel is the origin with clockwise rotation, θ , positive. The simplified vessel-block system showing coordinate θ at rest and when excited are shown in Figures 4.3 and 4.4 respectively. The moment equilibrium equation about the keel (origin) is:

$$\begin{aligned} \Sigma M_k &= I_k \ddot{\theta} + \overline{MKG}x_g - \overline{MKG}y_g \sin\theta \\ &= B/2(F_{1sv} - F_{1dv}) - B/2(F_{2sv} + F_{2dv}) + \overline{WKG} \sin\theta \quad (4.2.1) \end{aligned}$$

where I_k = Mass moment of inertia of vessel about the keel

M = Vessel Mass

F_{1sv}, F_{2sv} = static side block forces in the vertical direction
(Figure 4.4)

F_{1dv}, F_{2dv} = dynamic side block forces in the vertical

direction (Figure 4.4)

W = vessel weight (Mg)

and \ddot{x}_g, \ddot{y}_g = seismic ground accelerations in their respective directions

This equation can be simplified by the following:

- 1.) The left and right side block rows have the same vertical spring constant, K_{sv} , have the same static deflection and equal but opposite dynamic deflection due to symmetry, i.e.

$$F_{1sv} = F_{2sv} = F_{sv} \quad (4.2.2)$$

and $|F_{1dv}| = |F_{2dv}| = F_{dv}$. (4.2.3)

- 2.) The dynamic side block force, F_{dv} , as seen from Figure 4.5 equals to a force due to the modelled spring displacement plus a dissipative force due to system damping. In other words,

$$F_{dv}(\text{spring}) = (B/2)K_{sv} \sin \theta$$

and $F_{dv}(\text{dissipative}) = C(B/2) \dot{\theta}$

or when combined,

$$F_{dv} = B/2 (K_{sv} \sin \theta + C \dot{\theta}) \quad (4.2.4)$$

where K_{sv} = vertical spring constant of the side blocks

C = vertical damping coefficient of the side blocks

Substituting Equations 4.2.2, 4.2.3, and 4.2.4 into Equation 4.2.1 and rearranging components yields

$$\begin{aligned} I_K \ddot{\theta} + (B^2/2)C \dot{\theta} + [(B^2/2)K_{sv} - W \overline{KG}] \sin \theta \\ = -MKG \ddot{x}_g + MKG \ddot{y}_g \sin \theta \end{aligned} \quad (4.2.5)$$

An additional simplification is that since θ is very small,

$$\sin \theta \approx \theta.$$

The final simplification is that damping is expressed as a

fraction of critical damping. To do this, allow

$$(B^2/2)C = \xi C_{cr} = 2\xi I_k \omega_n$$

where ξ = viscous damping factor $(B^2C/2C_{cr})$

$$C_{cr} = \text{critical damping coefficient} = 2I_k \omega_n$$

ω_n = system undamped natural frequency.

Now, Equation 4.2.5 simplified to

$$\begin{aligned} I_k \ddot{\theta} + 2\xi I_k \omega_n \dot{\theta} + [(B^2/2)K_{sv} - WKG]\theta \\ = -M\overline{KG} \ddot{x}_g + M\overline{KG} \ddot{y}_g \theta \end{aligned} \quad (4.2.6)$$

The non-linear term, $M\overline{KG} \ddot{y}_g \theta$, found in the equation of motion will be removed at this time to linearize Equation 4.2.6 since θ is assumed to be small. The effects of the non-linear term will be evaluated in Section 6 and 7.

The final form of the linearized one degree of freedom equation of motion is

$$m_1 \ddot{\theta} + c_1 \dot{\theta} + k_1 \theta = -m_2 \ddot{x}_g \quad (4.2.7)$$

where $m_1 = I_k$

$$c_1 = 2\xi I_k \omega_n$$

$$k_1 = (B^2/2)K_{sv} - W\overline{KG}$$

$$m_2 = M\overline{KG}.$$

In matrix form,

$$\begin{bmatrix} 0 & m \\ m_1 & c_1 \end{bmatrix} \begin{bmatrix} \ddot{\theta} \\ \dot{\theta} \end{bmatrix} + \begin{bmatrix} -m_1 & 0 \\ 0 & k_1 \end{bmatrix} \begin{bmatrix} \theta \\ \dot{\theta} \end{bmatrix} = \begin{bmatrix} 0 \\ -m_2 \ddot{x}_g \end{bmatrix}.$$

To simplify the explanation, the matrices will be redefined as

$$[A]\{\dot{Y}\} + [B]\{Y\} = \{E(t)\} \quad (4.2.8)$$

where

$$[A] = \begin{bmatrix} 0 & m_1 \\ m_1 & c_1 \end{bmatrix} \quad [B] = \begin{bmatrix} -m_1 & 0 \\ 0 & k_1 \end{bmatrix}$$

$$\{\underline{y}\} = \begin{bmatrix} \dot{\theta} \\ \theta \end{bmatrix} \quad \{\underline{E}(t)\} = \begin{bmatrix} 0 \\ -m_2 \ddot{x}_g \end{bmatrix} .$$

Equations 4.2.6 and 4.2.8 will be solved in Sections 6 and 7.

4.3 Two Degree of Freedom: Rotational and Horizontal Translation Response

4.3.1 Approach

This section develops a two degree of freedom mathematical model of a drydocked submarine. As in the case of the one degree of freedom (Section 4.2.1), the model assumptions still hold, i.e. a rigid cylindrical body, keel and side piers remain vertical, no slippage between the block cradle and drydock, and the bases of the keel and side piers accelerate at the same rate as the drydock (ground).

The idealized model of the vessel-drydock system is shown in Figure 4.6. In this system, vessel motion is restricted to rotation about the keel, and in horizontal transverse translation relative to the keel and side pier supports. The approach for determining vessel-drydock failure is identical to the one degree of freedom case except for the addition of sliding and tipping failure modes.

The two degree of freedom mathematical model predicts and analyzes submarine rotational and translational response caused by seismic ground accelerations normal to the vessel's longitudinal axis. The rotational response is in radians, the translational response in inches, and both responses are expressed as a function of time. The keel and side pier forces are compared to applicable pier failure criteria found

in Section 3.

4.3.2 Two Degree of Freedom Equation of Motion Model

As in the one degree of freedom case, the keel is the origin for the two degree of freedom system with clockwise rotation, θ , is positive. The linear relative translation coordinate, x , is defined with respect to vessel and drydock translation relative to the ground. Defining u as the position of the submarine keel relative to the ground, then the following relationships hold:

$$\begin{aligned}x &= u - x_g \\u &= x + x_g \\ \text{and} \quad \ddot{u} &= \ddot{x} + \ddot{x}_g.\end{aligned}\tag{4.3.1}$$

The simplified vessel-block system showing coordinates (θ and x) at rest and when excited are shown in Figures 4.6 and 4.7 respectively.

A balance of forces in the x direction, as shown in Figure 4.7, yields the first equation of motion

$$\begin{aligned}\Sigma F_x = M\ddot{u} + \overline{MKG}\ddot{\theta} &= (F_{1sh} - F_{1dh}) - (F_{2sh} + F_{2dh}) \\ &\quad - (F_{3sh} + F_{3dh})\end{aligned}\tag{4.3.2}$$

where F_{1sh} , F_{2sh} , F_{3sh} = static block forces in the horizontal direction at their respective position

F_{1dh} , F_{2dh} , F_{3dh} = dynamic block forces in the horizontal direction at their respective position.

The above equation can be simplified by the following:

1) The left and right side block rows have the same horizontal spring constant, K_{sh} , have equal but opposite static horizontal deflection and the same dynamic horizontal

deflection due to symmetry, i.e.,

$$\begin{aligned}F_{1sh} + F_{2sh} &= 0 \\F_{1dh} &= F_{2dh} \end{aligned} \quad (4.3.3)$$

Also, the keel block rows do not experience any net static horizontal deflection since the inclination angle of the block cap is zero. Hence

$$F_{3sh} = 0. \quad (4.3.4)$$

2) The dynamic block forces, F_{dh} as seen from Figure 4.7 equals to a force due to the modelled springs plus a dissipative force due to system damping. In other words

$$\begin{aligned}F_{dh} \text{ (spring)} &= F_{1dh} \text{ (spring)} + F_{2dh} \text{ (spring)} + F_{3dh} \text{ (spring)} \\&= K_{sh}x + K_{sh}x + K_{kh}x\end{aligned}$$

$$F_{dh} \text{ (spring)} = (2K_{sh} + K_{kh})x$$

Likewise

$$F_{dh} \text{ (dissipative)} = C_x \dot{x}$$

so

$$F_{dh} = (2K_{sh} + K_{kh})x + C_x \dot{x} \quad (4.3.5)$$

where K_{sh} = side pier stiffness

K_{kh} = keel pier stiffness

C_x = system horizontal damping coefficient.

Substituting Equations 4.3.1, 4.3.3, 4.3.4, and 4.3.5 into Equation 4.3.2 and rearranging components yields

$$m_{11} \ddot{x} + m_{12} \ddot{\theta} + c_1 \dot{x} + k_{11} x = -m_{11} \ddot{x}_g \quad (4.3.6)$$

where $m_{11} = M$

$$m_{12} = M \overline{KG}$$

$c_1 = C_x$ = system horizontal damping coefficient

$k_{11} = (2K_{sh} + K_{kh})$ = system horizontal stiffness

Summing the moments about the origin in a similar fashion

as the previous degree of freedom case, as shown in Figure 4.7, yields the second equation of motion,

$$\begin{aligned} \Sigma M_K &= I_k \ddot{\theta} + \overline{MKG} \ddot{u} - \overline{MKG} \ddot{y}_g \sin \theta \\ &= B/2(F_{1sv} - F_{1dv}) - B/2(F_{2sv} + F_{2dv}) + \overline{WKG} \sin \theta \end{aligned} \quad (4.3.7)$$

The second equation can be reduced as it was in the one degree of freedom case to

$$\begin{aligned} I_k \ddot{\theta} + \overline{MKG} \ddot{x} + c_\theta \dot{\theta} + (B^2/2 K_{sv} - \overline{WKG}) \theta \\ = MKG \ddot{x}_g + MKG \ddot{y}_g \theta. \end{aligned} \quad (4.3.8)$$

Once again, the non-linear term, $\overline{MKG} y_g \theta$, found in Equation 4.3.8 will be removed leaving a linearized equation since θ is assumed to be small. The effects of the nonlinear term will be evaluated in Sections 6 and 7.

Now the system of equations for the two degree of freedom vessel-drydock system is as follows,

$$m_{11} \ddot{x} + m_{12} \ddot{\theta} + c_{11} \dot{x} + k_{11} x = -m_{11} \ddot{x}_g \quad (4.3.9a)$$

and

$$m_{22} \ddot{\theta} + m_{21} \ddot{x} + c_{12} \dot{\theta} + k_{22} \theta = -m_{21} \ddot{x}_g \quad (4.3.9b)$$

where $m_{11} = M$

$$m_{21} = m_{12} = \overline{MKG}$$

$$m_{22} = I_k$$

c_1 = system horizontal damping coefficient

c_2 = system rotational damping coefficient

$$k_{11} = 2K_{sh} + K_{kh}$$

$$k_{22} = B^2/2 K_{sv} - \overline{WKG}.$$

These two equations of motion are coupled in the mass times

acceleration term, which is known as inertial coupling. Also the equations are coupled in the damping term, because the system's two natural modes have translation and rotation involved in them. This model uses 5 percent of the critical damping coefficient as system damping. To evaluate damping, a modal analysis for the system is performed. This analysis is performed in Appendix 3. Substituting damping coefficients into Equations 4.3.9a and 4.3.9b, the equations of motion can be expressed in matrix notation as Equation 4.3.10:

$$[\underline{M}] \{\ddot{\underline{y}}'\} + [\underline{C}] \{\dot{\underline{y}}'\} + [\underline{K}] \{\underline{y}'\} = \{\underline{E}'(t)\} \quad (4.3.10)$$

where

$$\{\underline{y}'\} = \text{Response Vector} = \begin{Bmatrix} x \\ \theta \end{Bmatrix}$$

$$[\underline{M}] = \text{Mass Matrix} = \begin{bmatrix} m_{11} & m_{12} \\ m_{21} & m_{22} \end{bmatrix}$$

$$[\underline{C}] = \text{Damping Matrix} = \begin{bmatrix} c_{11} & c_{12} \\ c_{21} & c_{22} \end{bmatrix}$$

$$[\underline{K}] = \text{Stiffness Matrix} = \begin{bmatrix} k_{11} & 0 \\ 0 & k_{22} \end{bmatrix}$$

$$\{\underline{E}'(t)\} = \text{Seismic Forcing Vector} = \begin{Bmatrix} -m_{11} \ddot{x}_g \\ -m_{21} \ddot{x}_g \end{Bmatrix} .$$

To simplify the explanation, the matrices will be redefined as

$$[\underline{A}] \{\dot{\underline{y}}\} + [\underline{B}] \{\underline{y}\} = \{\underline{E}(t)\} \quad (4.3.11)$$

where

$$[\underline{A}] = \begin{bmatrix} 0 & [\underline{M}] \\ [\underline{M}] & [\underline{C}] \end{bmatrix}$$

$$\begin{aligned}
 [\underline{B}] &= \begin{bmatrix} -[\underline{M}] & 0 \\ 0 & [\underline{K}] \end{bmatrix} \\
 \{y\} &= \begin{Bmatrix} \{\underline{y}'\} \\ \{\underline{y}'\} \end{Bmatrix} \\
 \{\underline{E}(t)\} &= \begin{Bmatrix} 0 \\ \{\underline{E}'(t)\} \end{Bmatrix} .
 \end{aligned}$$

Equations 4.3.6, 4.3.8, and 4.3.11 will be solved in Sections 6 and 7.

4.4 Three Degree of Freedom: Rotational, Horizontal, and Vertical Translation Response

4.4.1 Approach

This section develops a three degree of freedom mathematical model of a drydocked submarine. The idealized model of the vessel-drydock system is shown in Figure 4.8. In this system, vessel motion is restricted to rotation about the keel, and in horizontal transverse and vertical translations relative to the keel and side pier supports. The approach for determining vessel-drydock failure is identical to the two degree of freedom case.

The three degree of freedom mathematical model predicts and analyzes submarine rotational, horizontal and vertical

transitional responses caused by seismic ground accelerations normal to the vessel's longitudinal axis. The rotational response is in radians, the translational response in inches, and all three responses are expressed as a function of time. The keel and side pier forces generated by the responses are compared to applicable pier failure criteria found in section 3 to check blocking stability.

4.4.2 Three Degree of Freedom Equation of Motion Model

As in the two degree of freedom case, the keel is the origin for the three degree of freedom system with absolute rotation, θ , and translation coordinate, x , is the horizontal vessel motion relative to the drydock. The linear relative translation coordinate, y , is defined with respect to vessel and drydock translation relative to the ground. This coordinate y describes the vertical motion of the vessel hull relative to the drydock and the drydock blocks. Defining v as the position of the submarine keel relative to the ground, then the following relationships hold;

$$y = v - y_g$$

$$v = y + y_g$$

and

$$\ddot{v} = \ddot{y} + \ddot{y}_g \quad (4.4.1)$$

Likewise,

$$\ddot{u} = \ddot{x} + \ddot{x}_g \quad (4.4.2)$$

The simplified vessel-block system showing coordinates (x , y and θ) at rest and when excited are shown in Figure 4.8 and 4.9 respectively.

As developed in Section 4.3.2, the first and third equations of motion in the three degree of freedom model are

$$M\ddot{x} + MKG\ddot{\theta} + C_x\dot{x} + (2K_{sh} + K_{kh})\ddot{x} = -M\ddot{x}_g \quad (4.4.3)$$

and

$$I_k \ddot{\theta} + \overline{MKG} \ddot{x} - \overline{MKG} y \ddot{\theta} + c \dot{\theta} + [(B^2/2)K_{sv} - \overline{WKG}] \theta = -\overline{MKG} \ddot{x}_g + \overline{MKG} \ddot{y}_g \theta . \quad (4.4.4)$$

A balance of forces in the y direction, as shown in Figure 4.9, yields the second equation of motion

$$\Sigma F_y = M \ddot{v} = (F_{1sv} - F_{1dv}) + (F_{2sv} - F_{2dv}) + (F_{3sv} - F_{3dv}) - W. \quad (4.4.5)$$

The above equations can be simplified by the following:

1) The vessel weight, W, must be equal to the summation of static block forces so that static equilibrium holds true, i.e.

$$F_{1sv} + F_{2sv} + F_{3sv} = W \quad (4.4.6)$$

2) The dynamic block forces, F_{dv} , as seen from Figure 4.9 equals to a force due to the modelled springs plus a dissipative force due to system damping. These dynamic block forces are only a function of vertical displacement, y, and velocity, \dot{y} . The formulation of these forces is identical to the procedure used in Section 4.3.2 and will not be repeated. The final form of the dynamic block forces, F_{dv} , is

$$F_{dv} = (2K_{sv} + K_{kv})y + C_y \dot{y} \quad (4.4.7)$$

where K_{sv} = side pier vertical stiffness

K_{kv} = keel pier vertical stiffness

C_y = system vertical damping coefficient.

Substituting Equations 4.4.1, 4.4.2, 4.4.6 and 4.4.7 into Equation 4.4.5 and rearranging components yields

$$M \ddot{y} + C_y \dot{y} + (2K_{sv} + K_{kv})y = -M \ddot{y}_g. \quad (4.4.8)$$

The above equation along with Equations 4.4.3 and 4.4.4

formulate the three equations of motion for the three degree of freedom model.

The non-linear terms, $\overline{MKG}\ddot{\theta}$ and $\overline{MKG}\ddot{y}_g$, found in Equation 4.4.4 will be removed at this time leaving a linearized equation since θ is assumed to be small. The effects of the non-linear terms will be evaluated in Section 6 and 7.

Now the system of equations for the three degree of freedom is as follows;

$$m_{11} \ddot{x} + m_{13} \ddot{\theta} + c_1 \dot{x} + k_{11} x = -m_{11} \ddot{x}_g \quad (4.4.9a)$$

$$m_{22} \ddot{y} + c_2 \dot{y} + k_{22} y = -m_{22} \ddot{y}_g \quad (4.4.9b)$$

$$m_{33} \ddot{\theta} + m_{31} \ddot{x} + c_3 \dot{\theta} + k_{33} \theta = -m_{31} \ddot{x}_g \quad (4.4.9c)$$

where $m_{11} = m_{22} = M$

$$m_{13} = m_{31} = \overline{MKG}$$

$$m_{33} = I_k$$

c_1 = system horizontal damping coefficient

c_2 = system vertical damping coefficient

c_3 = system rotational damping coefficient

$$k_{11} = 2K_{sh} + K_{kh}$$

$$k_{22} = 2K_{sv} + K_{kv}$$

$$k_{33} = B^2/2 K_{sv} - \overline{WKG}.$$

The first and third equations of motions, Equations 4.4.11a and 4.4.11c, respectively, are coupled in the mass times acceleration term, which is known as inertial coupling. Also, these equations are coupled in the damping term because two of the system's three natural modes have horizontal translation and rotation involved in them. The second equation of motion, Equation 4.4.11b, is uncoupled from the rest of equations.

Hence, the last natural mode of the system only depends on vertical translation.

In order to introduce damping, this model uses 5 percent of the critical damping coefficient as system damping. To evaluate damping, a modal analysis for the system in question must be performed. This analysis is performed in Appendix 3. System damping coefficients can be found using this modal analysis technique, but for now, the coefficients will be left in terms of c_{11} , c_{13} , c_{22} , c_{31} and c_{33} . Substituting these coefficients into Equations 4.4.11a, 4.4.11b, and 4.4.11c, the equations of motion can be expressed in matrix notation as Equation 4.4.12:

$$[M] \{\ddot{y}'\} + [C] \{\dot{y}'\} + [K] \{y'\} = \{E'(t)\} \quad (4.4.10)$$

where

$$\{y'\} = \text{Response Vector} = \begin{Bmatrix} x \\ y \\ \theta \end{Bmatrix}$$

$$[M] = \text{Mass Matrix} = \begin{bmatrix} m_{11} & 0 & m_{13} \\ 0 & m_{22} & 0 \\ m_{31} & 0 & m_{33} \end{bmatrix}$$

$$[K] = \text{Stiffness Matrix} = \begin{bmatrix} k_{11} & 0 & 0 \\ 0 & k_{22} & 0 \\ 0 & 0 & k_{33} \end{bmatrix}$$

$$\{E'(t)\} = \text{Seismic Forcing Vector} = \begin{Bmatrix} -m_{11} \ddot{x}_g \\ -m_{22} \ddot{y}_g \\ -m_{31} \ddot{x}_g \end{Bmatrix}$$

$$[C] = \text{Damping Matrix} = \begin{bmatrix} c_{11} & 0 & c_{13} \\ 0 & c_{22} & 0 \\ c_{31} & 0 & c_{33} \end{bmatrix}$$

To simplify the explanation the matrices will be redefined as

$$[\underline{A}] \{\dot{\underline{Y}}\} + [\underline{B}] \{\underline{Y}\} = \{\underline{E}(t)\} \quad (4.4.11)$$

where

$$[\underline{A}] = \begin{bmatrix} 0 & [\underline{M}] \\ [\underline{M}] & [\underline{C}] \end{bmatrix}$$

$$[\underline{B}] = \begin{bmatrix} -[\underline{M}] & 0 \\ 0 & [\underline{K}] \end{bmatrix}$$

$$\{\underline{Y}\} = \begin{pmatrix} \{\dot{\underline{Y}}\} \\ \{\underline{Y}'\} \end{pmatrix}$$

$$\{\underline{E}(t)\} = \begin{pmatrix} 0 \\ \{\underline{E}'(t)\} \end{pmatrix}$$

Equations 4.4.3, 4.4.4, 4.4.8, and 4.4.11 will be solved in Section 6 and 7.

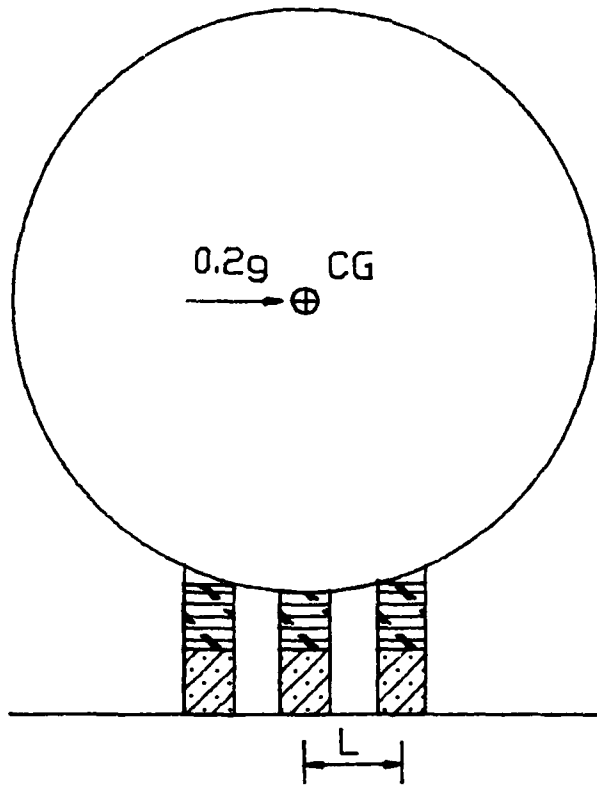


FIGURE 4.1
Vessel-Drydock System with Applied Quasi- static Force

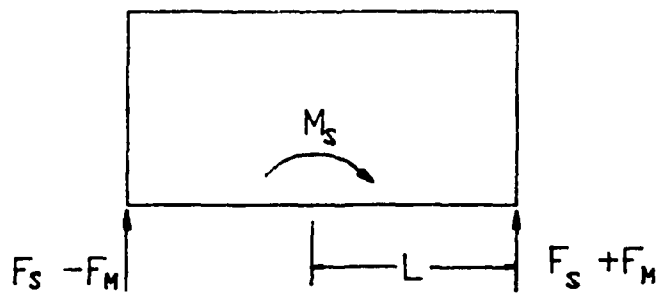


FIGURE 4.2
Vessel-Drydock System Force Diagram with Applied Quasi-static Force

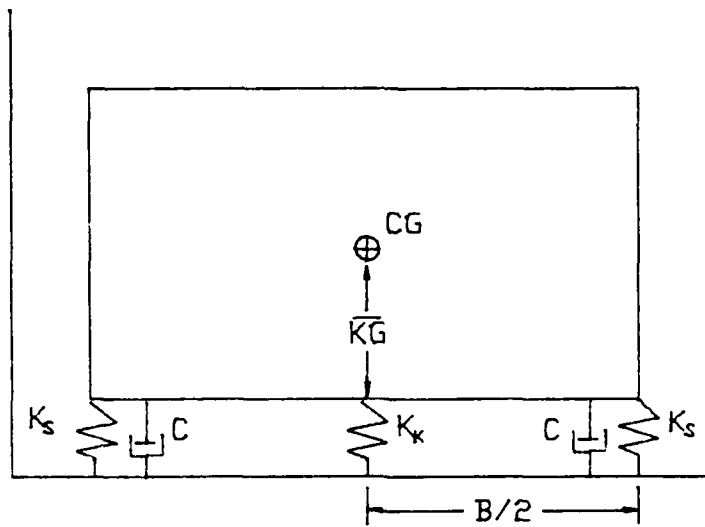


FIGURE 4.3
Idealized One Degree of Freedom Vessel- Drydock System at Rest

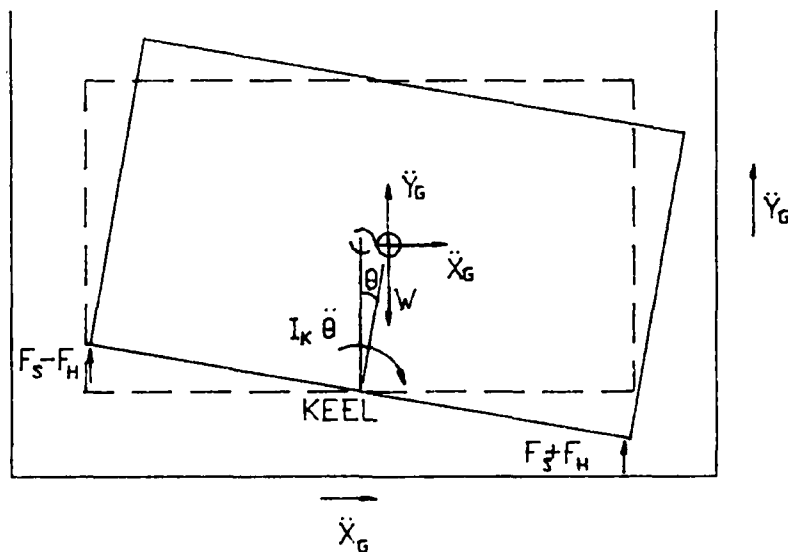


FIGURE 4.4
Idealized One Degree of Freedom Vessel- Drydock System,
Excited

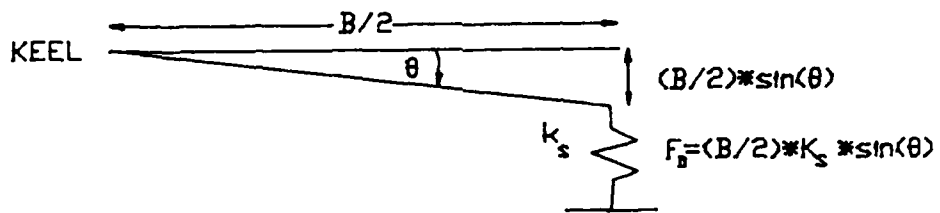


FIGURE 4.5
Dynamic Side Block Force

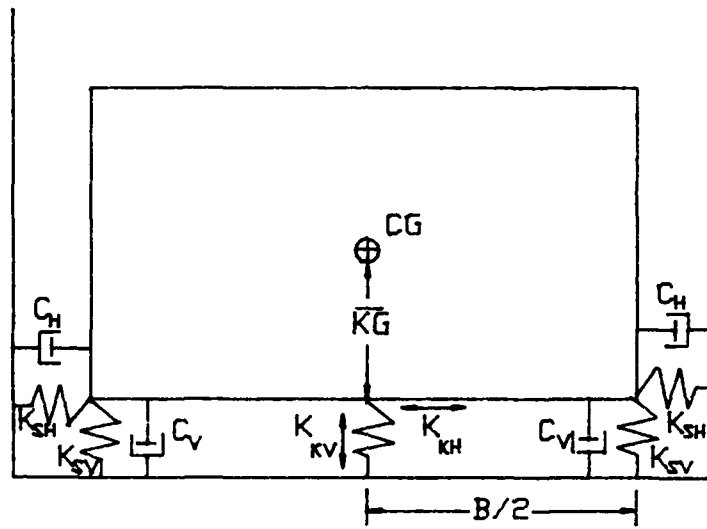


FIGURE 4.6
Idealized Two Degree of Freedom Vessel-Drydock System at Rest

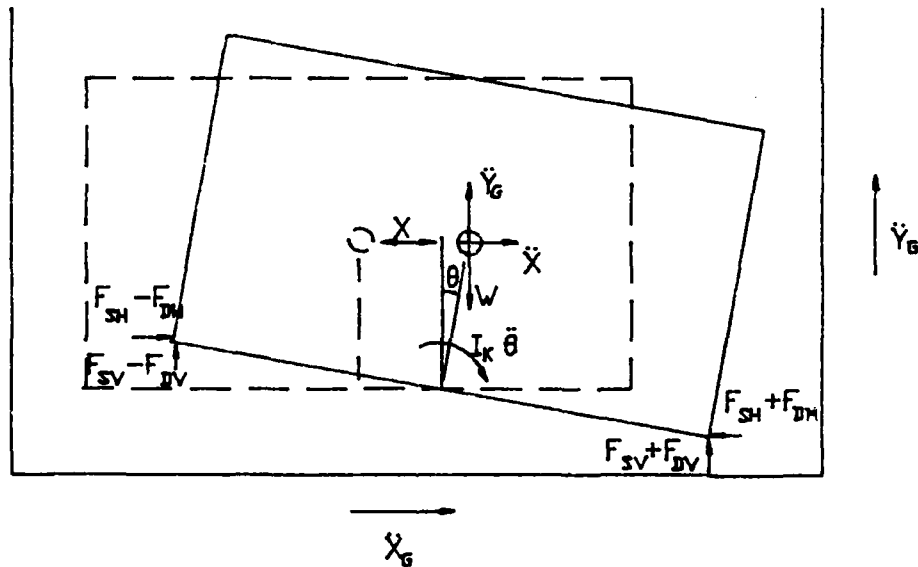


FIGURE 4.7
Idealized Two Degree of Freedom Vessel-Drydock System,
Excited

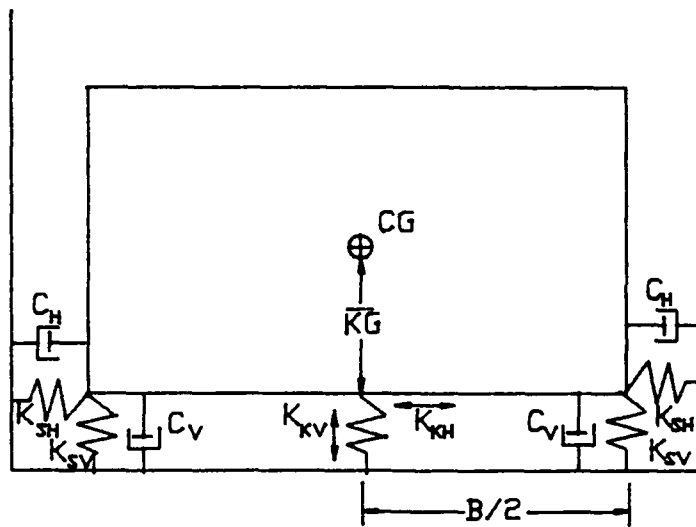


FIGURE 4.8
Idealized Three Degree of Freedom Vessel-Drydock System at Rest

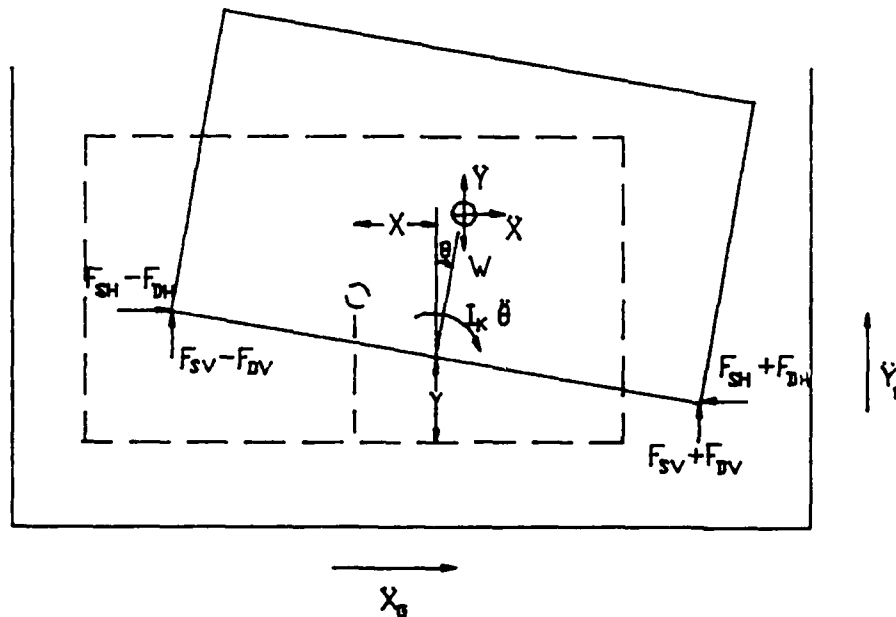


FIGURE 4.9
Idealized Three Degree of Freedom Vessel-Drydock System, Excited

5.0 SYSTEM PARAMETERS

In order to study the response of a vessel-drydock system to seismic loading, eleven typical configurations have been selected for implementation into the one, two and three degrees of freedom models developed in the previous section. This section explores these eleven systems along with the modeling of the pier blocks for stiffness.

5.1 Vessel-Drydock System Parameters

Eleven drydock system configurations have been chosen for analysis and are defined in Table 5.1. The vessel-drydock parameters, corresponding to each system, were taken from the appropriate NAVSEA drawings.

TABLE 5.1

Vessel-Drydock Configurations

<u>System</u>	<u>Hull</u>	<u>Block Type</u>	<u>Longitudinal Block Spring</u>	<u>NAVSEA Drawing</u>
1	616	Composite	8 ft	845-2006640
2	616	Composite	16 ft	845-2006640
3	616	Timber	8 ft	845-2006640
4	616	Timber	16 ft	845-2006640
5	616	Timber Side/ Concrete Keel	16 ft	845-2006640
6	726	Composite	8 ft	845-4862749
7	726	Composite	12 ft	845-4862749
8	726	Composite	16 ft	845-4862749
9	688	Composite/Timber	12 ft	845-4403511
10	637	Composite/Timber	12 ft	845-2140554
11	637	Composite/Timber	12 ft	845-2140554

Table 5.2 lists the vessel radii, weight, distance from center of gravity to keel, KG, moments of inertia about vessel center of gravity, $I_{C.g.}$ and keel, I_k , and side block transverse spacing, B.

TABLE 5.2

Key Vessel Parameters

SYSTEM	Hull Radius (inches)	Weight (Kips)	KG (inches)	I_{Cg} (K-in-sec ²)	I_k (K-in-sec ²)	B (inches)
1-5	198	16,396	193	831,257	2,411,000	144
6-8	252	37,656	223	3,097,535	7,949,000	180
9	198	13,624	193	691,852	2,007,000	138
10-11	190	9,529	174	445,592	1,193,000	138

5.2 Block Parameters¹¹

The models developed in Section 4 require the evaluation of the block's vertical and horizontal spring stiffness constants, K_v and K_h . The spring stiffness is the amount of force required to produce one unit of displacement in the respective direction. In order to facilitate the use of Hooke's law in evaluating spring constants, the assumption of homogeneous isotropic behavior will be used for the block materials: wood and concrete. Both the side and keel piers must be analyzed for K_v and K_h .

5.2.1 Vertical Stiffness K_v ¹¹

Using Hooke's Law, the linear relationship between vertical applied force and deformation can be written as

$$\frac{F}{A} = \frac{Eh}{H}$$

where F = vertical force
 A = area under applied force
 E = modulus of elasticity
 h = change in height
 H = original height.

Hence, the spring constant for a given material is

$$k_v = \frac{F}{h} = \frac{EA}{H} \quad (5.1)$$

For the eleven drydock configurations, two types of standard blocks (composite and timber) are used. A standard composite block which is composed of a softwood cap, a hardwood middle portion, and a concrete bottom can be modelled as a series of three springs (Figure 5.1). The resultant block spring stiffness is

$$k_v \text{ block} = [(1/k_{\text{cap}}) + (1/k_{\text{oak}}) + (1/k_{\text{con}})]^{-1} \quad (5.2)$$

where

k_{cap} = softwood cap spring constant
 k_{oak} = hardwood middle spring constant
 k_{con} = concrete bottom spring constant.

All three constants listed above are calculated from Equation 5.1. A standard timber block is composed of a softwood cap and a hardwood body (Figure 5.2). Its block spring constant is

$$k_v \text{ block} = [(1/k_{\text{cap}}) + (1/k_{\text{oak}})]^{-1} \quad (5.3)$$

The total vertical stiffness for a drydock configuration can be computed by multiplying $k_v \text{ block}$ times the number of blocks. The keel pier has a total vertical stiffness of

$$K_{kv} = k_v \text{ block} * n_k$$

and for the side pier

$$K_{sv} = k_v \text{ block} * n_s$$

where n_k and n_s are the number of blocks in one row for their respective pier.

The values of total vertical stiffness for both keel and side blocks of the eleven drydock configurations are found in Table 5.4. The following parameters are used in the formulation of Table 5.4:

A = cross-sectional area of softwood cap

E_{cap} = 22.5 ksi

E_{oak} = 31.675 ksi

E_{con} = 2,000 ksi

H_{cap} = 4 inches

H_{oak} = 29 inches for composite block

= 56 inches for timber block

H_{con} = 27 inches.

5.2.2 Horizontal Stiffness K_h ¹¹

In order to determine the horizontal stiffness, two types of deformation must be looked at. They are the block-cap displacements due to bending and shear deformations. Modelling as a continuous cantilever beam subjected to a concentrated lateral force at the cap surface (Figure 5.3), the bending displacement due to the applied force P of a composite block is

$$d_B = \frac{P(H_1 + H_2 + H_3)}{3E_1 I} + \frac{P(E_1 - E_2)(H_2 + H_3)}{3E_1 E_2 I}$$

$$+ \frac{P(E_2 I - E_3 I_3) H_3}{3E_2 E_3 I I_3} \quad (5.4)$$

where H_1 = height of concrete (27 inches)

H_2 = height of hardwood (29 inches)

H_3 = height of softwood cap (4 inches)

E_1 = modulus of elasticity of concrete

E_2 = modulus of elasticity of hardwood

E_3 = modulus of elasticity of softwood cap

I = moment of inertia of block's cross-section

I_3 = moment of inertia of cap's cross-section.

For the bending displacement of a timber block, Equation 5.4 still holds true with the alterations:

H_1 = height of hardwood (27 inches)

E_1 = modulus of elasticity of hardwood.

In shear, deformation can be determined by modelling the composite block as an element subjected to shear stress at the top (Figure 5.4). The shear displacement becomes

$$d_s = \frac{(1+\nu_{con})PH_1}{AE} + \frac{2(1+\nu_{wood})PH_2}{AE_2} + \frac{2(1+\nu_{wood})PH_3}{AE_3} \quad (5.5)$$

where A = area of cap's cross section

ν_{wood} = Poisson's ratio for wood (0.30 is used)

ν_{con} = Poisson's ratio for concrete (0.15 is used).

By redefining H_1 and E_1 , Equation 5.5 yields the shear displacement of a timber block.

The horizontal spring constant of any one block can be determined through the Hooke's Law relation

$$k_h = P/(d_B + d_S) \quad (5.6)$$

The total horizontal stiffnesses for the keel and side piers are

$$K_{kh} = k_h * n_k$$

and $K_{sh} = k_h * n_s$.

The values for the total area of the rows of blocks for each of the eleven systems are listed in Table 5.3. Also listed are the corresponding total area of the cap blocks for a row of side or keel blocks. The values of total horizontal and vertical stiffnesses of the keel and side piers for the eleven drydock configurations are listed in Table 5.4.

TABLE 5.3
Keel Pier Cross-Sectional Area Analysis

Systems	Cap			Block			Total			Block			Cement			Block		
	Width (ins)	Depth (ins)	Area (in ²)	Width (ins)	Depth (ins)	Area (in ²)	Number of Keel	Area (in ²)	Depth (ins)	Area (in ²)	Number of Keel	Area (in ²)	Height (ins)	Area (in ²)	Number of Keel	Area (in ²)	Height (ins)	Area (in ²)
1	24	42	1008	48	42	2016	55	55440	48	42	2016	55	110880	4	29	27	60	60
2	24	42	1008	48	42	2016	55	55440	48	42	2016	55	110880	4	29	27	60	60
3	24	42	1008	48	42	2016	55	55440	48	42	2016	55	110880	4	56	0	60	60
4	24	42	1008	48	42	2016	55	55440	48	42	2016	55	110880	4	56	0	60	60
5	24	42	1008	48	42	2016	55	55440	48	42	2016	55	110880	4	29	27	60	60
6	36	42	1512	48	42	2016	72	108864	48	42	2016	72	145152	4	29	27	60	60
7	36	42	1512	60	42	2520	72	108864	60	42	2520	72	181440	4	29	27	60	60
8	36	42	1512	60	42	2520	72	108864	60	42	2520	72	181440	4	29	27	60	60
9	24	42	1008	60	42	2520	42	42336	60	42	2520	42	105840	4	56	0	60	60
10	24	42	1008	48	42	2016	30	30240	48	42	2016	30	60480					
	12	42	504	48	42	2016	4	2016	48	42	2016	4	8064					
								32256					68544		4	56	0	60
11	24	42	1008	48	42	2016	30	30240	48	42	2016	30	60480					
12	12	42	504	48	42	2016	4	2016	48	42	2016	4	8064					
								32256					68544		4	56	0	60

TABLE 5.3 (continued)

Side Pier Cross-Sectional Area Analysis

Systems	Cap Width (ins)	Cap Depth (ins)	Cap Area (in ²)	Number of Keel	Cap Area (in ²)	Block Width (ins)	Block Depth (ins)	Block Area (in ²)	Number of Keel	Block Area (in ²)	Cap Height (ins)	Block Height (ins)	Wood Height (ins)	Cement Height (ins)
1	24	12	288	29	8532	48	42	2016	29	58464	4	29	27	60
2	24	12	288	15	4320	48	42	2016	15	30240	4	29	27	60
3	24	12	288	29	8352	48	42	2016	29	58464	4	56	0	60
4	24	12	288	15	4320	48	42	2016	15	30240	4	56	0	60
5	24	12	288	15	4320	48	42	2016	15	30240	4	56	0	60
6	36	36	1296	44.5	57672	48	42	2016	44.5	89712	4	29	27	60
7	36	36	1296	29.5	38232	60	42	2520	29.5	74340	4	29	27	60
8	36	36	1296	22.5	29160	60	42	2520	22.5	56700	4	29	27	60
9	24	20	480	19	9120	60	42	2520	19	47880	4	29	27	60
10	24	24	576	13	7488	48	42	2016	13	26208	4	29	27	60
11	24	24	576	10.5	6048	48	42	2016	10.5	21168	4	29	27	60

TABLE 5.4

Total Keel and Side Pier Stiffness in Pounds Per Inch

System	K _{kv}	K _{sv}	K _{kh}	K _{sh}
1	50089159	7545899.	14018741	2612721
2	50089159	3903051.	14018741	1351407.
3	28493109	4292468.	5161684.	1282216.
4	28493109	2220242.	5161684.	663215.3
5	50089159	2220242.	14018741.	663215.3
6	98356895	52105736	24330635	16104611
7	98356895	34542004	24330635	10676090
8	98356895	26345596	24330635	8142780.
9	21758374	8239775.	3941650.	2683291.
10	16577809	6765289.	3072572.	2139500.
11	16577809	5464271.	3072572.	1728057.

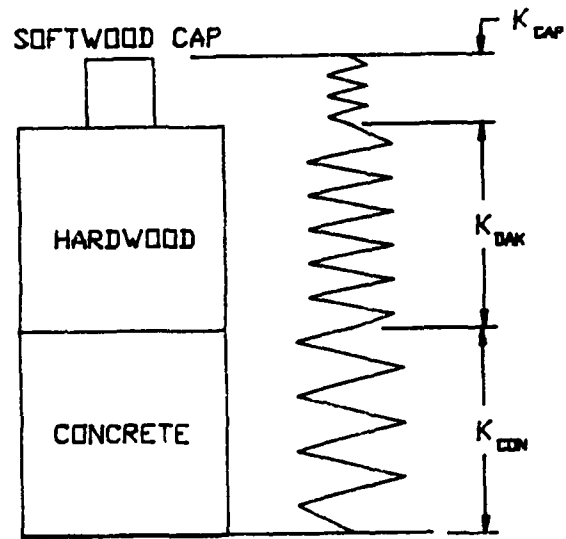


FIGURE 5.1
Standard Composite Block Stiffness Model

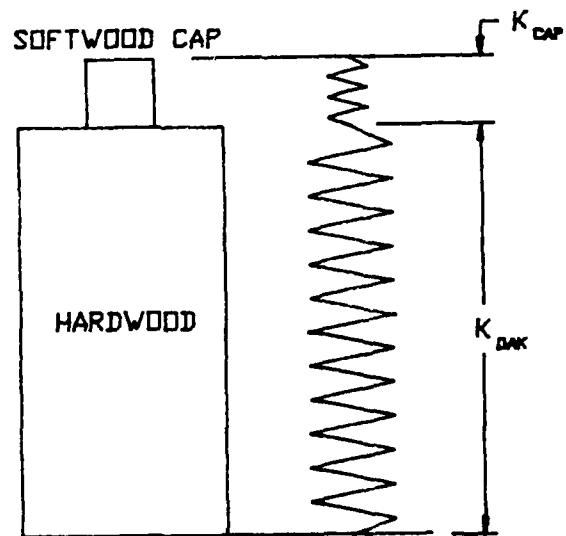


FIGURE 5.2
Standard Timber Block Stiffness Model

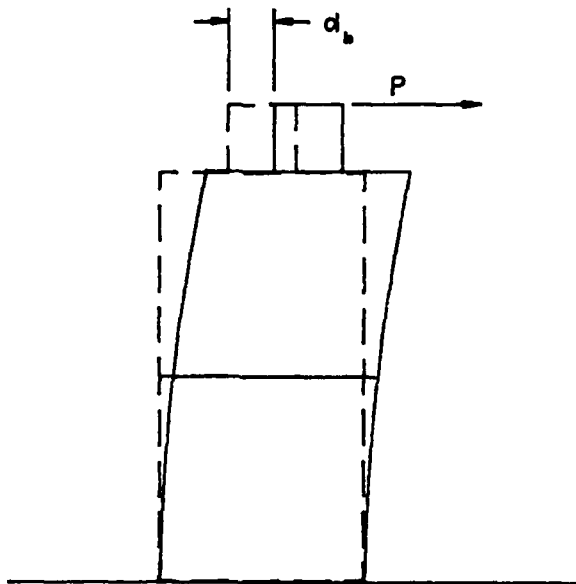


FIGURE 5.3
Standard Block in Bending

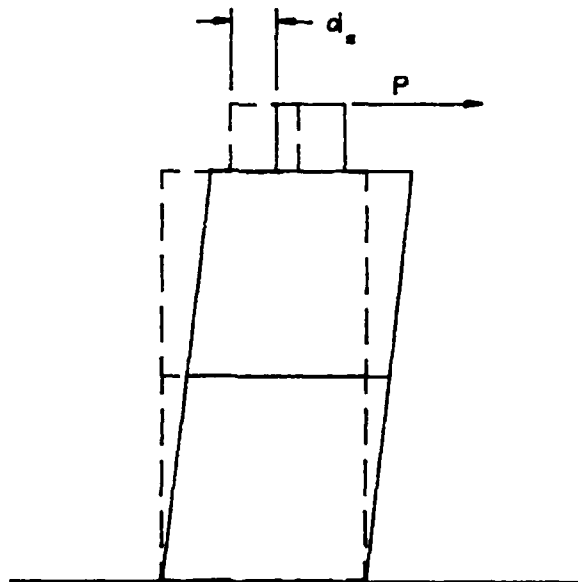


FIGURE 5.4
Standard Block in Shear

6.0 VESSEL RESPONSE TO SEISMIC EXCITATION

This portion of the thesis discusses methods of determining the seismic response of the vessel-drydock system mathematical models developed in Section 4. The numerical analysis schemes to be implemented are a modal analysis method (Section 6.1) which looks at the linearized equations of motion, and a fourth order Runge-Kutta numerical method (Section 6.2) which analyzes the non-linear aspect and also verifies the linear solution. Section 6.3 incorporates a response spectrum analysis to solve the mathematical models. Finally, Section 6.4 generates system response for the eleven vessel-drydock configurations using the quasi-static force method.

6.1 Vessel Response Using Modal Analysis

In order to use the modal analysis method described herein, only the linearized equations of motion mathematical models can be evaluated. These are Equations 4.2.8, 4.3.11 and 4.4.11 which correspond to the one, two, and three degree of freedom models respectively. Since all three linearized equations are in the form

$$[A]\{\dot{Y}\} + [B]\{Y\} = \{E(t)\},$$

the three degree of freedom model will be analyzed. The other two cases are just a reduced version of the third.

To solve the linearized three degree of freedom equations of motion (4.4.11) in matrix notation and obtain system responses as a function of time, the problem is solved as an eigenvalue problem with a procedure described in reference [13]. As a first step, the equations are decoupled.

To accomplish this, first consider the free vibration problem

$$[\underline{A}]\{\dot{\underline{Y}}\} + [\underline{B}]\{\underline{Y}\} = 0 \quad (6.1.1)$$

Assuming Equation 6.1.1 has a solution in the form

$$\{\underline{Y}\} = \{\psi\} e^{\lambda t},$$

Equation 6.1.1 can be expressed as

$$\lambda[\underline{A}]\{\psi\} + [\underline{B}]\{\psi\} = 0. \quad (6.1.2)$$

where λ = complex eigenvalues

$\{\psi\}$ = modal vectors.

Solving the matrix determinant problem

$$|\lambda[\underline{A}] + [\underline{B}]| = 0 \quad (6.1.3)$$

yields the eigenvalues. In the three degree of freedom case, $[\underline{A}]$ and $[\underline{B}]$ are 6 x 6 matrices hence the solution of Equation 6.1.3 will yield 6 eigenvalues. These eigenvalues will be comprised of three sets of complex conjugates. Now the modal vectors can be found by substituting the eigenvalues back into Equation 6.1.2 and solving. The modal vectors are then combined to form the modal matrix $[\Psi]$ where

$$[\Psi] = [\{\psi\}_1 \{\psi\}_2 \{\psi\}_3 \{\psi\}_4 \{\psi\}_5 \{\psi\}_6].$$

The equations of motion can then be decoupled by using the modal matrix, i.e.

$$[\Psi]^T [\underline{A}][\Psi] = [\underline{A}]$$

and

$$[\Psi]^T [\underline{B}][\Psi] = [\underline{B}]$$

where $[\underline{A}]$ and $[\underline{B}]$ are diagonal matrices.

Once the modal matrix is found, the forced vibration problem is analyzed. Assume the following

$$\{\underline{Y}\} = [\Psi] \{\underline{z}\}$$

and

$$\{\underline{z}\} = [\Psi]^{-1} \{\underline{Y}\},$$

where z is a complex coordinate system. Equation 4.4.1 is now expressed as

$$[A] [\psi] \{\dot{z}\} + [B] [\psi] \{z\} = \{E(t)\}.$$

Using $[\psi]^T$, the above equation can now be in the form

$$[\underline{A}] \{\dot{z}\} + [\underline{B}] \{z\} = [\psi]^T \{E\} \equiv \{N(t)\}.$$

This will yield six uncoupled equation of motion in the form

$$a_{ii} \dot{z}_i(t) + b_{ii} z_i(t) = N_i(t), \quad i = 1, 6$$

$$\text{or } \dot{z}_i(t) - v_i z_i(t) = (1/a_{ii}) N_i(t) \quad (6.1.4)$$

where $v_i = -b_{ii}/a_{ii}$.

The solution of Equation 6.1.4 is

$$z_i(t) = \frac{1}{a_{ii}} \int_0^t e^{v_i(t-\tau)} N_i(\tau) d\tau, \quad i = 1, 6. \quad (6.1.5)$$

Once Equation 6.1.5 is solved, the $\{y\}$ matrix is found by the relationship

$$\{y\} = [\psi] \{z\}.$$

Recalling from Section 4.4.2 the terms of the three degree of freedom equations of motion $\{y\}$ matrix is

$$\{y\} = \begin{bmatrix} \dot{x} \\ y \\ \dot{\theta} \\ x \\ y \\ \theta \end{bmatrix}.$$

Hence, the desired vessel-drydock system response can be found in the fourth, fifth and sixth terms of the $\{y\}$ matrix, i.e. x , y and θ .

6.2 Vessel Response: Fourth Order Runge-Kutta Numerical Method

A fourth order Runge-Kutta numerical scheme is chosen to analyze the non-linear equations of motion due to its simplicity and easy use of computer programming. It also will be used to verify solutions found by other methods. The non-linear Equations 4.2.6; 4.3.6 and 4.3.8; 4.4.3. 4.4.4 and 4.4.8 correspond to the one, two and three degree of freedom models respectively. Since all three systems of equations are similar in form, only the three degree of freedom non-linear model will be developed.

The three degree of freedom non-linear equations of motion are

$$m_{11} \ddot{x} + m_{13} \ddot{\theta} + c_{11} \dot{x} + c_{13} \dot{\theta} + k_{11} x = -m_{11} \ddot{x}_g$$

$$m_{22} \ddot{y} + c_{22} \dot{y} + k_{22} y = -m_{22} \ddot{y}_g$$

and

$$m_{33} \ddot{\theta} + m_{31} \ddot{x} - m_{31} \ddot{y} + c_{33} \dot{\theta} + c_{31} \dot{x} + k_{31} \theta = -m_{31} \ddot{x}_g + m_{31} \ddot{y}_g \theta.$$

The coefficient of the above equations can be found in Section 4.4.2. These equations can be rearranged into

$$\ddot{x} + \frac{m_{13}}{m_{11}} \ddot{\theta} = -\frac{c_{11}}{m_{11}} \dot{x} - \frac{c_{13}}{m_{11}} \dot{\theta} - \frac{k_{11}}{m_{11}} x - x_g \quad (6.1.2a)$$

$$\ddot{y} = -\frac{c_{22}}{m_{22}} \dot{y} - \frac{k_{22}}{m_{22}} y - y_g \quad (6.1.2b)$$

and

$$\ddot{\theta} + \frac{m_{31}}{m_{33}} \ddot{x} = -\frac{c_{33}}{m_{33}} \dot{\theta} - \frac{c_{31}}{m_{33}} \dot{x} - \left(\frac{k_{33}}{m_{33}} + \frac{m_{31} c_{22}}{m_{33} m_{22}} \dot{y} + \frac{m_{31} k_{22}}{m_{22} m_{33}} y \right) \theta - \frac{m_{31}}{m_{33}} \ddot{x}_g \quad (6.2.1c)$$

Equations 6.2.1a, 6.2.1b and 6.2.1c can be made into an equivalent first order system by the following substitutions

$$\dot{x} = R = e_1(t, x, R, T)$$

$$\dot{y} = S = f_1(t, y, S)$$

$$\dot{\theta} = T = g_1(t, \theta, y, R, S, T)$$

$$\dot{R} + \frac{m_{13}}{m_{11}} \dot{T} = e_2(t, x, R, T)$$

$$\dot{S} = f_2(t, y, S)$$

$$\dot{T} + \frac{m_{31}}{m_{13}} R = g_2(t, \theta, y, R, S, T).$$

The Runge-Kutta formulas [8] for this system are

$$\begin{aligned} k_{11} &= hR_n & \ell_{11} &= h\{e_2(t, x_n, R_n, T_n)\} \\ k_{12} &= hS_n & \ell_{12} &= h\{f_2(t, y_n, S_n)\} \\ k_{13} &= hT_n & \ell_{13} &= h\{g_2(t, \theta_n, y_n, R_n, S_n, T_n)\} \\ k_{21} &= h(R_n + \frac{1}{2}\ell_{11}) & \ell_{21} &= h\{e_2(t, x_n + \frac{1}{2}k_{11}, R_n + \frac{1}{2}\ell_{11}, T_n + \frac{1}{2}\ell_{13})\} \\ k_{22} &= h(S_n + \frac{1}{2}\ell_{12}) & \ell_{22} &= h\{f_2(t, y_n + \frac{1}{2}k_{12}, S_n + \frac{1}{2}\ell_{12})\} \\ k_{23} &= h(T_n + \frac{1}{2}\ell_{13}) & \ell_{23} &= h\{g_2(t, \theta_n + \frac{1}{2}k_{13}, y_n + \frac{1}{2}k_{12}, \\ & & & R_n + \frac{1}{2}\ell_{11}, S_n + \frac{1}{2}\ell_{12}, T_n + \frac{1}{2}\ell_{13})\} \\ k_{31} &= h(R_n + \frac{1}{2}\ell_{21}) & \ell_{31} &= h\{e_2(t, x_n + \frac{1}{2}k_{21}, R_n + \frac{1}{2}\ell_{21}, T_n + \frac{1}{2}\ell_{23})\} \\ k_{32} &= h(S_n + \frac{1}{2}\ell_{22}) & \ell_{32} &= h\{f_2(t, y_n + \frac{1}{2}k_{22}, S_n + \frac{1}{2}\ell_{22})\} \\ k_{33} &= h(T_n + \frac{1}{2}\ell_{23}) & \ell_{33} &= h\{g_2(t, \theta_n + \frac{1}{2}k_{23}, y_n + \frac{1}{2}k_{22}, R_n + \frac{1}{2}\ell_{21}, \\ & & & S_n + \frac{1}{2}\ell_{22}, T_n + \frac{1}{2}\ell_{23})\} \end{aligned}$$

$$\begin{aligned}
k_{41} &= h(R_n + l_{31}) & l_{41} &= h\{e_2(t, x_n + k_{31}, R_n + l_{31}, T_n + l_{33})\} \\
k_{42} &= h(S_n + l_{32}) & l_{42} &= h\{f_2(t, y_n + k_{32}, S_n + l_{32})\} \\
k_{43} &= h(T_n + l_{33}) & l_{43} &= h\{g_2(t, \theta_n + k_{33}, y_n + k_{32}, R_n + l_{31}, \\
& & & S_n + l_{32}, T_n + l_{33})\}
\end{aligned}$$

and lastly,

$$\begin{aligned}
x_{n+1} &= x_n + \frac{1}{6}(k_{11} + 2k_{21} + 2k_{31} + k_{41}) \\
y_{n+1} &= y_n + \frac{1}{6}(k_{12} + 2k_{22} + 2k_{32} + k_{42}) \\
\theta_{n+1} &= \theta_n + \frac{1}{6}(k_{13} + 2k_{23} + 2k_{33} + k_{43}) \\
R_{n+1} &= R_n + \frac{1}{6}(l_{11} + 2l_{21} + 2l_{31} + l_{41}) \\
S_{n+1} &= S_n + \frac{1}{6}(l_{12} + 2l_{22} + 2l_{32} + l_{42}) \\
T_{n+1} &= T_n + \frac{1}{6}(l_{13} + 2l_{23} + 2l_{33} + l_{43})
\end{aligned}$$

where h is the time step. Hence, the desired vessel-drydock system response can be found and system failure analyzed by the iteration of the Runge-Kutta scheme.

6.3 Vessel Response: Response Spectrum Analysis

The degrees of freedom mathematical models developed in previous sections produce a time history of the seismic response of a drydocked vessel. These models use numerous computer iterations to find their time history in order to evaluate the system's maximum seismic response. Another way to determine the maximum seismic response of a drydocked vessel is the response spectrum analysis method. Simplicity and fast results are characteristic of this spectrum method. However, only maximum response is produced and no time history is generated.

The response spectra are graphs of the maximum seismic response of single degree of freedom systems over a range of

system natural frequencies. These graphs are generated for particular earthquake and can contain acceleration, velocity, displacement, or combination of all three responses for the given system. Simplified response spectra are plotted for earthquake design analysis. The El Centro earthquake response spectra graph, shown in Figure 6.1, will be used to confirm the results of the mathematical models in this thesis. The simplified spectrum portion of this graph is described in reference [2] and updated in reference [7].

The simplified El Centro earthquake response spectra used described the maximum relative displacement of the system shown in the insert of Figure 6.1. The linear equation of motion for this simple system is

$$\ddot{m}u + c\dot{u} + ku = -m\ddot{y}_{sa} f_a(t)$$

where $u(t)$ = relative displacement of the mass with respect to the support

and \ddot{y}_{sa} = maximum support acceleration.

The natural frequency of the system is given by

$$\omega^2 = k/m$$

$$f = \omega/2\pi$$

Using the response spectra graph and the particular frequency, f , of the system of interest, the maximum value of the relative displacement, u_m , is determined. In equation form, the relative displacements of a single degree of freedom system with 5% critical damping subjected to the El Centro earthquake ground motions are:

for $\omega < 2.24$ rad/sec,

$$u_{\max} = 1.4 (y_{sa})_{\max} = 11.62 \text{ inches}, \quad (6.3.1)$$

for $2.24 < \omega < 12.74$,

$$u_{\max} = 1.9 (Y_{sa})_{\max}/\omega = 26.03/\omega \text{ inches,} \quad (6.3.2)$$

for $\omega > 12.74$,

$$u_{\max} = 2.6 (Y_{sa})_{\max}/\omega^2 = 331.53/\omega^2 \text{ inches.} \quad (6.3.3)$$

These formulas generated the simplified response spectrum shown in Figure 6.2.

In order to use Figure 6.2 to verify the one, two and three degree of freedom vessel-drydock models, some manipulation must be performed. This is because the linear equations of motion of the models do not exactly match those of the system pictured in Figure 6.1. Examining the one degree of freedom linear equation of motion (Equation 4.2.7);

$$I_k \ddot{\theta} + 2\xi I_k \omega_n \dot{\theta} + [(B^2/2)K_{sv} - W\overline{KG}] \theta = -M \overline{KG} \ddot{x}_g$$

or

$$\ddot{\theta} + 2\xi \omega_n \dot{\theta} + ((B^2/2)K_{sv} - W \overline{KG})/I_k \theta = -(M \overline{KG}/I_k) \ddot{x}_g.$$

The natural frequency for the above equation is defined as

$$\omega_n^2 = ((B^2/2)K_{sv} - W \overline{KG})/I_k.$$

Using Figure 6.2, this frequency gives a corresponding u_{\max} .

Hence, the maximum rotational response of the system, θ_{\max} , is then determined by the relation

$$\theta_{\max} = M \overline{KG}/I_k u_{\max}.$$

Table 6.1 lists the maximum rotational response for the eleven configurations found in Section 5.

TABLE 6.1

One Degree of Freedom Vessel-Drydock System
Maximum Response Using Response Spectrum Analysis

System	ω_n (rad/sec)	θ_{max} (rads.)
1	5.580	0.01594
2	3.933	0.02619
3	4.141	0.02149
4	2.870	0.03100
5	2.870	0.03100
6	10.254	0.00698
7	8.327	0.00860
8	7.255	0.00987
9	6.147	0.01445
10	7.253	0.01299
11	6.498	0.01450

The response spectrum analysis to the two and three degree of freedom systems is applied by means of the modal method described in reference [2]. Concisely, the modal method requires that the system natural modes be determined. Then, the response of the system to a known forcing input can be developed by mode superposition. Treating each natural mode as a single degree of freedom system with its own natural frequency, this method is good for simplifying seismic response analysis. Since each natural mode acts as a separate system, the maximum response may be determined. Then, a conservative estimate for the maximum response of the original system can be made by adding up the maximum response of each mode.

The method of adding maximum modal responses gives an upper bound for the maximum system response. Since there is a known response spectrum, the amount in which each natural mode contributes to the maximum response for a given input can be

determined. This is known as the participation factor of each given mode. A full description and derivation of participation factors including implementation techniques can be found in reference [2], and will not be presented here. The participation factor for each natural mode in the two and three degree of freedom case is calculated to confirm computer generated results of maximum responses in Appendix 3.

6.4 Vessel Response: Quasi-Static Force Analysis

As described in Section 4.1, the quasi-static force method replaces the earthquake motions by a force corresponding to the vessel mass times 0.2g. This analysis only allows rotation about the vessel's keel hence, the quasi-static force analysis is itself a one degree of freedom model with system response, in radians, determined by Equation 4.1.4, i.e.

$$\theta = M_S / L^2 K_{SV}$$

where $M_S = 448 * \Delta * \overline{KG}$

Δ = displacement in tons

$L = B/2$.

The results of this method are listed in Table 6.2.

TABLE 6.2

System Response using Quasi-Static Force Analysis

<u>SYSTEM</u>	<u>θ, IN RADIANS</u>
1	0.00809
2	0.01564
3	0.01422
4	0.02749
5	0.02749
6	0.00199
7	0.00300
8	0.04419
9	0.00670
10	0.00051
11	0.00637

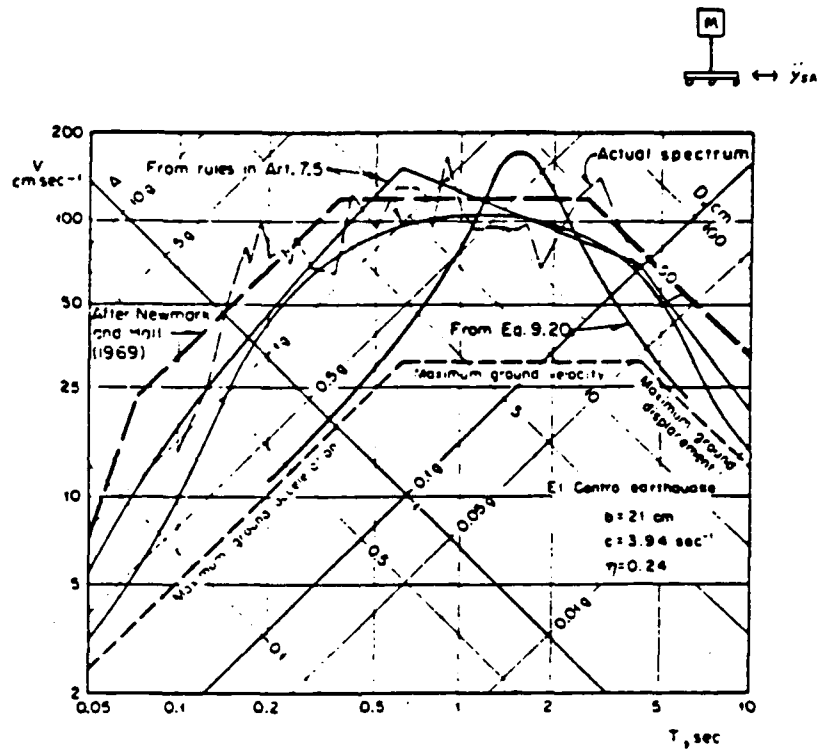


FIGURE 6.1
 Actual El Centro Earthquake Response Spectrum

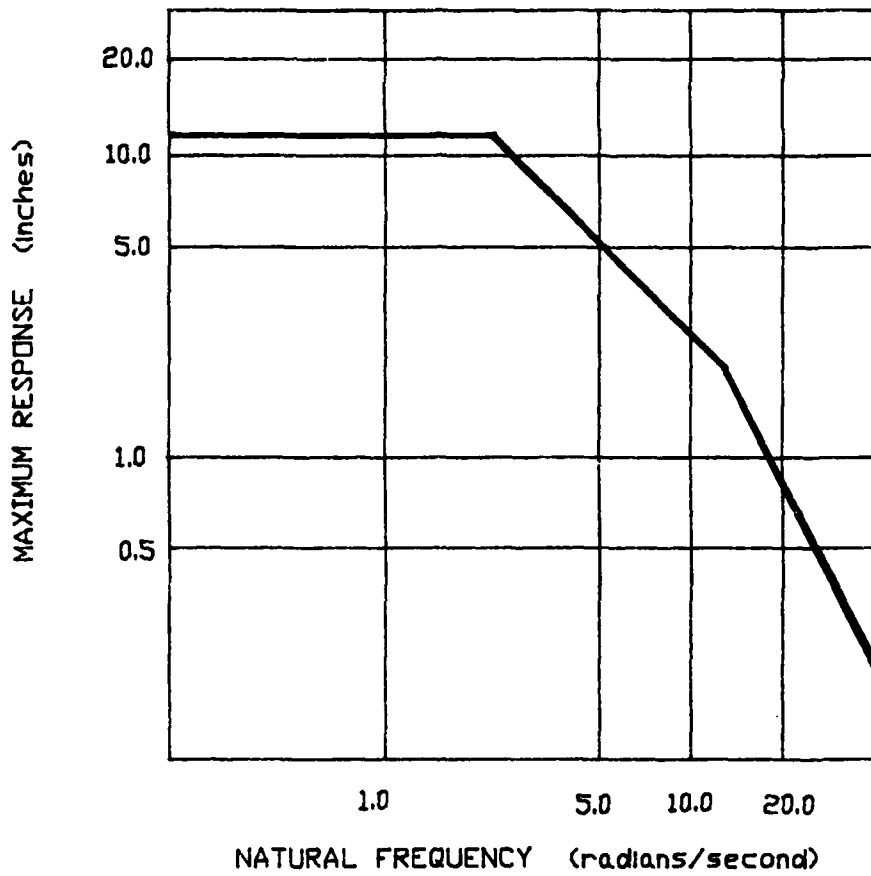


FIGURE 6.2
Idealized El Centro Earthquake Response Spectrum, 5% Damping

7.0 COMPUTER SOLUTIONS

In this section of the thesis, the computer programs needed to implement the mathematical models and the associated seismic response are developed. Due to the numerous iterations that is required for the modal analysis and Runge-Kutta methods to effectively determine vessel-drydock response, all computer work is performed at the MIT Joint Computer Facility (JCF). The required computer programs are written in Fortran 77.

In order to check the computer generated results, the vessel-drydock mathematical models are subjected to a sinusoidal earthquake input. The advantage being that closed form solutions of responses to sinusoidal inputs can be calculated. Thus, closed form response can be compared to the computer generated responses.

Upon obtaining the correct results for a sinusoidal earthquake, the El Centro earthquake's acceleration time history is applied to the vessel-drydock system. The maximum value of these computer generated results is compared to the maximum response for the system predicted by the response spectrum method found in Section 6.3.

7.1 Modal Analysis Solution

7.1.1 Computer Program Development

As described in Section 6.3, the program approaches the problem by first assembling matrices A and B. The program then uses the International Mathematical and Statistical Library (IMSL) subroutine EIGZF resident on JCF to perform the

system free vibration eigenvalue problem on matrices A and B. The output of subroutine EIGZF is the modal matrix [ψ] of the vessel-drydock system. Reference [4] contains further information about subroutine EIGZF.

The equations of motion can now be de-coupled by using the modal matrix. De-coupling the equations of motion leaves equations of the form

$$a_{ii} \ddot{z}_i(t) + b_{ii} \dot{z}_i(t) = N_i(t) , \quad i = 1, m$$

where m is equal to twice the number of the particular degree of freedom model, i.e. for the one degree of freedom $m = 2$. The solution to the above equation is

$$z_i(t) = \frac{1}{a_{ii}} \int_0^t e^{-b_{ii}/a_{ii}(t-\tau)} N_i(\tau) d\tau, \quad i = 1, m,$$

where a_{ii} and b_{ii} represent the diagonal elements of the diagonalized A and B matrices, respectively. The integral

$$\int_0^t e^{-b_{ii}/a_{ii}(t-\tau)} N_i(\tau) d\tau$$

can be evaluated using Simpson's rule, which is

$$\begin{aligned} \Sigma A_i(t) = & [(A_i(t - 2\Delta\tau) + N_i(t - 2\Delta\tau))e^{-(b_{ii}/a_{ii})2\Delta\tau} \\ & + 4N_i(t - \Delta\tau)e^{-(b_{ii}/a_{ii})\Delta\tau} + N_i(t)] \end{aligned}$$

where $\Delta\tau$ = data time increments

and $A(t - 2\Delta\tau) = \Sigma A(t)$ evaluated two time increments previously.

The value $z_i(t)$ is evaluated as

$$z_i(t) = (1/a_{ii})(\Delta\tau/3)(\Sigma A_i(t)), \quad i = 1, m.$$

To obtain the values of the system response for a particular time, the relationship

$$\{Y\} = [\psi] \{z\}$$

where $\{Y\}$ = system response vector is used, using the column vector $\{z\}$ for the time at which results are desired. The values of block forces caused by the system response are calculated every 0.02 seconds for the first 30 seconds of the earthquake. Only the first 30 seconds are needed due to the nature of the El Centro earthquake the seismic acceleration after 30 seconds are small when compared to the first 30 seconds. The resultant block forces and vessel motions are then checked against failure criteria established in Section 3. The amplitude of the seismic acceleration is reduced until no block failure occurs. Hence, the maximum earthquake acceleration, in g's, that the vessel-drydock system can withstand without failure can be found.

The three degree of freedom vessel response computer program is listed in Appendix 1. Since all three linearized models found in Equations 4.2.8, 4.3.11 and 4.4.11 are in the form

$$[A]\dot{\{Y\}} + [B]\{Y\} = \{E(t)\},$$

the three degree of freedom computer program is modified to give the one and two degree model results.

7.1.2 Computer Program Input

The computer program listed in Appendix 1 evaluates the horizontal and vertical translations and rotation of the three degree of freedom vessel-drydock system in increments of 0.02 seconds. The program requires the following input: vessel

weight, WEIGHT, in kips, keel to center of gravity height (\overline{KG}), H, in inches, vessel mass moment of inertia about the keel, I_K , in kip-in-sec², time increments of ground acceleration data, DTAU, in seconds, side and keel piers vertical and horizontal stiffnesses, K_{sv} , K_{kv} , K_{sh} , and K_{kh} , in kips/inch, gravitational constant, GRAVITY, in inch/sec², side and keel pier dimensions of width and height, BASE SIDE, BASE KEEL, HTSIDE and HTKEEL, in inches, the coefficient of friction between the block-block and ship-block interfaces, U1 and U2, horizontal distance between the center of vessel contact with port and starboard side piers, BR, in inches, vertical/horizontal ground acceleration ratio, AMP, proportional limits of side and keel block materials, PLSIDE and PLKEEL, in kips/in², total cross-sectional area of side and keel piers, SIDE AREA and KEEL AREA, in in², percent critical damping, ZETA, vessel hull number, HULL, and finally the vessel-drydock configuration number, NSYS. The following is where these inputs can be found:

Table 5.1	NSYS and HULL
Table 5.2	WEIGHT, H, I_K , and BR
Table 5.3	BASESIDE, BASEKEEL, HTSIDE, SIDEAREA and KEELAREA
Table 5.4	K_{kv} , K_{sv} , K_{kh} and K_{sh} .

The rest of the inputs are assumed to be

$$\text{GRAVITY} = 384 \text{ in/sec}^2$$

$$U1 = U2 = 0.5$$

$$\text{PLSIDE} = \text{PLKEEL} = 0.7 \text{ kips/in}^2$$

and AMP = 0.5.

The value of 0.5 for the vertical/horizontal ground acceleration ratio (AMP) parameter is used because no vertical component of the El Centro earthquake acceleration was available at the time of this thesis.

Damping coefficients equal to 5% of critical damping (i.e. ZETA = 0.05) are assumed for the entire system. This analysis for damping coefficients can be found in Appendix 3 and is implemented directly into the computer program.

Certain idealized system failure criteria from Section 3 need to be modified to accurately represent the vessel-drydock system as it actually exists. As stated in Section 3.1, block crushing occurs when the stress on the block exceeds the block's proportional limit. The vessel rests upon soft wood caps placed on top of the keel and side piers when in the drydock cradle. Crushing of the cap is not considered a failure due to its small size. For the blocking system considered, the generated stresses are transferred through the cap to the top drydock block.

Also, a side pier cannot tip inboard because the vessel hull is not physically attached to the pier and cannot pull the pier beyond its upright position. The softwood cap on top of the side pier causes the vessel force to be applied 12 inches from the inboard edge. As shown in Figure 7.3, this causes the static force vector to fall outside of the middle one-third of the pier base, as discussed in Section 3. Since the pier will only tip in the outboard direction, the resultant vessel force must fall in the outboard one-third of

the pier base. Thus, this failure criteria (from Figure 7.3) for the side pier is

$$\frac{\text{HORIZONTAL FORCE}}{\text{VERTICAL FORCE}} < \frac{2/3 \text{ Width} - 120}{\text{Pier Height}} .$$

7.1.3 Computer Program Testing

In order to validate the modal analysis method, the one degree of freedom mathematical model is checked with a set of sinusoidal ground accelerations for input. The input ground motion was

$$E(\tau) = \ddot{x}_g = 323.95 \sin(3.92\tau). \quad (7.1.1)$$

This sample function is selected because its magnitude and frequency closely match that of the maximum acceleration portion of the El Centro earthquake. Also, vessel-drydock system configuration #1 is chosen for this initial analysis. The results of the one degree of freedom case will be compared to the closed form solution.

The one degree of freedom linear equation of motion (Equation 4.2.7) is of the form

$$\ddot{\theta} + 2\xi\omega_n \dot{\theta} + \omega_n^2 \theta = -\frac{M \overline{KG}}{I_k} E(\tau).$$

The closed form solution of this equation is

$$\begin{aligned} \theta(t) &= -\frac{M \overline{KG}}{I_k \omega_d} \int_0^t E(\tau) e^{-\xi\omega_n(t-\tau)} \sin\omega_d(t-\tau) d\tau \\ &= -\frac{M \overline{KG}}{I_k \omega_d} [A(t) \sin\omega_d t - B(t) \cos\omega_d t] \end{aligned} \quad (7.1.2)$$

where

$$A(t) = \int_0^t E(\tau) \frac{e^{-\xi\omega_n t} \cos\omega_d \tau}{e^{-\xi\omega_n \tau}} d\tau$$

$$\text{and } B(t) = \int_0^t E(\tau) \frac{e^{\xi \omega_n \tau}}{e^{\xi \omega_n t}} \sin \omega_d \tau \, d\tau.$$

The results of a computer run with vessel-drydock system #1 and sinusoidal excitation (Equation 7.1.1) indicate that the maximum rotation angle θ is 0.038243 radians at a time of 2.02 seconds. To confirm this value, Equation 7.1.2 has to be evaluated

$$\theta(2.02) = -\frac{M \overline{KG}}{I_k \omega_d} [A(2.02) \sin \omega_d(2.02) - B(2.02) \cos \omega_d(2.02)]$$

$$\text{where } A(2.02) = \int_0^{2.02} 323.95 \sin(3.92\tau) \frac{e^{\xi \omega_n \tau}}{e^{2.02 \xi \omega_n}} \cos \omega_d \tau \, d\tau$$

$$\text{and } b(2.02) = \int_0^{2.02} 323.95 \sin(3.92\tau) \frac{e^{\xi \omega_n \tau}}{e^{2.02 \xi \omega_n}} \sin \omega_d \tau \, d\tau.$$

From Section 6.3,

$$\begin{aligned} \omega_n &= [((B^2/2)K_{sv} - W \overline{KG})/I_k]^{1/2} \\ &= 5.580 \text{ rad/sec} \end{aligned}$$

$$\begin{aligned} \text{and } \omega_d &= \omega_n(1 - \xi^2)^{1/2} \\ &= 5.573 \text{ rad/sec.} \end{aligned}$$

With these values of natural and damped natural frequencies, the value of $A(2.02)$ can be evaluated using the relationship

$$\int_0^t e^{at} \sin bt \cos ct \, dt = e^{at} \frac{[a \sin(b-c)t - (b-c) \cos(b-c)t]}{2[a^2 + (b-c)^2]} + e^{at} \frac{[a \sin(b+c)t - (b+c) \cos(b+c)t]}{2[a^2 + (b+c)^2]} \Big|_0^t$$

Substituting the values

$$t = 2.02$$

$$a = \omega_n = .279$$

$$b = 3.92$$

and $c = \omega_d = 5.573$

The value of $A(2.02)$ becomes

$$323.95(e^{-.5636})^{-1} * -.8307 = -153.1629$$

Similarly, for $B(2.02)$,

$$\int_0^t e^{at} \sin bt \sin ct \, dt = e^{at} \frac{[(b-c) \sin(b-c)t + c \cos(b-c)t]}{2[a^2 + (b-c)^2]} - e^{at} \frac{[(b+c) \sin(b+c)t + c \cos(b+c)t]}{2[a^2 + (b+c)^2]} \Big|_0^t$$

with the same values of a , b and c as before.

Evaluating, $B(2.02)$ becomes

$$323.95 (e^{-.5636})^{-1} * -.2191 = -40.3973$$

Now,

$$\theta(2.02) = \frac{1}{2.54} * \frac{42.6979 * 193.0}{2411000. * 5.573} [-153.1629 * \sin(2.02 * 5.573) - (-40.3973 * \cos(2.02 * 5.573))]$$

$$= .038247 \text{ radians.}$$

Comparing the computer generated solution (0.038243 radians) with the closed form solution (.038247 radians), it can be seen that the computer program is calculating the one degree of freedom rotation formula correctly.

One other simple method to check to see if the rotation displacement time history is correct is to look at the waveform. At steady state condition, $\theta(t)$ will be a sinusoidal with the same frequency as the sinusoidal ground acceleration. An amplitude different and a phase shift will

be present. The steady state solution [12] of a equation of motion in the form

$$m\ddot{x} + c\dot{x} + kx = F \sin\omega t$$

is

$$x = \frac{|F|}{k} = \frac{1}{\sqrt{(1-r^2)^2 + (2\xi r)^2}} \sin\left(\omega t - \tan^{-1} \frac{2\xi r}{1-r^2}\right)$$

where

$$r = \omega/\omega_n$$

$$\omega_n = (k/m)^{1/2} = \text{Natural Frequency}$$

$$\xi = 1/2 c/\sqrt{km} = \text{percent critical damping.}$$

In this case,

$$\omega_n = 5.580 \text{ rad/sec}$$

$$r = 3.92/5.580 = .703$$

$$\xi = .05$$

$$|F| = M \overline{KG} \frac{|\ddot{x}_g|}{2.54} = 1051012.9 \text{ lb.in}$$

$$k = 75071464 \text{ lb in.}$$

so now,

$$e \text{ steady state} = .027402 \sin(3.92t - .1381) \text{ radians (7.1.3)}$$

Figure 7.1 represents the sinusoidal ground acceleration (Equation 7.1.1) and Figure 7.2 which represents the rotation, $\epsilon(t)$, of the vessel-drydock system as generated by the modal analysis computer program. Note the same frequency between Figures 7.1 and 7.2. The steady state portion of Figure 7.2 is matched to Equation 7.1.3. In conclusion the model analysis method correctly predicts the one degree of freedom mathematical model.

7.1.4 Computer Program Results

The modal analysis method can now be used with the El Centro earthquake data to predict the system response. Eleven vessel-drydock configurations (Section 5.0) are analyzed for maximum ground acceleration that the system can withstand without block failure. Also, the first block failure modes exhibited by the systems are found.

For the eleven vessel-drydock systems, the linearized one, two and three degree of motion mathematical model responses are calculated and listed in Table 7.3, 7.4, and 7.5, respectively. These tables can be found on pages 91 thru 93. The program further calculates that vessel liftoff (Section 3.4) will be the first failure mode to occur when ground accelerations are greater than the maximum permissible ground acceleration listed in Table 7.3, 7.4, and 7.5. The maximum permissible ground acceleration is based on the reduction of the El Centro acceleration amplitude until no failure occur. However, the waveform remains unchanged.

In order to get a visual picture of the various responses, vessel-drydock system #1 is selected to be plotted. Figures 7.4; 7.5a and b and 7.6a, b, and c are the appropriate responses for the one, two and three degree of freedom models. Only the first thirty seconds of the earthquake are required to give the maximum system response as seen by the plots. Note that the relative horizontal displacement (Figure 7.6a) and rotation (7.6b) time histories of the three degree of freedom model are indential to the ones found in the two degree of freedom model. This is due to the uncoupled

vertical equation of motion found in the linearized three degree of freedom case.

As a check for the computer generated results, the system maximum responses due to full magnitude El Centro earthquake accelerations are compared to the system maximum responses determined by response spectrum analysis in Table 7.1 and 7.2. These tables are generated by combining the computer results of various models and Tables 6.1 (Section 6.3) and A.3.3 (Appendix 3). Since the response spectrum method is an approximate one (Section 6.3), the maximum 20% error between its results and the computer results in the one degree of freedom case is reasonable. Thus, the one degree program is generating accurate results.

In the two degree of freedom case, the response spectrum method predicts the worst case if the system's two natural modes reach a maximum at the same time, and add together. This happened in the rotational case, but only twice in the relative displacement case. In the majority of the systems, the computer generated rotational response actually exceeded the rotational response predicted by modal analysis. The maximum 35% difference between the two results can be accounted for because of the approximate, simplified response spectrum mentioned earlier. The three degree of freedom case has the same order of error as found in the two degree case as shown in Table 7.2. Hence, all mathematical models perform satisfactory using the modal analysis computer program.

TABLE 7.1

One Degree of Freedom Equation of Motion Response Comparison
 Modal Analysis Computer Results of Linear System

<u>System</u>	<u> θ </u> <u>radians</u>
1	0.01474
2	0.01618
3	0.01436
4	0.02966
5	0.02966
6	0.00832
7	0.0115
8	0.01712
9	0.01512
10	0.01714
11	

Response Spectrum Method Results of Linear System

<u>System</u>	<u> θ </u> <u>radians</u>
1	0.01594
2	0.02619
3	0.02149
4	0.031
5	0.031
6	0.00698
7	0.0068
8	0.00987
9	0.01445
10	0.01299
11	0.0145

TABLE 7.2

Three Degree of Freedom Equation of Motion Response Comparison
 Modal Analysis Computer Results of Linear System

<u>System</u>	<u> x </u> <u>(inches)</u>	<u> y </u> <u>(inches)</u>	<u> θ </u> <u>(radians)</u>
1	0.27971	0.07374	0.01458
2	0.22661	0.10948	0.01636
3	0.53288	0.15395	0.01546
4	0.58122	0.18352	0.03130
5	0.24721	0.11703	0.02992
6	0.36179	0.06123	0.00814
7	0.39118	0.06870	0.00879
8	0.39889	0.07140	0.01154
9	0.61065	0.11749	0.01587
10	0.57808	0.11970	0.01547
11	0.61730	0.11676	0.01734

Response Spectrum Method Results of Linear System

<u>System</u>	<u> x </u> <u>(inches)</u>	<u> y </u> <u>(inches)</u>	<u> θ </u> <u>(radians)</u>
1	0.33275	0.10859	0.01646
2	0.27141	0.12225	0.02348
3	0.65142	0.19089	0.02350
4	0.53788	0.21491	0.02350
5	0.21468	0.12980	0.03202
6	0.45271	0.08025	0.00683
7	0.46833	0.09708	0.00866
8	0.46597	0.10762	0.01009
9	0.64366	0.15381	0.01552
10	0.65864	0.13662	0.01342
11	0.67467	0.14955	0.01552

NOTE: Two Degree of Freedom System Maximum Response correspond to x and θ .

7.2 Fourth Order Runge-Kutta Analysis Solution

7.2.1 Computer Program Development

As described in Section 6.2, the Runge-Kutta scheme uses a set of first order differential equations to describe the second order vessel-drydock system. A simple example of this procedure is done on the following equation

$$m\ddot{x} + c\dot{x} + kx = f(t) + g(t)x$$

let $r = \dot{x}$ and rearranging yields two first order equations,
 $\dot{x} = r$

$$\dot{r} = -\frac{c}{m} r - \frac{k}{m} x + f(t) + g(t)x$$

Now, the first order system can be implemented into a computer program.

Briefly, the fourth order Runge-Kutta numerical scheme is one that makes use of predicted velocity and acceleration at a given time to compute the displacement and velocity for the next time increment. This can be done by the basic relationships

$$x_{n+1} = x_n + \dot{x}_n \Delta t$$

and
$$\dot{x}_{n+1} = \dot{x}_n + \ddot{x}_n \Delta t$$

However, \dot{x} and \ddot{x} are not found by differentiation but through the manipulations of the second order equation into a set of first order equations. This can be done by procedure shown in the previous paragraph.

The first step in the computer program development is to place the set of first order differential equations into the Runge-Kutta formulas shown in Section 6.2. The evaluation of these formulas will predict the velocity and acceleration

that will be used in the next time increment. Now, the system response, both displacements and associated velocities, can be calculated using the previous information. This process is marched through time steps in our to produce a time history of the system response.

Now, the values of block forces caused by the system response are calculated every 0.01 seconds for the first 30 seconds of the earthquake. The first 30 seconds are only required to analyze for maximum seismic response. The resultant block forces and vessel motions are then checked against failure criteria found in Section 3. The amplitude of the seismic acceleration is reduced until no block failure occurs. Like in the modal analysis method (Section 7.1), the maximum earthquake acceleration, in g's, that the vessel-drydock system can withstand without failure can be found.

The Runge-Kutta analysis gives the ability to analyze both the linear and non-linear equations of motion for the one, two and three degree of motion mathematical models. The non-linear three degree of freedom vessel response computer program is listed in Appendix 2. The program is developed around Equations 4.4.5, 4.4.6 and 4.4.8 and those found in Section 6.2. Since all linear and non-linear models developed in this thesis can be arranged into the Runge-Kutta formulas, the non-linear three degree of freedom computer program is modified to give desired model results.

7.2.2 Computer Program Input

The computer program listed in Appendix 2 evaluates the horizontal and vertical translations and rotation of the non-linear three degree of freedom vessel-drydock system in increments of 0.01 seconds. The program requires the identical input found in Section 7.1.2 for the modal analysis method. Hence, the program inputs needs not be listed again. Like in the previous case, Appendix 3 provides the damping coefficients to be implemented into the computer program.

7.2.3 Computer Program Testing

In order to validate the fourth order Runge-Kutta numerical scheme, the linear one degree of freedom mathematical model is checked with a set of sinusoidal ground accelerations for input. The same input ground motion that is used to validate the modal analysis is implemented in this case, i.e.

$$E(\tau) = \ddot{x}_g = 329.95 \sin(3.92t). \quad (7.2.1)$$

This sample function is selected because its magnitude and frequency closely match that of the maximum acceleration portion of the El Centro earthquake. Also, vessel-drydock system configuration #1 is chosen for this initial analysis. The results of the linearized one degree of freedom case will be compared to the modal analysis and closed form solutions.

The results of a computer run with vessel-drydock system #1 and sinusoidal excitation (Equation 7.2.1) indicate that the maximum rotation angle θ is 0.038236 radians at a time of 2.02 seconds. Comparing this the computer generated solution with the modal analysis solution (0.038243 radians) and the

closed form solution (0.038247 radians) found in Section 7.1.3, it can be seen that the computer program is calculating the linearized one degree of freedom rotation formula correctly. Also, Figure 7.7 which represents the rotation, θ (t), of the vessel-drydock system as generated by the Runge-Kutta computer program is essentially identical to Figure 7.2 generated by the modal analysis computer program.

In conclusion, the fourth order Runge-Kutta method correctly predicts the linearized one degree of freedom mathematical model. Now, the computer program will be used for the linear and non-linear one, two and three degree of freedom systems.

7.2.4 Computer Program Results

The fourth order Runge-Kutta analysis can be implemented with the El Centro earthquake data to predict the system response. Eleven vessel-drydock configurations (Section 5.0) are analyzed for maximum ground acceleration that the system can withstand without block failure. Also, the first block failure modes exhibited by the systems are found.

For the eleven vessel-drydock systems, the linear and non-linear one, two and three degree of motion mathematical model responses are calculated and listed in Table 7.3, 7.4 and 7.5, respectively. These tables can be found on pages 91 thru 93. The program further calculates that vessel liftoff (Section 3.4) will be the first failure mode to occur when ground accelerations are greater than the maximum permissible ground acceleration listed in Table 7.3, 7.4 and 7.5.

In order to get a visual picture of the various linear and non-linear responses, vessel-drydock system #1 is selected to be plotted. Figures 7.8, 7.9 a and b, 7.10 a, b and c are the appropriate response for the linear one, two and three degree of freedom models and Figures 7.11, 7.12a and b and 7.13 a, b and c are for the non-linear models. Note that these figures are almost identical to Figures 7.3, 7.4a and b and 7.5 a, b and c generated by the modal analysis method (Section 7.1.5). This reinforces the equivalency of the results found by the two numerical schemes. This can also be seen by comparing the system maximum responses of the Runge-Kutta method to that of the modal analysis method. Both are listed in Table 7.3, 7.4 and 7.5. The maximum error for any given case is 5%. Hence, all mathematical models perform satisfactory using the fourth order Runge-Kutta computer program.

TABLE 7.3

Modal Analysis Method Results of Linear System

System	θ_{\max} (radians)	Time (sec)	Maximum Acceleration (g's)
1	0.003390	6.64	0.0759
2	0.003883	9.28	0.0792
3	0.006033	9.22	0.1368
4	0.006822	8.68	0.0759
5	0.004513	8.68	0.0462
6	0.001999	5.36	0.0792
7	0.002422	5.84	0.0924
8	0.002760	8.98	0.0792
9	0.005138	7.54	0.0990
10	0.004537	8.98	0.0990
11	0.004972	7.92	0.0957

4th Order Runge-Kutta Numerical Method Results of Linear System

System	θ_{\max} (radians)	Time (sec)	Maximum Acceleration (g's)
1	0.003390	6.64	0.0759
2	0.003882	9.27	0.0792
3	0.006032	9.22	0.1386
4	0.006822	8.68	0.0759
5	0.004153	8.68	0.0462
6	0.002004	5.35	0.0792
7	0.002426	5.83	0.0924
8	0.002763	8.97	0.0792
9	0.005141	7.54	0.0990
10	0.004543	8.98	0.0990
11	0.004972	7.92	0.0957

4th Order Runge-Kutta Numerical Method Results of
Non-Linear System

System	θ_{\max} (radians)	Time (sec)	Maximum Acceleration (g's)
1	0.003391	6.64	0.0759
2	0.003883	9.27	0.0792
3	0.006032	9.23	0.1386
4	0.006825	8.68	0.0759
5	0.004154	8.68	0.0462
6	0.002004	5.35	0.0792
7	0.002427	5.83	0.0924
8	0.002764	8.97	0.0792
9	0.005139	7.54	0.0990
10	0.004546	8.98	0.0990
11	0.004970	7.91	0.0957

TABLE 7.4
Two Degree of Freedom Equation of Motion Response
Modal Analysis Method Results of Linear System

System	x_{\max} (inches)	Time (seconds)	θ_{\max} (radians)	Time (seconds)	Maximum Acceleration (g's)
1	0.064335	8.38	0.003355	9.02	0.0759
2	0.063873	5.38	0.003927	9.26	0.0792
3	0.207826	5.42	0.006033	9.24	0.1287
4	0.127868	5.72	0.006887	8.66	0.0726
5	0.032138	5.80	0.003891	8.72	0.0429
6	0.090448	5.78	0.002037	5.36	0.0825
7	0.109531	5.46	0.002463	5.86	0.0924
8	0.095734	5.98	0.002770	7.82	0.0759
9	0.195410	6.06	0.005080	7.60	0.1056
10	0.167644	6.04	0.004487	7.84	0.0957
11	0.172847	6.08	0.004856	7.54	0.0924

4th Order Runge-Kutta Numerical Method Results of Linear System

System	x_{\max} (inches)	Time (seconds)	θ_{\max} (radians)	Time (seconds)	Maximum Acceleration (g's)
1	0.064566	8.38	0.003358	9.02	0.0759
2	0.064934	5.38	0.003927	9.26	0.0792
3	0.207015	5.56	0.006034	9.24	0.1287
4	0.127317	5.72	0.006890	8.66	0.0726
5	0.032442	5.80	0.003891	8.72	0.0429
6	0.090984	5.78	0.002048	5.36	0.0825
7	0.110229	5.46	0.002466	5.86	0.0924
8	0.091996	5.98	0.002656	7.81	0.0759
9	0.194354	6.06	0.005074	7.59	0.1056
10	0.166760	6.03	0.004493	7.83	0.0957
11	0.174626	6.07	0.004860	7.55	0.0924

4th Order Runge-Kutta Numerical Method Results of Non-Linear System

System	x_{\max} (inches)	Time (seconds)	θ_{\max} (radians)	Time (seconds)	Maximum Acceleration (g's)
1	0.064597	8.38	0.003358	9.02	0.0759
2	0.064839	5.38	0.003926	9.26	0.0792
3	0.206443	5.56	0.006035	9.24	0.1287
4	0.127281	5.72	0.006892	8.66	0.0726
5	0.032442	5.80	0.003891	8.72	0.0429
6	0.090984	5.78	0.002048	5.36	0.0825
7	0.110274	5.46	0.002467	5.86	0.0924
8	0.092031	5.98	0.002656	7.81	0.0759
9	0.194361	6.06	0.005075	7.59	0.1056
10	0.166763	6.03	0.004493	7.83	0.0957
11	0.174636	6.07	0.004859	7.55	0.0924

TABLE 7.5

Three Degree of Freedom Equation of Motion Response
Modal Analysis Method Results of Linear System

System	x_{\max} (inches)	Time (sec.)	y_{\max} (inches)	Time (sec.)	θ_{\max} (radians)	Time (sec.)	Maximum Acceleration (g's)
1	0.067132	8.38	0.017698	5.68	0.003501	9.02	0.0792
2	0.061211	5.38	0.025181	8.06	0.003765	9.26	0.0759
3	0.207826	5.42	0.060041	5.64	0.006033	9.24	0.1287
4	0.122056	5.72	0.038540	5.64	0.006574	8.66	0.0693
5	0.032138	5.70	0.015215	5.38	0.003891	8.72	0.0429
6	0.090448	5.78	0.019865	5.32	0.002037	5.36	0.0825
7	0.105619	5.46	0.018550	6.68	0.002375	5.86	0.0891
8	0.091745	5.98	0.016424	5.36	0.002654	7.82	0.0759
9	0.201516	6.06	0.038773	5.80	0.005238	7.60	0.1089
10	0.161863	6.04	0.033516	5.38	0.004332	7.84	0.0924
11	0.179020	6.08	0.033861	5.40	0.005030	7.54	0.0957

4th Order Runge-Kutta Numerical Method Results of Linear System

System	x_{\max} (inches)	Time (sec.)	y_{\max} (inches)	Time (sec.)	θ_{\max} (radians)	Time (sec.)	Maximum Acceleration (g's)
1	0.067373	8.38	0.017858	5.37	0.003504	9.02	0.0792
2	0.062228	5.39	0.025102	8.06	0.003761	9.27	0.0759
3	0.207015	5.43	0.059736	5.64	0.006304	9.25	0.1287
4	0.121529	5.73	0.038651	5.65	0.006577	8.67	0.0693
5	0.032442	5.81	0.014985	5.39	0.003891	8.79	0.0429
6	0.094623	5.78	0.019463	5.77	0.002130	5.37	0.0858
7	0.106292	5.47	0.018152	6.69	0.002378	5.87	0.0891
8	0.091996	5.99	0.016558	5.37	0.002656	7.82	0.0759
9	0.200428	6.06	0.039205	5.40	0.005233	7.60	0.1089
10	0.161009	6.04	0.033887	5.39	0.004338	7.84	0.0924
11	0.180863	6.08	0.034608	5.40	0.005033	7.55	0.0957

4th Order Runge-Kutta Numerical Method Results of Non-linear System

System	x_{\max} (inches)	Time (sec.)	y_{\max} (inches)	Time (sec.)	θ_{\max} (radians)	Time (sec.)	Maximum Acceleration (g's)
1	0.067283	8.38	0.017858	5.37	0.003507	9.02	0.0792
2	0.062050	5.39	0.025102	8.06	0.003763	9.27	0.0759
3	0.206406	5.57	0.059736	5.64	0.006037	9.25	0.1287
4	0.121484	5.73	0.038651	5.65	0.006580	8.67	0.0693
5	0.032443	5.81	0.014985	5.39	0.003891	8.79	0.0429
6	0.094523	5.78	0.019463	5.77	0.002130	5.37	0.0858
7	0.106348	5.47	0.018152	6.69	0.002379	5.87	0.0891
8	0.091968	5.99	0.016558	5.37	0.002656	7.82	0.0759
9	0.200131	6.06	0.039205	5.40	0.005234	7.61	0.1089
10	0.160892	6.04	0.033887	5.39	0.004337	7.84	0.0924
11	0.180674	6.08	0.034608	5.40	0.005032	7.55	0.0957

7.3 Discussion of the Models and Associated Results

Both the modal analysis and the Runge-Kutta numerical methods give satisfactory results in determining the system maximum response in the various models and configurations. The maximum error in the comparison of the two methods for any given run is 5%. This is excellent when considering that each method has completely different basic concepts behind them. The modal analysis method runs faster to obtain the result due to less computer operations. But, the Runge-Kutta method is much easier to program into the computer and is more flexible. In all, both methods can be used to predict the seismic response of the linearized one, two and three degree of freedom models.

In the comparison of the one, two and three degree of freedom responses, certain conclusions can be drawn. The one degree of freedom model need only be used if system maximum rotational response is the main concern to drydock system design. This model gives results sufficiently close to the rotation generated by the other two models. Since vessel liftoff of the side block is the first block failure to be exhibited by the vessel-drydock system, the one degree of freedom model adequately predicts the maximum earthquake amplitude the system can withstand. Most of the vertical displacement at the side pier is due to rotation and not of relative vertical displacement as found in the three degree model. Hence, the one degree of freedom system response should be used to determine vessel rotation and maximum earthquake amplitude.

The three degree of freedom system results should be used for a parameter study on block failure modes and for block design. This is because only the three degree model produces all required displacements for estimation of generated forces in both keel and side blocks. However, when the relative vertical translations generated are small, the two degree model can be used in block design,. The one degree model is truly inadequate for block design since crushing and vessel liftoff of the side blocks are the only failure modes.

The non-linear equations of motion mathematical models needs to be addressed. As shown in Table 7.3, 7.4 and 7.5, the non-linearity of the system caused less than 1% difference between the linear and non-linear responses. Under the eleven representative vessel-drydock configurations, the non-linear terms (ie. $\dot{\gamma}\theta$ and $\ddot{\gamma}\theta$) should be removed from the equations of motion. This linearization of the equations of motion will be verified in the proceeding discussion.

The next step in the studying of the non-linearity of the system is to determine, when the non-linear terms mentioned earlier should be included in the equations of motion. The non-linear equation of motion for the one degree of freedom model is

$$\ddot{\theta} + \frac{c}{I_k} \dot{\theta} + \frac{k_1}{I_k} \theta - \frac{-M \overline{KG}}{I_k} \ddot{x}_g + \frac{M \overline{KG}}{I_k} \ddot{y}_g = \theta$$

Let $\ddot{x}_g = a \sin t$

$$\ddot{y}_g = \gamma \ddot{x}_g$$

AD-A173 312

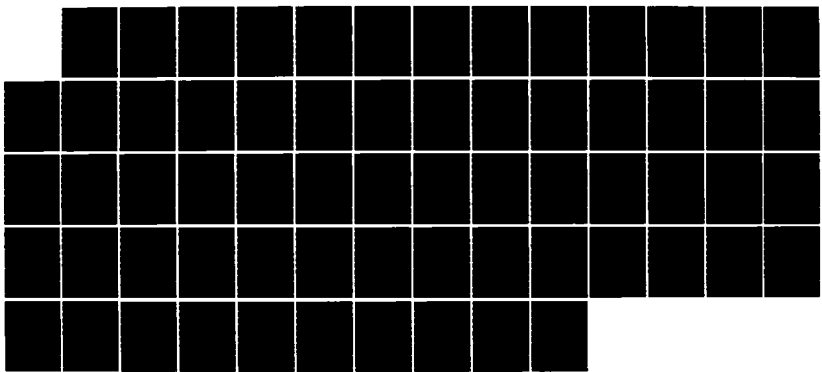
THE COUPLED THREE DEGREE OF FREEDOM MOTION RESPONSE OF
A DRYDOCKED SUBMAR. (U) MASSACHUSETTS INST OF TECH
CAMBRIDGE DEPT OF OCEAN ENGINEERIN.. D E SIGHAN JUN 86
N00228-85-G-3262

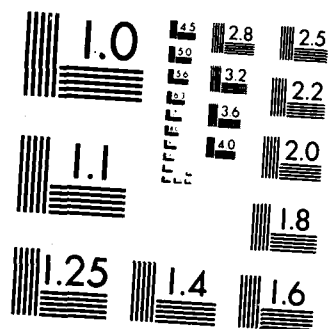
2/2

UNCLASSIFIED

F/G 13/13

NL





MICROCOPY RESOLUTION TEST CHART
NATIONAL BUREAU OF STANDARDS 1963-A

$$M \overline{KG} a/I_k = \beta$$

$$\lambda^2 = k_1/I_k$$

$$\text{and } 2\xi\lambda = C_\theta/I_k.$$

Substituting and rearranging the Equation of motion gives

$$\ddot{\theta} + 2\xi\lambda\dot{\theta} + \lambda^2\theta = -\beta \sin\omega t(1 - \gamma\theta). \quad (7.3.1)$$

where λ = system natural frequency

β = normalized maximum amplitude

γ = ratio of vertical/horizontal amplitude.

Equation 7.3.1 not only represents the vessel-drydock system but any other system than can be reduced to this form. A parameter study is performed using λ , β and γ to determine whether or not to use non-linear terms in the equations of motion. The selection criterion will be when the non-linear response (ie. $\gamma \neq 0$) is different to the linear response (ie $\gamma = 0$) by 10%. If for a given λ , β and γ this criterion is exceeded, then the non-linear term, $\gamma\theta$, should be included. If not, exclude them. For this study, let $\omega = 3.92$ rad/sec and $\xi = 0.05$ to emulate the sinusoidal excited system with 5% damping discussed in Section 7.1.3. Using a Runge-Kutta numerical scheme, Figures 7.14 a, b, c, d and e are generated by varying the three parameters. Note that a negative γ indicates a phase shift of 180° between the vertical and horizontal sinusoidal excitation. The linearity selection criterion of 10% difference holds true for the region marked "N-L" for non-linear for a given β . In the case of the one degree of freedom vessel-drydock systems, the linearizing of the equations of motion can be shown on Figure 7.14b since $\beta = 0.5$, $\gamma = 0.5$ and λ ranges from 2.870 rad/sec to 10.254 rad/sec

(Table 6.1).

In order to verify the linearity selection criterion, a linear point selected off of Figure 7.14b of $\beta = 0.5$, $\gamma = 5.58$ and $\lambda = 20.0$ is implemented into the Runge-Kutta computer program in Section 7.2. The nonlinear response equals 0.015839 radians compared to the linear response of 0.014741 radians when using the El Centro earthquake input. This is a difference of 7.5% which is less than 10%. The linearity selection criterion holds true. Now, a non-linear point of $\beta = 0.5$, $\lambda = 8.327$ and $\gamma = 15.0$ is implemented into the Runge-Kutta scheme. The non-linear and linear responses are .009652 and .008664, respectively. This is a difference of 11.4% which is greater than 10%. The linearity selection criterion is validated. Thus, vessel-drydock system should be checked before selection of linear or non-linear models.

As mentioned earlier, Equation 7.3.1 can be used to validate systems other than the vessel-drydock systems subjected to sinusoidal ground acceleration whose frequency matches that of the El Centro earthquake, ie. $\omega = 3.92$ rad/sec. this can be done by modifying the appropriate linearity selection criteria figure with

$$\lambda_1 = \lambda/3.92$$

and replotting the figure. This essentially changes Equation 7.3.1 into a non-dimensional of

$$\ddot{\theta}_1 + 2\xi\lambda_1\dot{\theta}_1 + \lambda_1^2\theta_1 = -\beta_1 \sin t_1 (1 - \gamma_1\theta_1)$$

where

$$\ddot{\theta}_1 = \ddot{\theta}/\omega^2$$

$$\dot{\theta}_1 = \dot{\theta}/\omega$$

$$\theta_1 = \theta$$

$$\lambda_1 = \lambda/\omega$$

$$\beta_1 = \beta/\omega^2$$

$$\gamma_1 = \gamma$$

$$t_1 = \omega t$$

and in this case, $\omega = 3.92$ rad/sec.

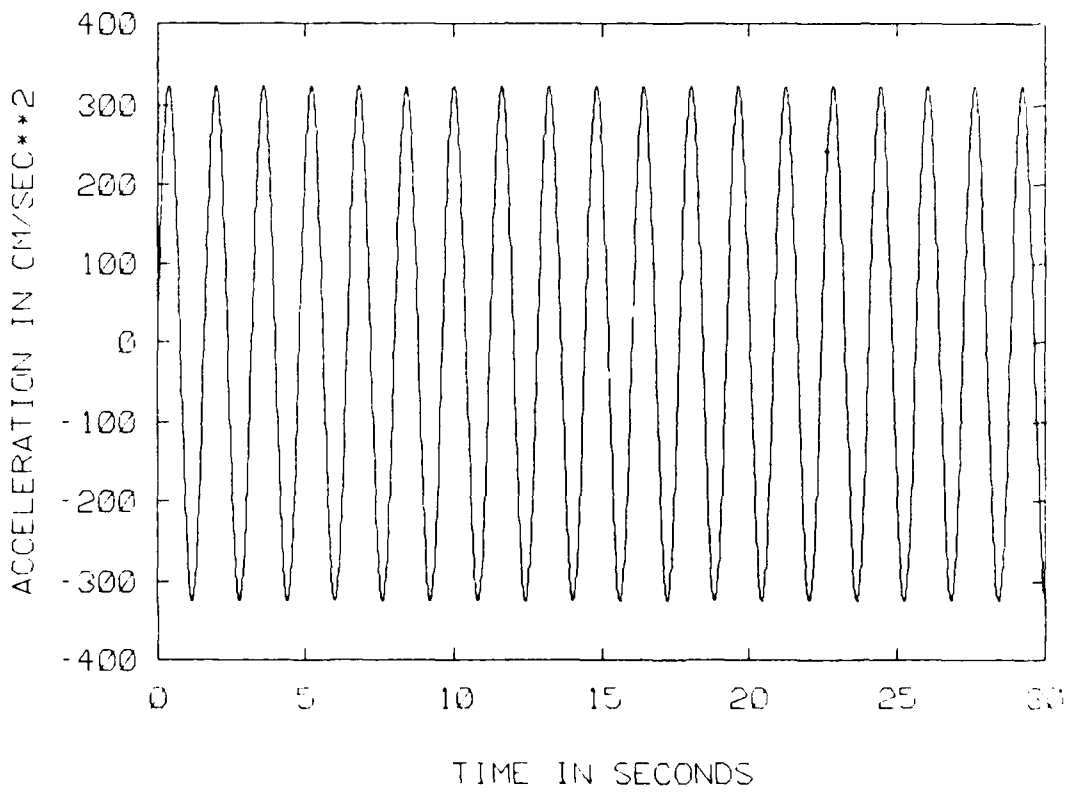


FIGURE 7.1
Sinusoidal Ground Acceleration

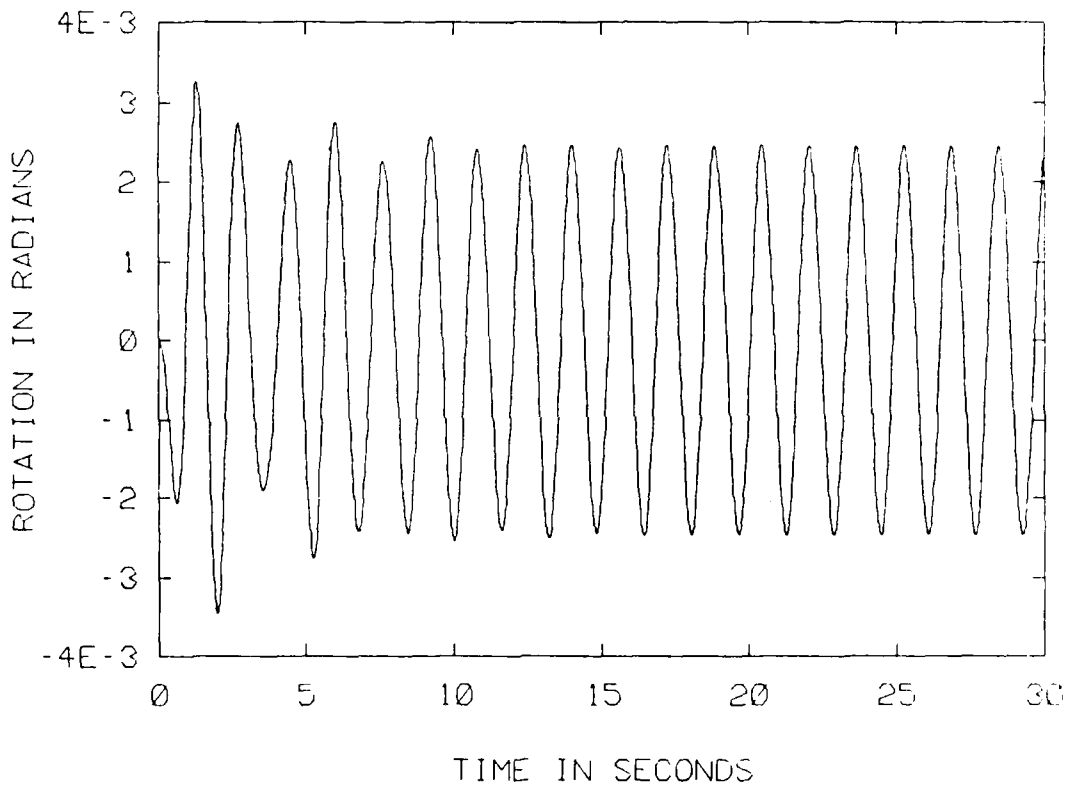


FIGURE 7.2
Vessel Seismic Response in Rotation using Modal Analysis with
Sinusoidal Ground Acceleration

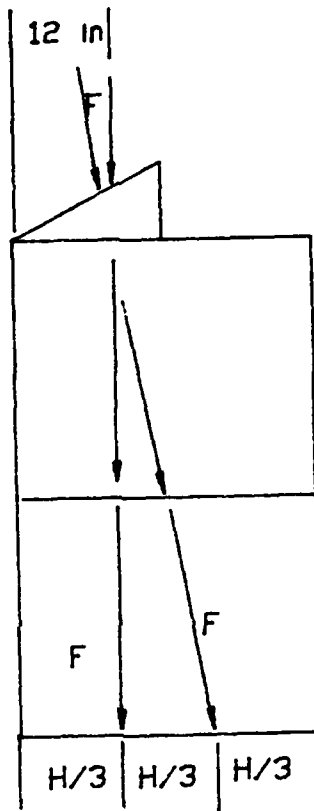


FIGURE 7.3
Side Pier Forces, with Softwood Cap Block

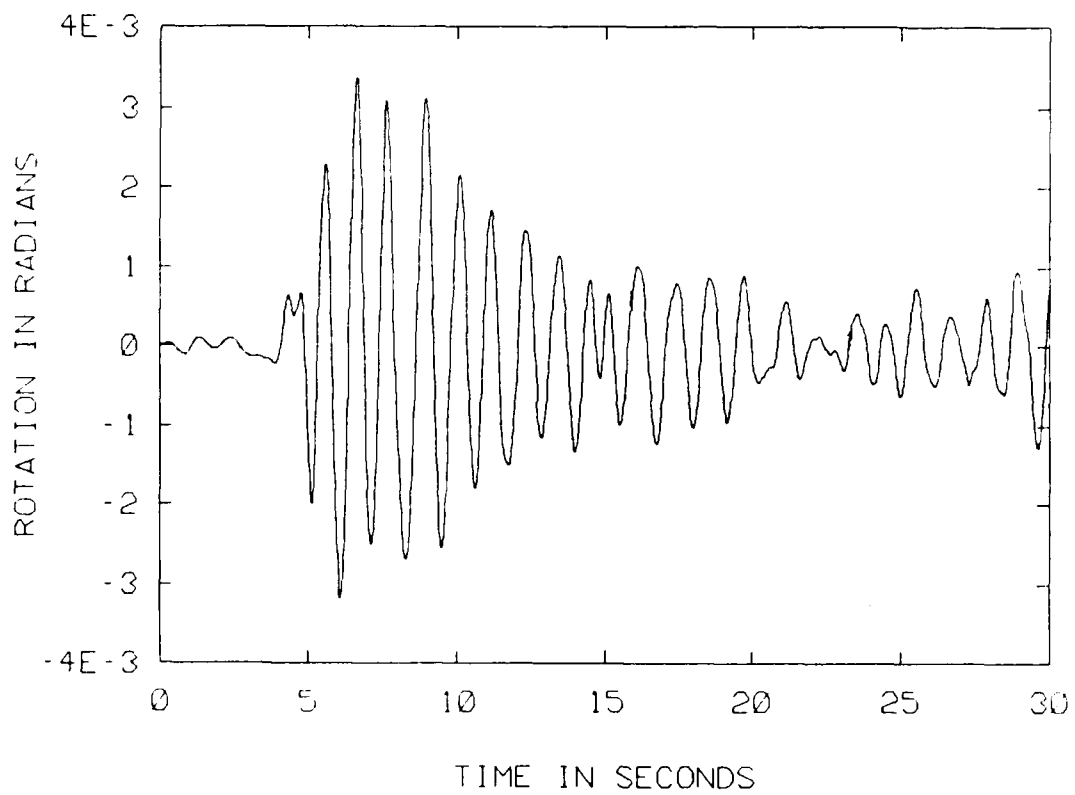


FIGURE 7.4
Vessel Seismic Response in Rotation for One Degree of Freedom
Model using Modal Analysis

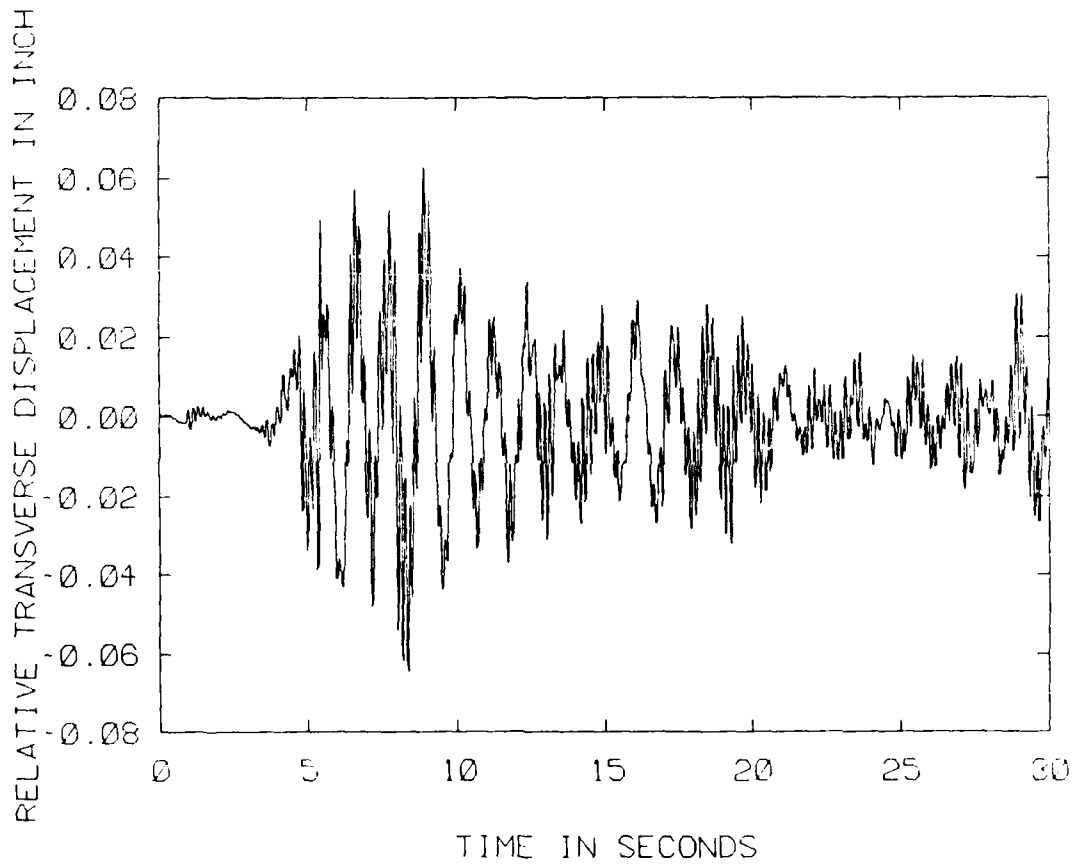


FIGURE 7.5a
Vessel Seismic Response in Relative Horizontal Translation for
Two Degree of Freedom Model using Modal Analysis

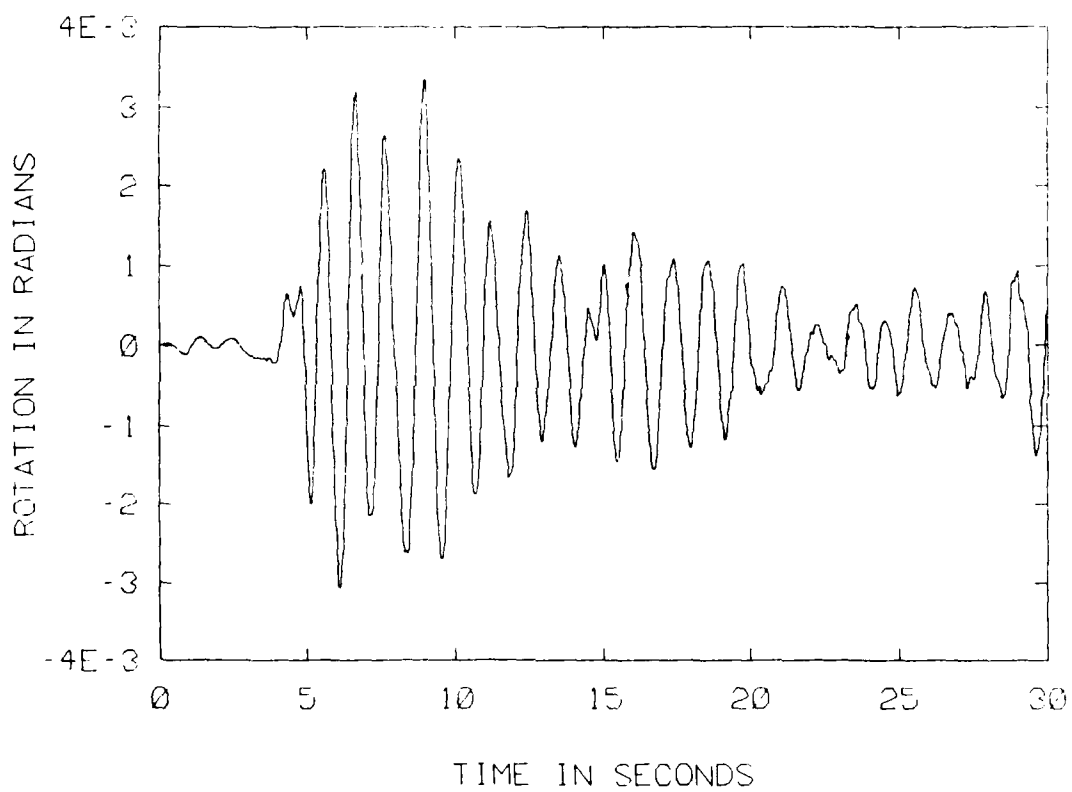


FIGURE 7.5b
Vessel Seismic Response in Rotation for Two Degree of Freedom
Model using Modal Analysis

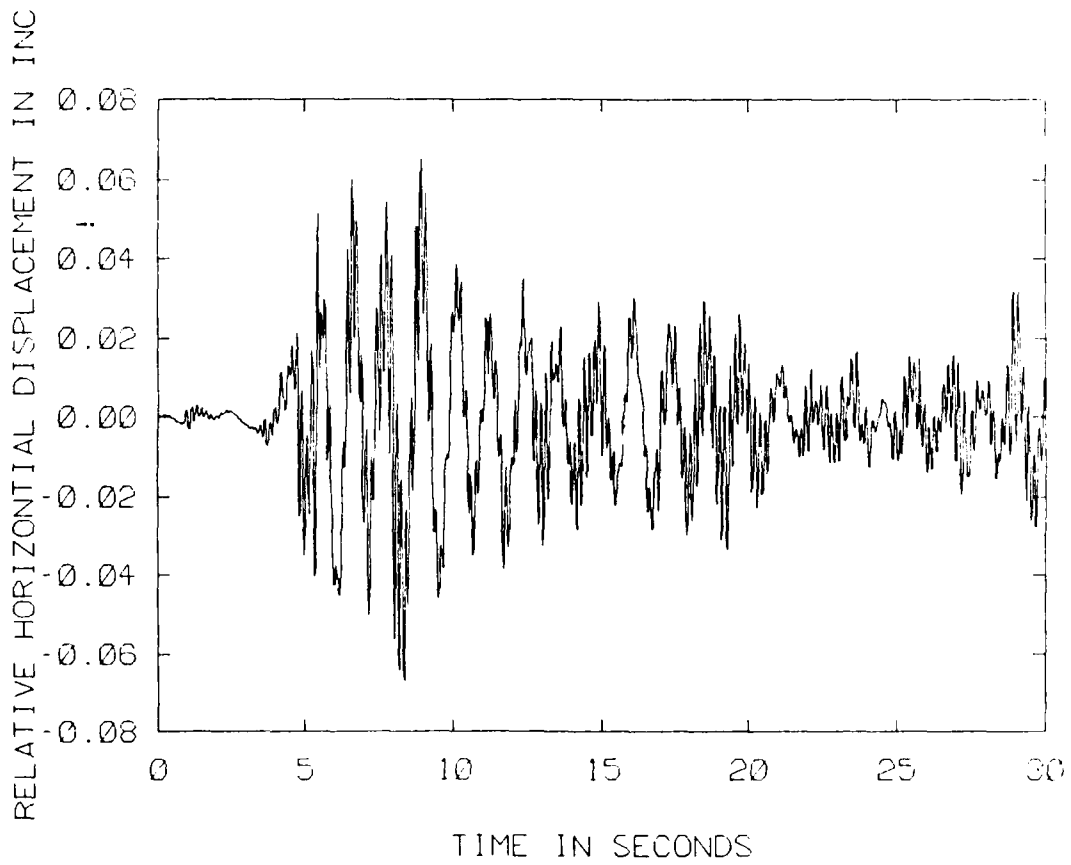


FIGURE 7.6a
Vessel Seismic Response in Relative Horizontal Translation for
Three Degree of Freedom Model using Modal Analysis

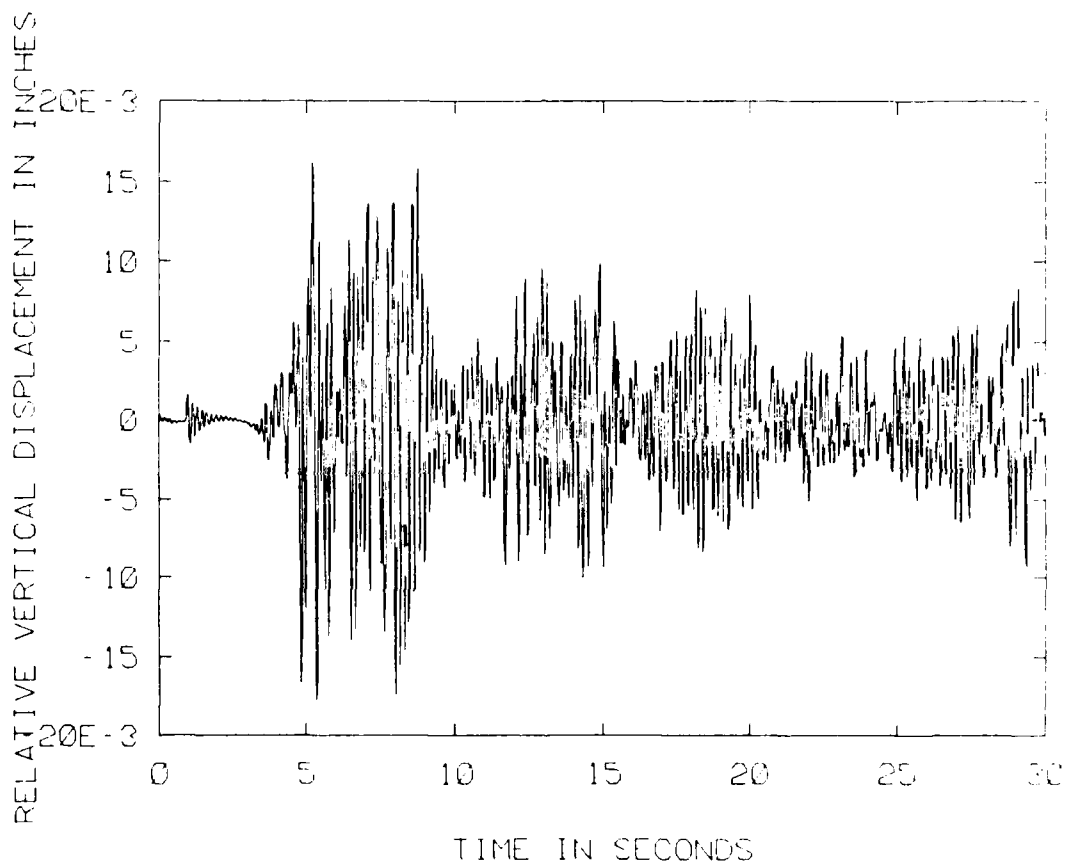


FIGURE 7.6b
Vessel Seismic Response in Relative Vertical Translation for
Three Degree of Freedom Model using Modal Analysis

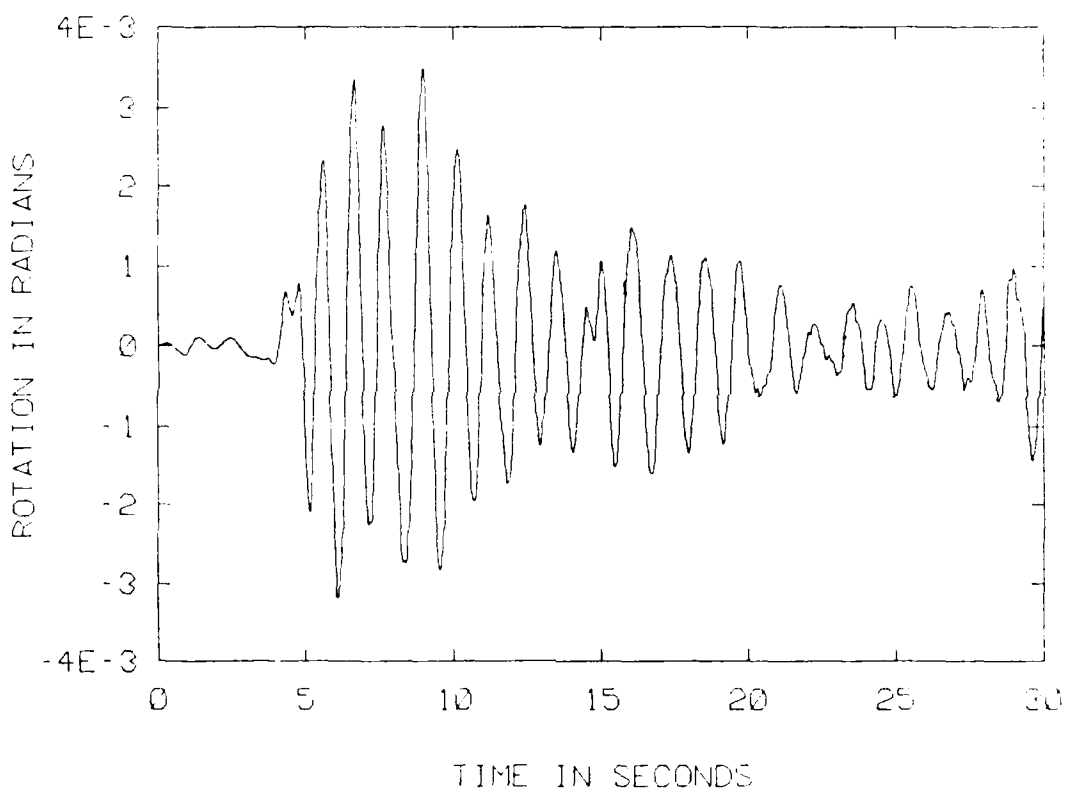


FIGURE 7.6c
Vessel Seismic Response in Rotation for Three Degree of
Freedom Model using Modal Analysis

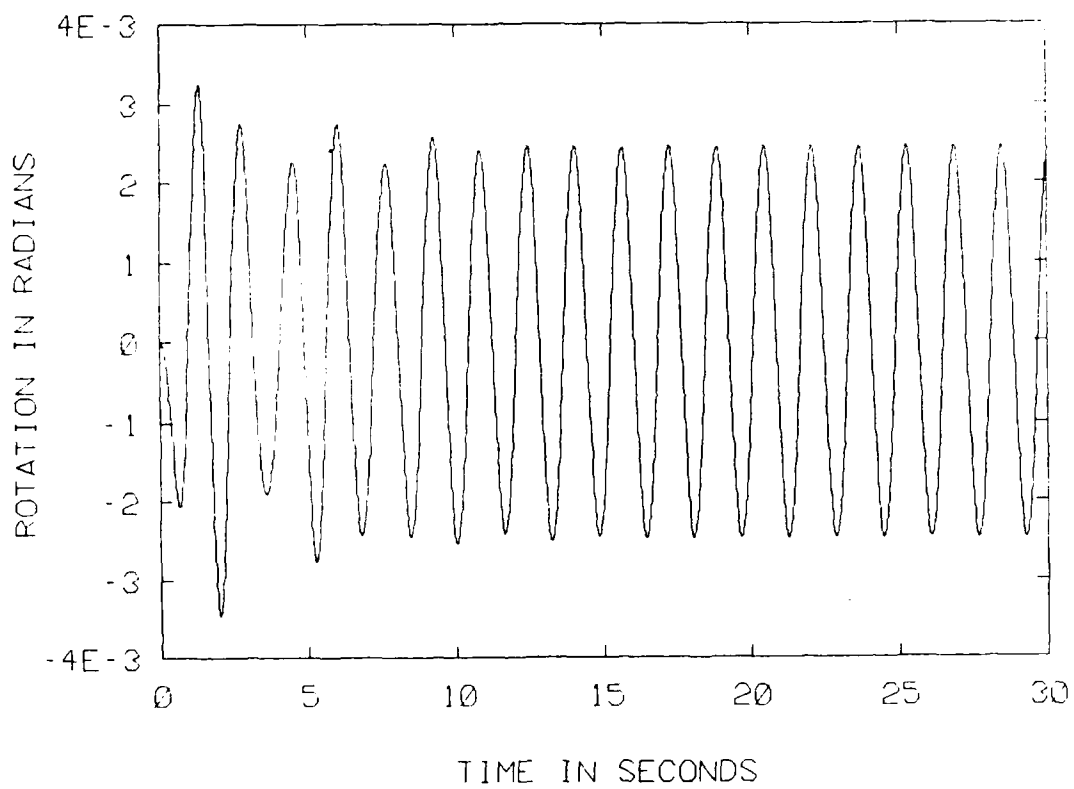


FIGURE 7.7
Vessel Seismic Response in Rotation using Runge-Kutta
Numerical Analysis with Sinusoidal Ground Acceleration

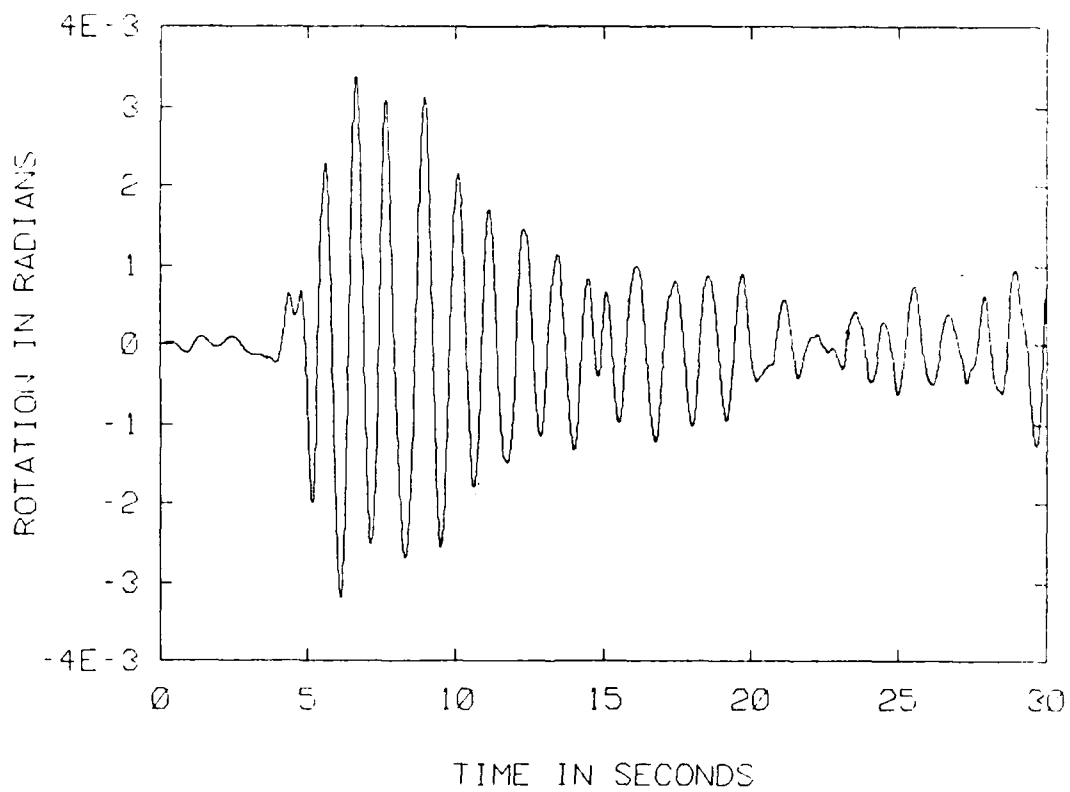


FIGURE 7.8
Vessel Seismic Response in Rotation for One Degree of Freedom
Model using Runge-Kutta Analysis

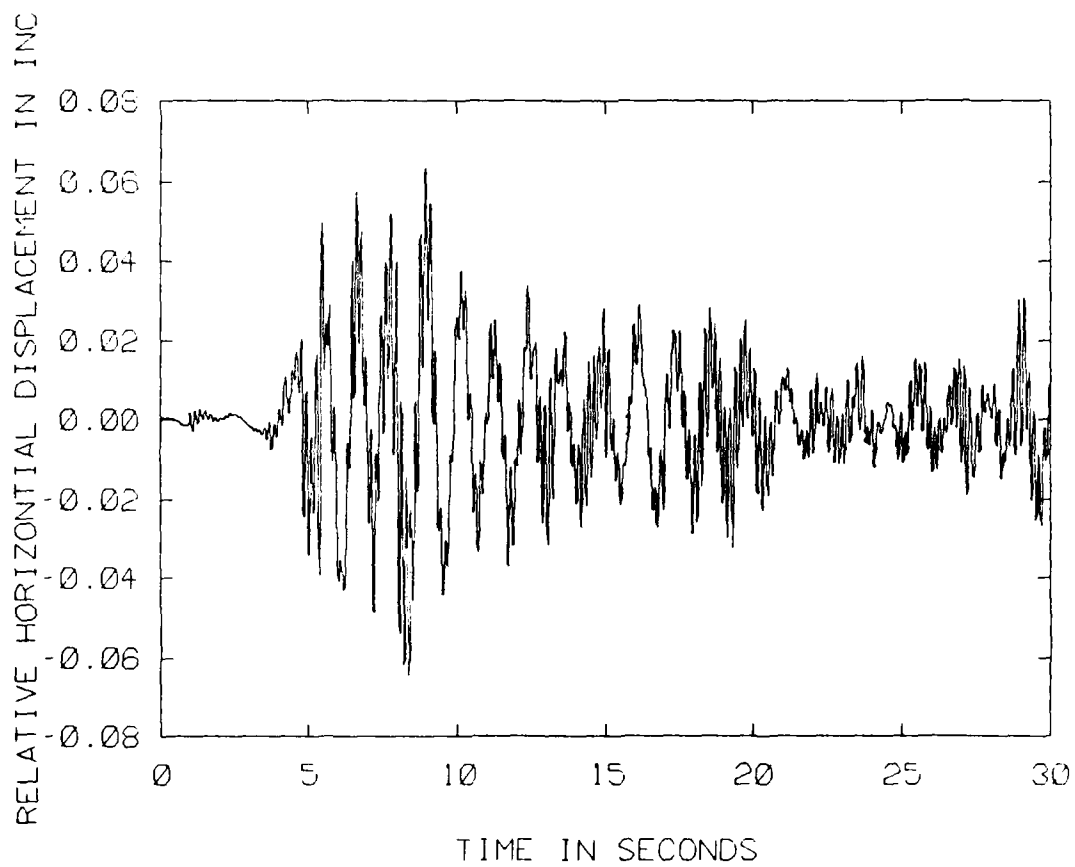


FIGURE 7.9a
Vessel Seismic Response in Relative Horizontal Translation for
Two Degree of Freedom using Runge-Kutta Analysis

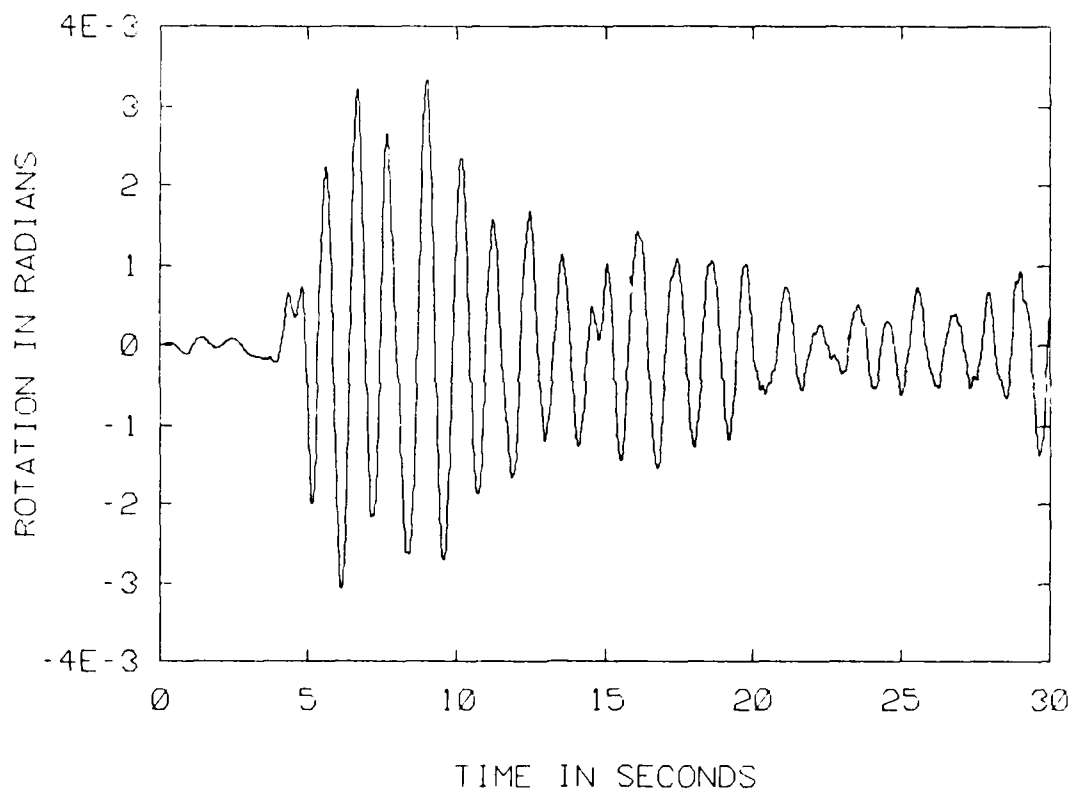


FIGURE 7.9b
Vessel Seismic Response in Rotation for Two-Degree of Freedom
Model using Runge-Kutta Analysis

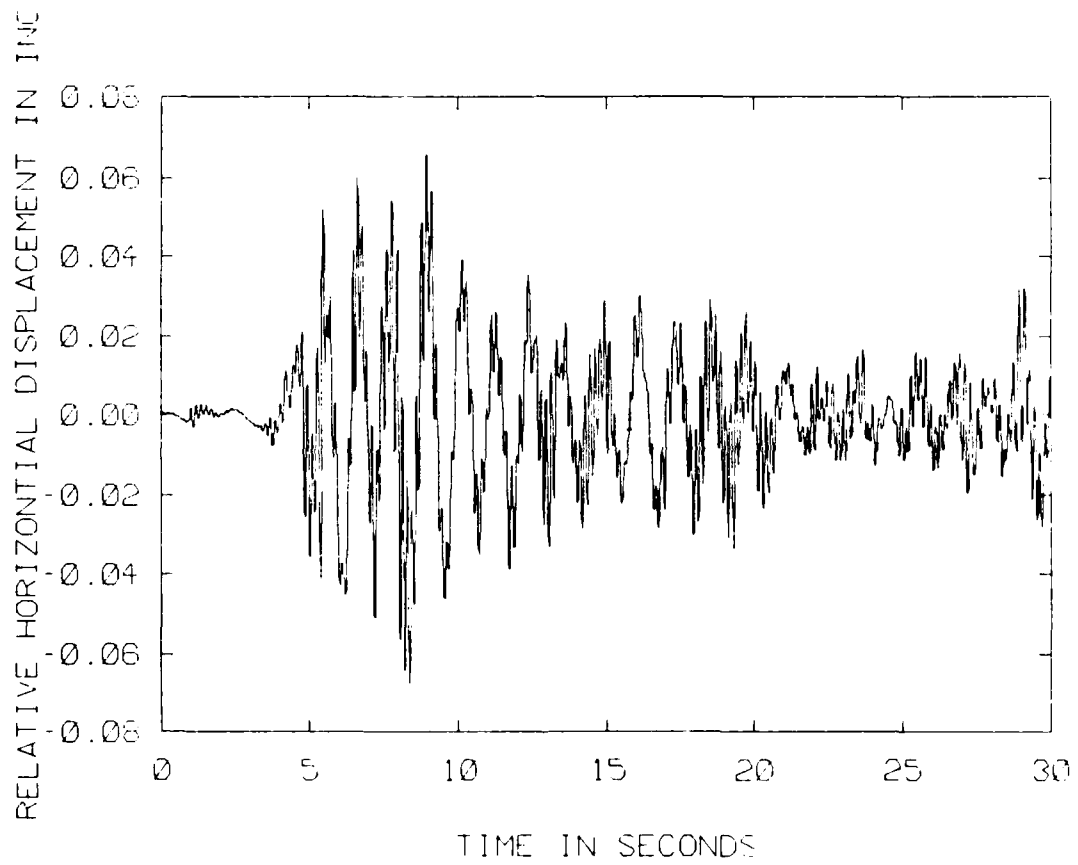


FIGURE 7.10a
Vessel Seismic Response in Relative Horizontal Translation for
Three Degree of Freedom Model using Runge-Kutta Analysis

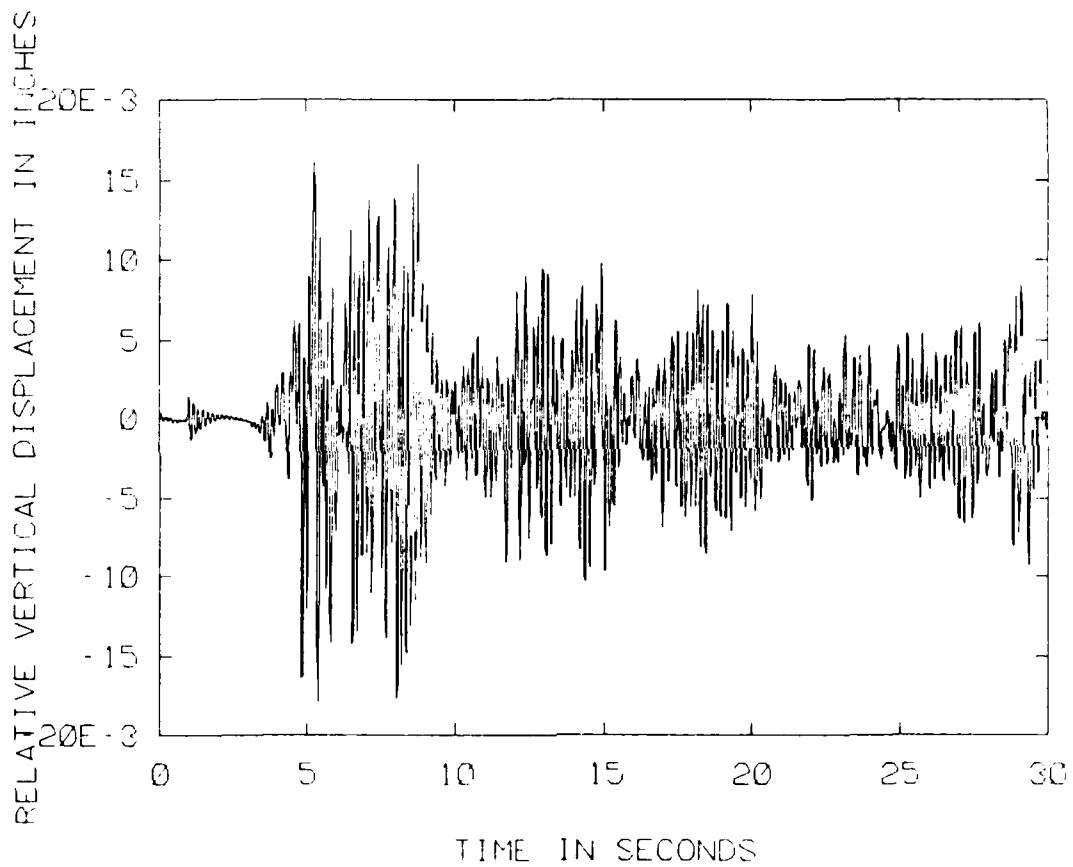


FIGURE 7.10b
Vessel Seismic Response in Relative Vertical Translation for
Three Degree of Freedom Model using Runge-Kutta Analysis

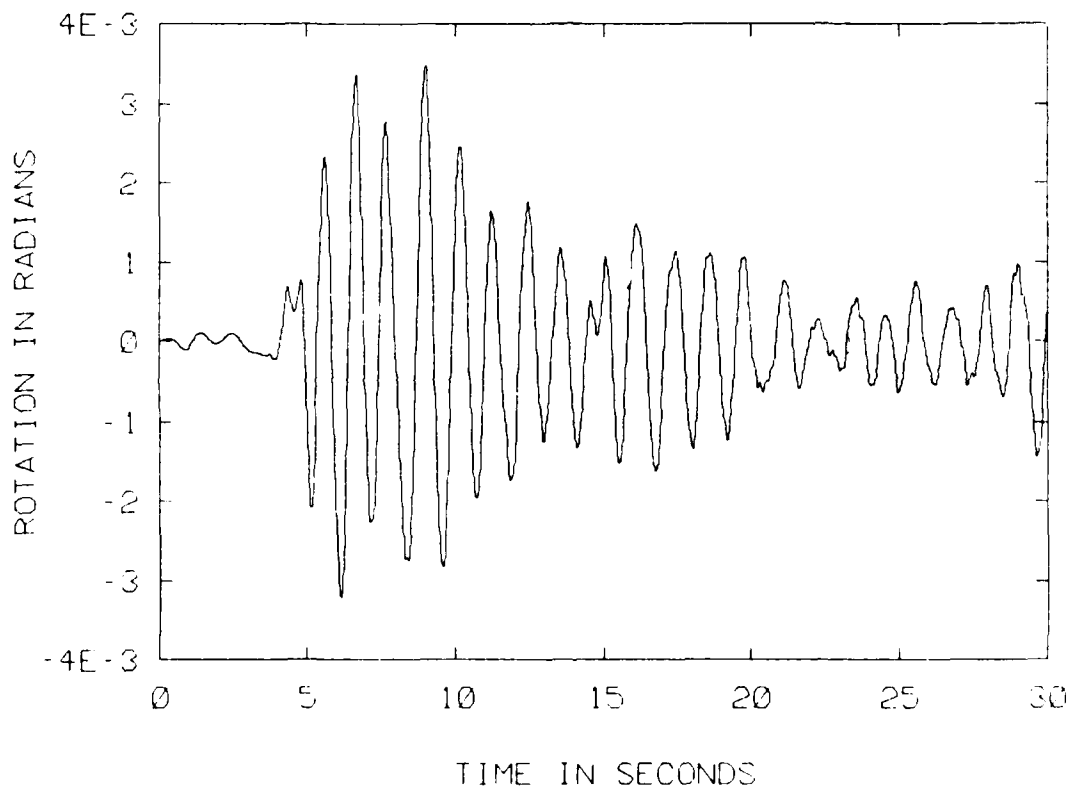


FIGURE 7.10c
Vessel Seismic Response in Rotation for Three Degree of Freedom Model using Runge-Kutta Analysis

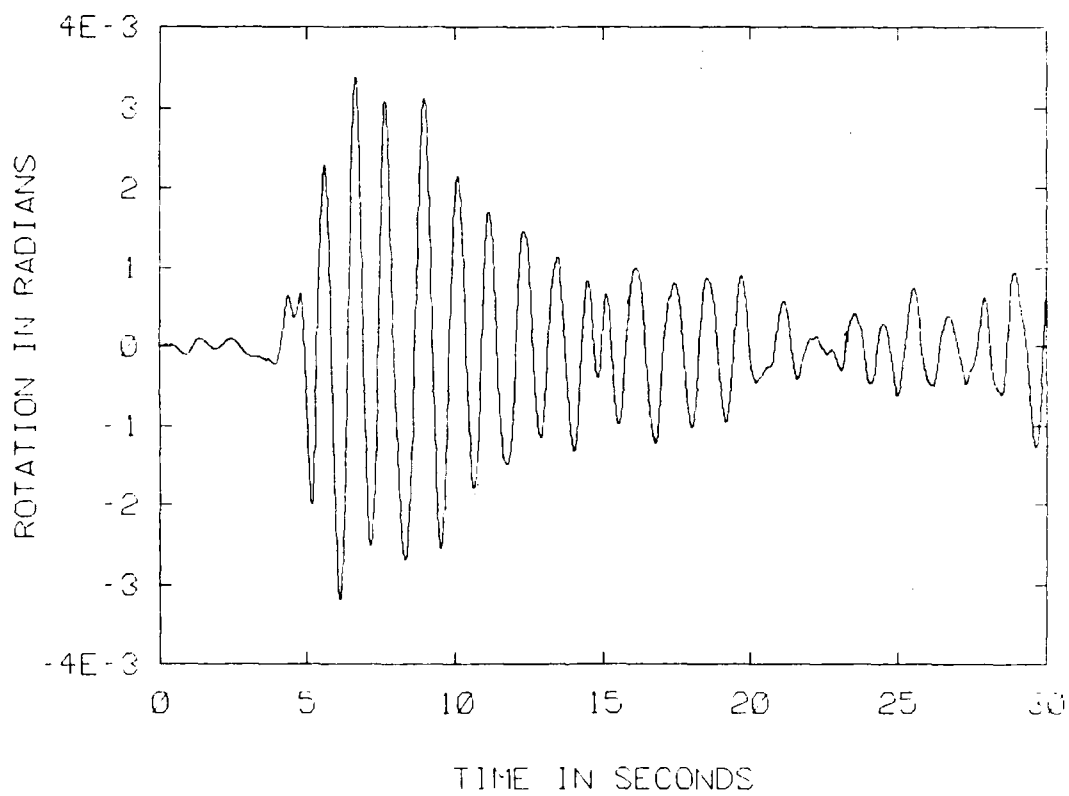


FIGURE 7.11
Vessel Seismic Response in Rotation for Non-Linear One Degree of Freedom Model using Runge-Kutta Analysis

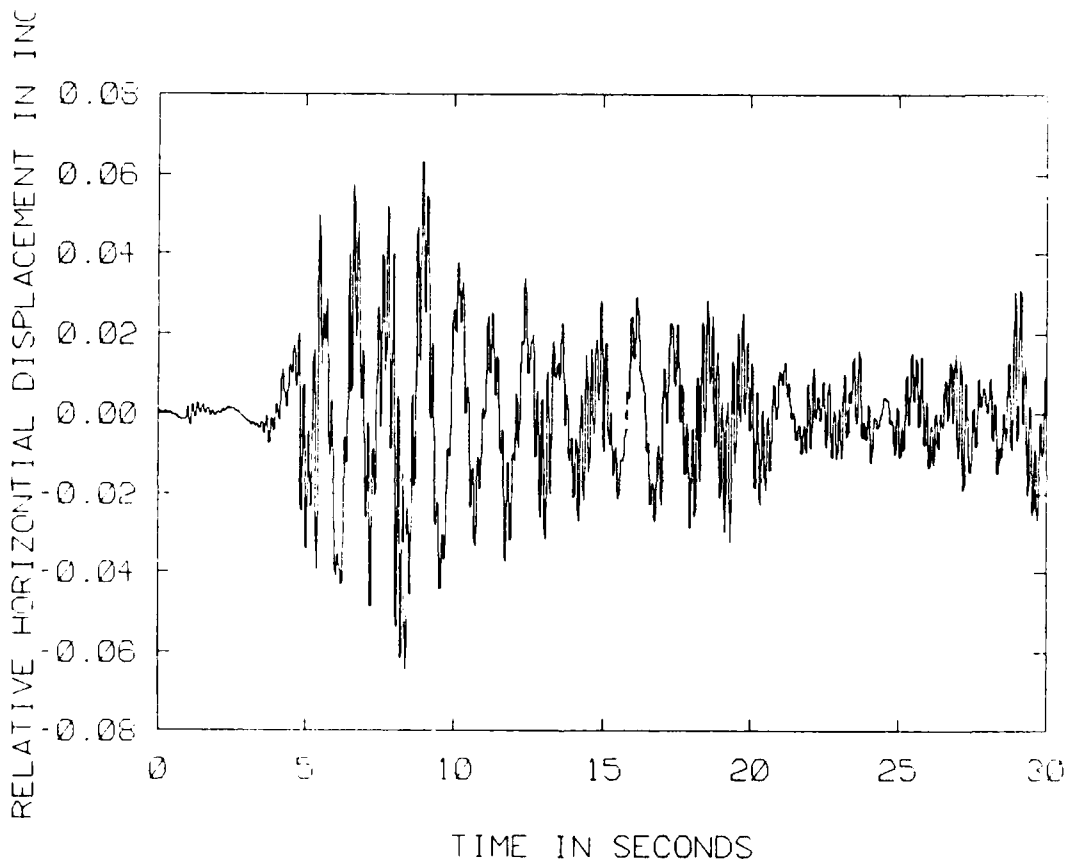


FIGURE 7.12a
Vessel Seismic Response in Relative Horizontal Translation
for Non-linear Two Degree of Freedom Model using Runge-Kutta
Analysis

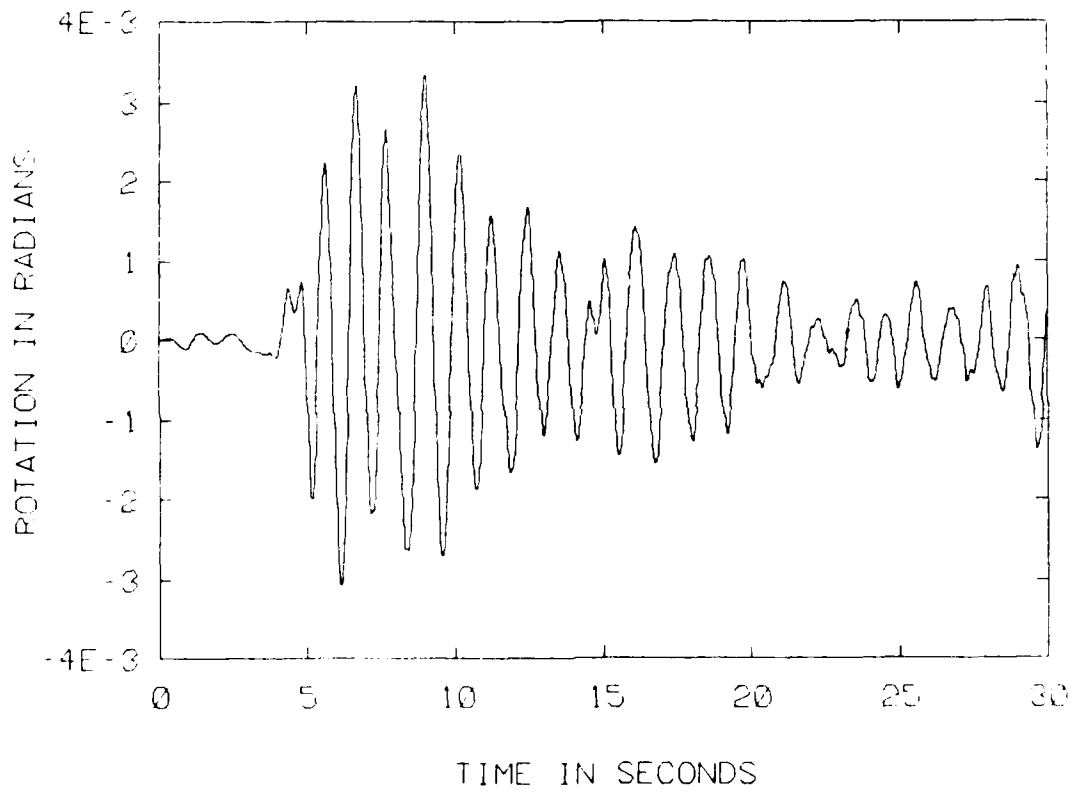


FIGURE 7.12b
Vessel Seismic Response in Rotation for Non-linear Two Degree
of Freedom Model using Runge-Kutta Analysis

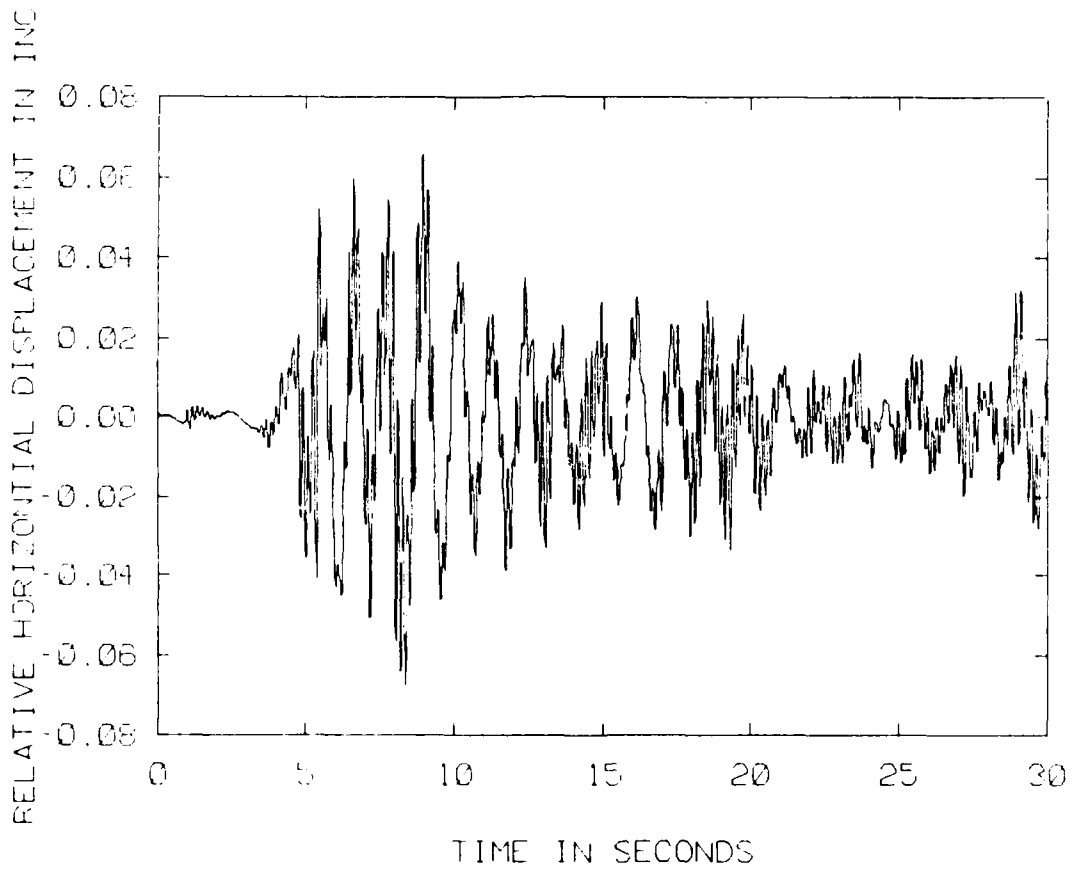


FIGURE 7.13a
Vessel Seismic Response in Relative Horizontal Translation
for Non-linear Three Degree of Freedom Model using Runge-
Kutta Analysis

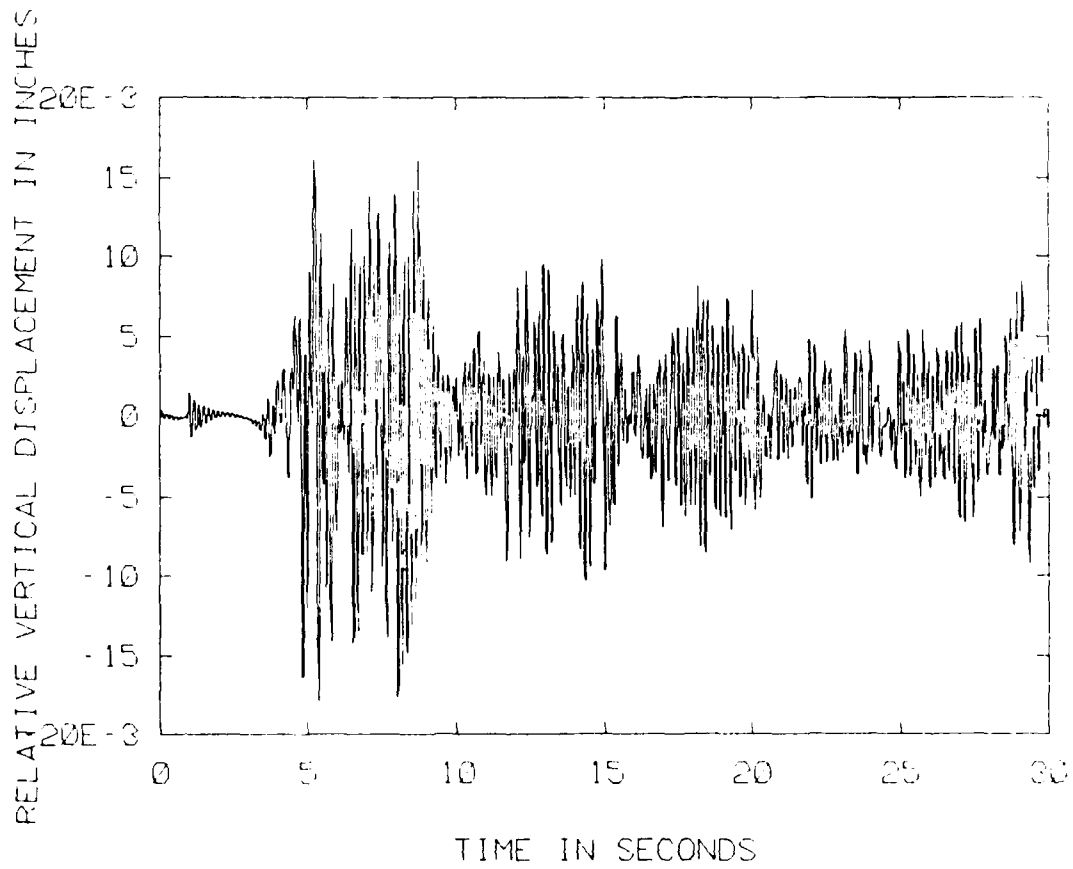


FIGURE 7.13b
Vessel Seismic Response in Relative Vertical Translation for
Non-linear Three Degree of Freedom Model using Runge-Kutta
Analysis

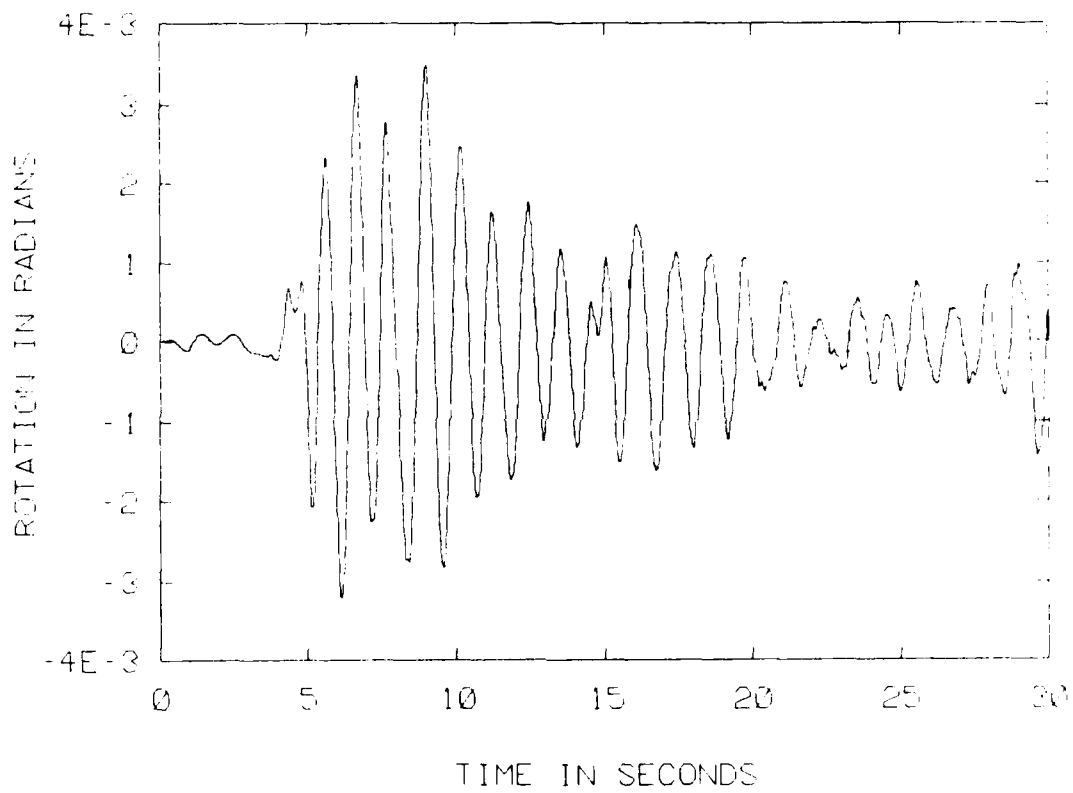


FIGURE 7.13c
Vessel Seismic Response in Rotation for Non-linear Three
Degree of Freedom Model using Runge-Kutta Analysis

LINEARITY SELECTION CRITERIA

5 % DAMPING, BETA=1

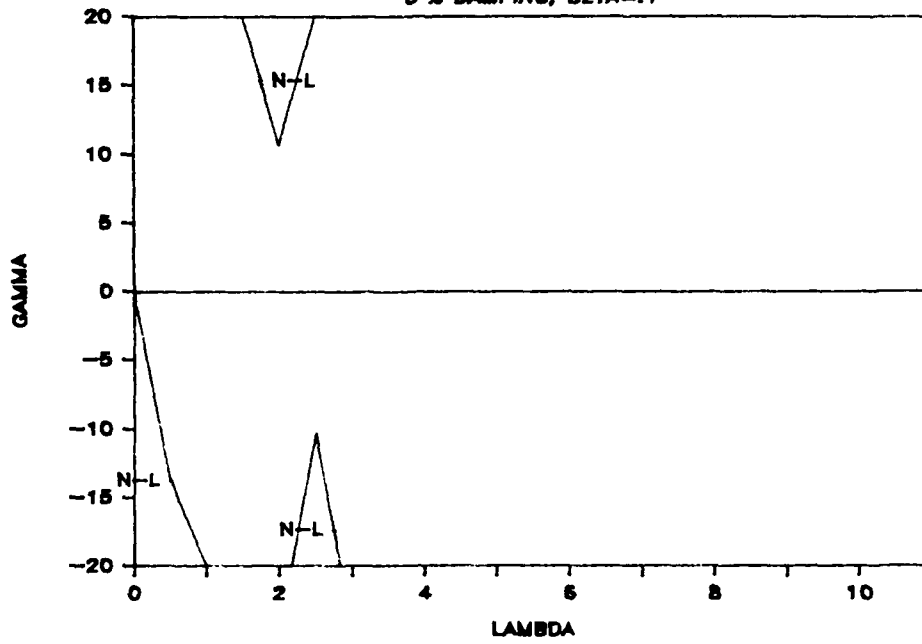


FIGURE 7.14a

Linearity Selection Criteria, 5% Damping, Bet = 0.1

LINEARITY SELECTION CRITERIA

5 % DAMPING, BETA=0.5

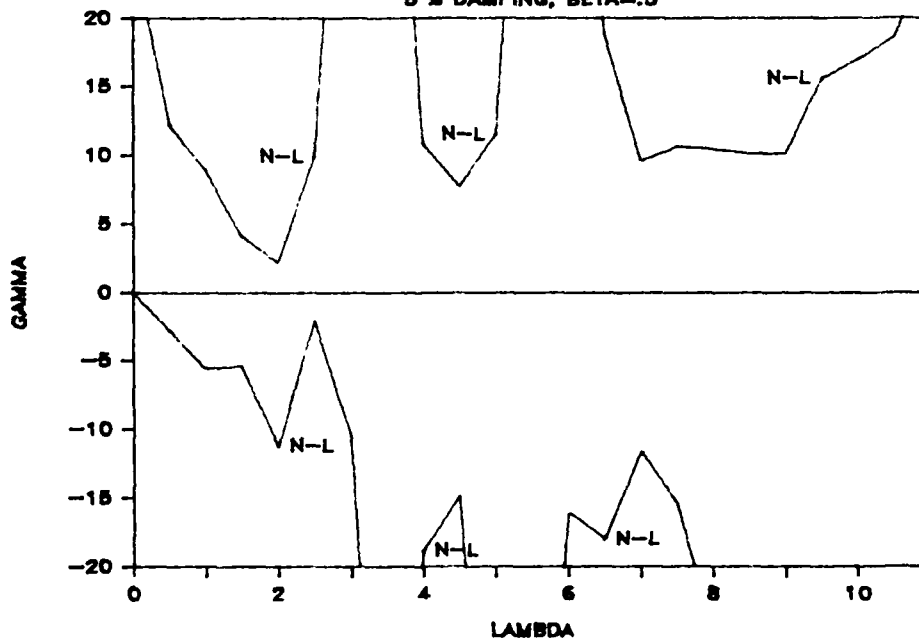


FIGURE 7.14b

Linearity Selection Criteria, 5% Damping, Beta = 0.5

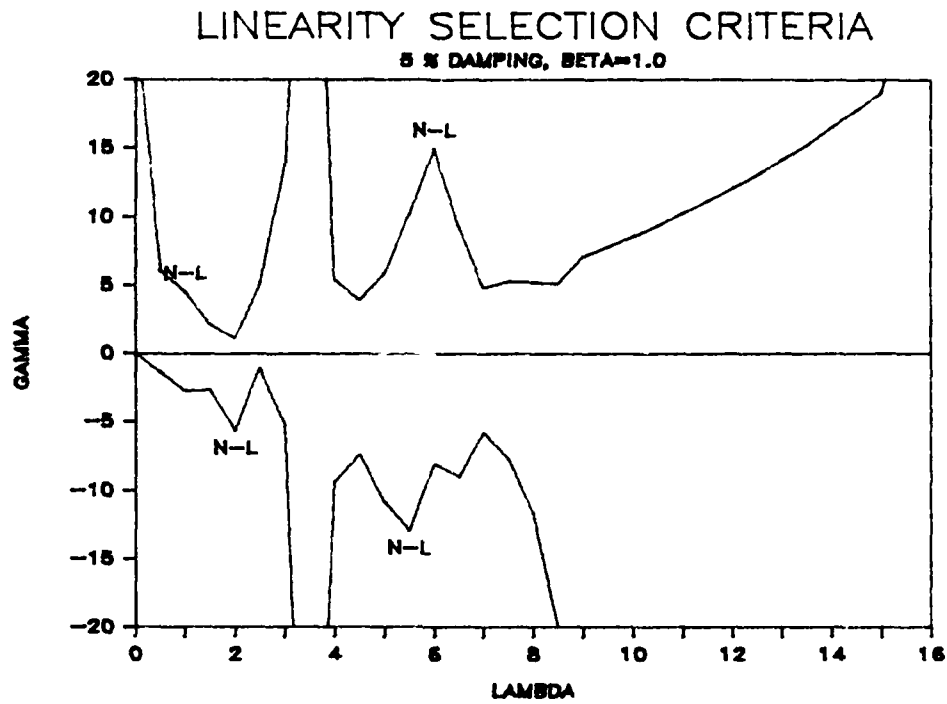


FIGURE 7.14c
Linearity Selection Criteria, 5% Damping, Beta = 1.0

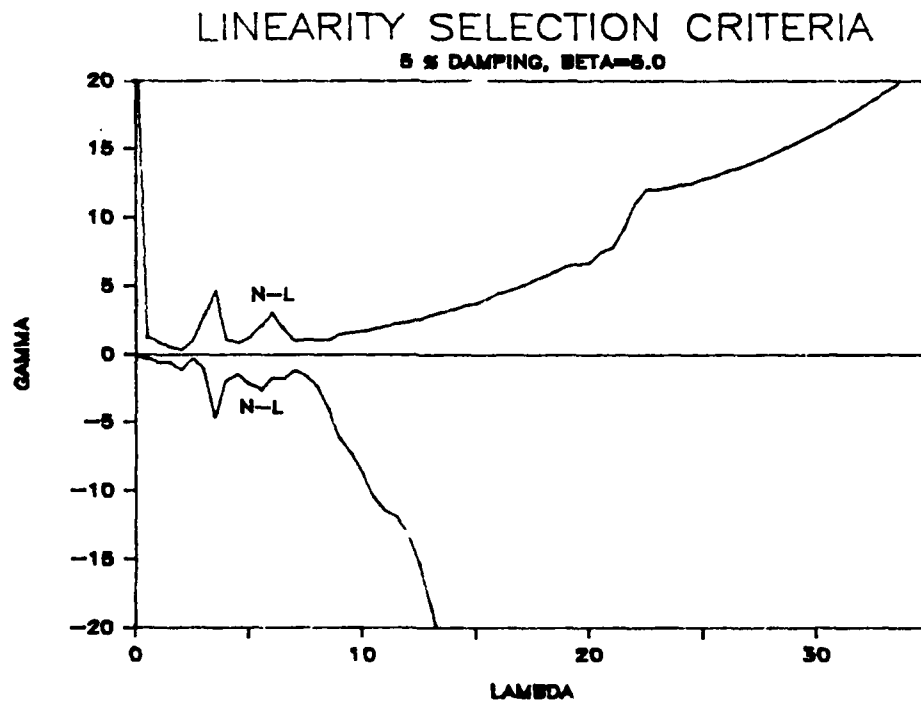


FIGURE 7.14d
Linearity Selection Criteria, 5% Damping, Beta = 5.0

LINEARITY SELECTION CRITERIA

5% DAMPING, BETA=10.

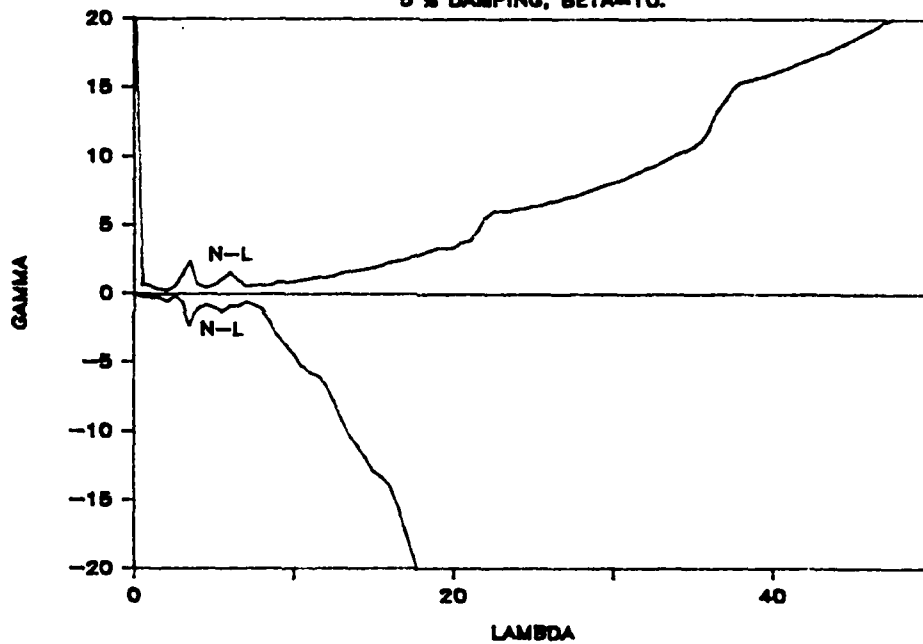


FIGURE 7.14e
Linearity Selection Criteria, 5% Damping, Beta = 10.0

8.0 SUMMARY, CONCLUSIONS, AND RECOMMENDATIONS FOR FURTHER STUDY

8.1 Summary

This thesis investigates four models of the vessel-drydock system for seismic analysis. These models are implemented to determine vessel response to seismic loading for eleven representative submarine-drydock systems. Using Equation 4.1.4, the quasi-static force model generates various vessel responses listed on Table 6.2. For example, the submarine in system #1 will rotate about its keel 0.00809 when subjected to a strong earthquake. The one degree of freedom model predicts a maximum vessel rotation for system #1 of 0.01471 radians in response to the El Centro earthquake ground acceleration history. This rotation of 0.01471 radians is verified by the two and three degree of freedom models. See Tables 7.2 and 7.3. This maximum seismic response of system #1 can also be confirmed by the response spectrum method as described in Section 6.3 and reference [1]. The response spectrum method gives the rotation as 0.01594 radians. All eleven systems have similar differences between the quasi-static force model and the various degree of freedom models.

More important than the maximum vessel response due to the El Centro earthquake of .33g magnitude is the maximum permissible earthquake acceleration that a vessel-drydock can withstand without failure. The maximum permissible accelerations and associated vessel responses for the one, two and three degree of freedom are listed in Table 7.3, 7.4 and 7.5, respectively. For example, the one degree of freedom

model for system #1 predicts a maximum permissible acceleration of 0.0759 g's with maximum vessel rotation of 0.00339 radians. The two degree of freedom determines a maximum permissible acceleration equalling .0759 g's with maximum vessel rotation and relative horizontal displacement of 0.003358 radians and 0.064566 inches, respectively. Finally, the maximum permissible acceleration of 0.0792 g's with associated vessel responses (rotation, relative horizontal and vertical displacements) of 0.003504 radians, 0.067373 inches, and 0.017858 inches. The slightly higher maximum permissible acceleration found in three degree model is due to the beneficial effect of the vertical displacement delaying failure of the system. However, as shown by the other systems, this is not always the case. In summary, the range of magnitudes known as maximum permissible accelerations that the eleven systems could withstand without liftoff is 13% to 42% of the magnitude of the El Centro earthquake depending on system and model used.

8.2 Conclusions

The quasi-static method currently used by the U.S. Navy for seismic response analysis underestimates the block forces caused by an earthquake the magnitude of the El Centro earthquake. The one degree of freedom model adequately predicts the vessel rotational response to seismic loading but is ineffective in the analysis of possible failures to the vessel-drydock system. The two degree of freedom model does a good job of predicting vessel rotational and horizontal translation response to seismic loading provided the response

due to vertical acceleration is small, which is the case for the eleven systems analyzed. Finally, the three degree of freedom model predicts the vessel rotational, horizontal, and vertical translation responses and can be used to completely investigate various types of failure to the vessel-drydock system in all eleven vessel-drydock systems examined. The vessel would experience side pier liftoff failure during an earthquake with the magnitude of the El Centro earthquake (ie. 0.33 g's). The various vessel-drydock systems would not remain intact during this magnitude of earthquake. Also noted that the fourth order Runge-Kutta numerical scheme should be used to evaluate system response because of its simplicity, results accuracy, and ease of introducing terms into the Equation of motion.

8.3 Recommendations for Further Study

The seismic response of drydocked vessels needs further investigation in three areas. First, a three degree of freedom model which will allow vessel liftoff should be studied so that other failure mode will occur. Second, a study of the vessel-drydock system parameters needs to be carried out to explore ways in which drydocked vessel seismic response can be decreased. Third, an in depth study of the drydock block itself in order to provide failure modes along with stiffness and damping characteristics for implementation into mathematical models.

REFERENCES

1. Barker, Charles, F., "The Response of Drydocked Ships to Seismic Loading", MIT Thesis, May 1985.
2. Biggs, John M., Introduction to Structural Dynamics, McGraw-Hill, Inc., New York, NY 1964.
3. Clough, Ray W., Penzien, Joseph, Dynamics of Structures, McGraw-Hill, Inc., New York, NY 1975.
4. International Mathematical and Statistical Library, Reference Manual Edition 9, 1982, IMSL, Houston, TX.
5. U.S. NAVY, NAVSEA Technical Manual, CH. 997 R1.
6. U.S. Navy, "Proposed Military Standard, Drydock Blocking Systems, Requirements for", prepared for NAVSEA by Gibbs and Cox, Inc., 31 July 1983.
7. Newmark, Nathan M., Rosenblueth, Emilio, Fundamentals of Earthquake Engineering, Prentice-Hall Inc., Englewood Cliffs, NJ, 1971.
8. Schrid, Francis, Theory and Problems of Numerical Analysis, Schaum's Outline Series, McGraw-Hill Book Co., New York, NY 1968.
9. Sunder, S. Shyam, Conner, Jerome J., "A New Procedure for Processing Strong-Motion Earthquake Signals", Bulletin of the Seismological Society of America, Vol. 72, No. 2, April, 1982, pp. 643-661.
10. Thomson, William T., Theory of Vibration with Applications, Prentice-Hall, Inc., Englewood Cliffs, NJ, 1972.
11. Timoshenko, S., Strength of Materials, Part 1, Robert E Krieger Publishing Co., Inc., Huntington, NY, 1955, reprinted 1976.
12. Timoshenko, S., Vibration Problems in Engineering, D. Van Nostrand Co., Inc., NY, Third Ed., 1955.
13. Tse, Francis S., Morse, Ivan E., Hinkle, Rolland T., Mechanical Vibrations, Theory and Applications, Second Edition, Allyn and Bacon, Inc., Boston, MA, 1978.
14. Viscomi, B. Vincent, "A Method of Predicting the Seismic Rotational Response of Submarines in Graving Drydocks", Structural Integrity Division, Ship Design and Integration Directorate, NAVSEA, U.S. Navy, Sept. 1981.

APPENDIX 1

C LINEARIZED THREE DEGREE OF FREEDOM SYSTEM RESPONSE USING
C MODAL ANALYSIS METHOD

```
integer ia,ib,ic,l,mm,n,ijob,iz,ier,hull,nsys,flag10
integer flag1,flag2,flag3,flag4,flag5,flag6,flag7,flag8
real a(6,6),b(6,6),beta,wk(72),weight,h,Ik,gravity
real m(3,3),cx(3,3),k(3,3),sidearea,keelarea,plside
real baseside,basekeel,htside,htkeel,crit1,crit2,crit3
real an(6,6),ac(6000),dtau,maxx,maxt,maxy,timex,timet
real rfl,rf2,rf3,hf1,hf2,hf3,ampacc,mass,ampacmax
real kvs,kvk,khs,khk,base,ht,counter
real time1,time2,time3,time4,time5,time6,time7,time8
real x(6000),t(6000),y(6000),r1(7),s1(7),pi(7),XSCL(6)
real bbb,ccc,w12,w1,w22,w2,w32,w3,model,mode3,capwidth
real mmx1,mmang1,mmx3,mmang3,br,amp,plkeel,crit4,u1,u2
real timey,mmmm1,mmmm2,mmmm3,mmmm4
complex alfa(6),z(6,6),ad(6,6),bd(6,6),aa(6,6),bb(6,6)
complex g(6),v(6),yy(6,6000),ABC(6),zt(6,6),beta1

CHARACTER*40 XLABEL,YLABEL,YYLABEL,YYLABLEL,DEC
```

C READ IN VESSEL AND DRYDOCK DATA; VESSEL WEIGHT,KG,I (ABOUT KEEL),
C TIME INCREMENT OF DATA POINTS,VERTICAL STIFFNESS OF SIDE AND
C KEEL PIERS,HORIZONTAL STIFFNESS OF SIDE AND KEEL PIERS,
C GAVITATIONAL CONSTANT,SIDE BLOCK BASE AND HEIGHT,
C KEEL BLOCK BASE AND HEIGHT,
C BLOCK-BLOCK AND BLOCK-HULL FRICTION COEFFICIENTS,
C SIDE AND KEEL BLOCK'S PROPORTIONAL LIMIT,
C SIDE PIER-VESSEL CONTACT AREA,KEEL PIER-VESSEL CONTACT AREA,
C CAP BLOCK INCLINATION ANGLE.

```
read(44,*) weight,h,Ik,dtau,kvs,kvk,khs,khk,gravity
read(44,*) baseside,basekeel,htside,htkeel,u1,u2
read(44,*) br,amp,plside,plkeel,sidearea,keelarea,zeta
read(44,*) hull,nsys
write(6,*) 'do you want response plots? (y or n) '
read(5,15) dec
15       format (a)
          do 10,i=1,6
          do 11,j=1,6
          a(i,j)=0.0
          b(i,j)=0.0
11       continue
10       continue
          do 12,i=1,3
          do 13,j=1,3
          m(i,j)=0.0
          k(i,j)=0.0
          cx(i,j)=0.0
13       continue
12       continue
```

```

C      CALCULATE SYSTEM PARAMETERS

      mass=weight/gravity

      beta=asin(sqrt(br**2/(4*h**2)))

      m(1,1)=mass
      m(1,3)=h*mass
      m(2,2)=mass
      m(3,1)=mass*h
      m(3,3)=Ik

      k(1,1)=(2*khs+khk)
      k(2,2)=(2*kvs+kvk)
      k(3,3)=(0.5*kvs*(br**2.0)-(weight*h))

C      DETERMINE NATURAL FREQUENCIES OF SYSTEM

      bbb=-(m(1,1)*k(3,3)+m(3,3)*k(1,1)-m(1,3)*k(3,1)-m(3,1)*k(1,3))
      + / (m(1,1)*m(3,3)-m(1,3)*m(3,1))
      ccc=(k(1,1)*k(3,3)-k(1,3)*k(3,1))/(m(1,1)*m(3,3)-m(1,3)*m(3,1))

C      NATURAL FREQ. MODE #1

      w12=(-bbb-sqrt(bbb**2.0-4*ccc))/2
      w1=sqrt(w12)

C      NATURAL FREQ. MODE #2

      w22=k(2,2)/m(2,2)
      w2=sqrt(w22)

C      NATURAL FREQ. MODE #3

      w32=(-bbb+sqrt(bbb**2.0-4*ccc))/2
      w3=sqrt(w32)

C      MODE SHAPE #1 & #3

      mode1=(m(1,3)*w12-k(1,3))/(-m(1,1)*w12+k(1,1))
      mode3=(m(1,3)*w32-k(1,3))/(-m(1,1)*w32+k(1,1))
C      DETERMINE C11,C13,C31,C33
      mmx1=m(1,1)+m(1,3)/mode1
      mmang1=mode1*m(3,1)+m(3,3)
      mmx3=m(1,1)+m(1,3)/mode3
      mmang3=mode3*m(3,1)+m(3,3)
      mmmm1=2*zeta*mmx1*w1
      mmmm2=2*zeta*mmx3*w3
      mmmm3=2*zeta*mmang1*w1
      mmmm4=2*zeta*mmang3*w3

      cx(1,3)=(mmmm1-mmmm2)/(1/mode1-1/mode3)
      cx(1,1)=mmmm1-(cx(1,3)/mode1)
      cx(2,2)=2*zeta*m(2,2)*w2

```

```

cx(3,1)=(mmmm3-mmm4)/(model-mode3)
cx(3,3)=mmmm3-(cx(3,1)*model)

C      SET UP A AND B MATRICES,PERFORM EIGENVALUE PROBLEM, AND
C      DECOUPLE EQUATIONS OF MOTION

a(1,4)=m(1,1)
a(1,6)=m(1,3)
a(2,5)=m(2,2)
a(3,4)=m(3,1)
a(3,6)=m(3,3)
a(4,1)=m(1,1)
a(4,3)=m(1,3)
a(4,4)=cx(1,1)
a(4,6)=cx(1,3)
a(5,2)=m(2,2)
a(5,5)=cx(2,2)
a(6,1)=m(3,1)
a(6,3)=m(3,3)
a(6,4)=cx(3,1)
a(6,6)=cx(3,3)

b(1,1)=-m(1,1)
b(1,3)=-m(1,3)
b(2,2)=-m(2,2)
b(3,1)=-m(3,1)
b(3,3)=-m(3,3)
b(4,4)=k(1,1)
b(4,6)=k(1,3)
b(5,5)=k(2,2)
b(6,4)=k(3,1)
b(6,6)=k(3,3)

do 100,i=1,6
do 110,j=1,6
an(i,j)=-1.0*a(i,j)
110 continue
100 continue

ia=6
ib=6
ic=6
iz=6
n=6
ljob=2
call eigzf(b,ia,an,ib,n,ljob,alfa,beta1,z,iz,wk,ier)
WRITE(6,*)wk(1),ier

DO 200,i=1,6
do 201,j=1,6
zt(j,i)=z(i,j)
201 continue
200 CONTINUE
call mult (zt,a,aa)
call multc (aa,z,ad)
call mult (zt,b,bb)
call multc (bb,z,bd)
do 204,i=1,6
v(i)=-1.0*bd(i,1)/ad(i,1)

```

```

204   continue
C     READ IN ACCELERATION DATA
      do 300,n=1,5001,5
      read (45,*) ac(n),ac(n+1),ac(n+2),ac(n+3),ac(n+4)
300   continue
C     ESTABLISH FAILURE CRITERIA AND FLAGS
      crit1= min(u1,(u2*cos(beta)+sin(beta))/
+      (cos(beta)-u2*sin(beta)))
      crit2=min(u1,u2)
      crit3= (0.66*baseside-12.0)/htside
      crit4=basekeel/(6*htkeel)
      ampacc=1.0
      counter=0.0
      ampacmax=0.0
10000  continue
      flag1=0
      flag2=0
      flag3=0
      flag4=0
      flag5=0
      flag6=0
      flag7=0
      flag8=0
      flag10=0
      do 50000 i=1,6
      ABC(i)=0.0
50000  continue
      maxx=0.0
      maxt=0.0
      maxy=0.0
      mm=0
C     SOLVE FOR Y, THE COLUMN MATRIX WHICH IS THE SOLUTION IN
C     THE IMAGINARY COORDINATE SYSTEM WHERE THE EQUATIONS OF MOTION
C     ARE DECOUPLED
      do 301,l=3,3501,2
      do 302,i=1,6
      g(i)=(ABC(i)+ac(1-2)/2.54)*exp(v(i)*2*dtau)
+      +4.0*(ac(1-1)/2.54)*exp(v(i)*dtau)+ac(1)/2.54
      ABC(i)=g(i)
      yy(i,1)=((zt(i,4)+amp*zt(i,5)+zt(i,6)*h)*mass/ad(i,1))*g(i)
+      *ampacc*-dtau/3
302   continue
      mm=mm+1
C     USING THE MODAL MATRIX ( 4th,5th, AND 6th ROWS ), OBTAIN
C     VALUES FOR TRANSLATIONS AND ROTATION
      do 303, i=1,6
      si(i)=z(4,i)*yy(i,1)+si(i-1)
303   continue
      x(mm)=si(6)
      if (abs(x(mm)).gt.abs(maxx)) then
          timex=dtau*(i-1)
          maxx=x(mm)
      endif
      do 304, i=1,6

```

```

304   r1(1)=z(6,1)*yy(1,1)+r1(1-1)
      continue
      t(mm)=r1(6)
      if (abs(t(mm)).gt.abs(maxt)) then
          timet=dtau*(1-1)
          maxt=t(mm)
      endif
      do 305, i=1,6
305   pi(1)=z(5,1)*yy(1,1)+pi(1-1)
      continue
      y(mm)=pi(6)
      if (abs(y(mm)).gt.abs(maxy)) then
          timey=dtau*(1-1)
          maxy=y(mm)
      endif

C     CALCULATE VERTICAL AND HORIZONTAL FORCES CAUSED BY VESSEL,
C     TEST FOR FAILURE

C     CALCULATE FORCES ON SIDE/KEEL BLOCKS
      rf1=kvs*((weight/k(2,2))-y(mm)-(br/2)*t(mm))
      rf2=kvs*((weight/k(2,2))-y(mm)+(br/2)*t(mm))
      rf3=kvk*((weight/k(2,2))-y(mm))
      hf1=khs*(x(mm))
      hf2=khs*(x(mm))
      hf3=khk*x(mm)
C     TEST FOR SIDE BLOCK SLIDING

      if (flag1.eq.1) then
          go to 400
      else if (hf1.lt.0.0.and.rf1.gt.0.0.and.abs(hf1/rf1).gt.crit1) then
          time1= dtau*(1-1)
          flag1=1
      else if (hf2.gt.0.0.and.rf2.gt.0.0.and.abs(hf2/rf2).gt.crit1) then
          time1=dtau*(1-1)
          flag1=1
      endif
      x1=x(mm)
      y1=y(mm)
      t1=t(mm)
400   continue

C     TEST FOR KEEL BLOCK SLIDING

      if (flag2.eq.1) then
          go to 410
      else if (rf3.gt.0.0.and.abs(hf3/rf3).gt.crit2) then
          time2=dtau*(1-1)
          flag2=1
      endif
      x2=x(mm)
      y2=y(mm)
      t2=t(mm)
410   continue
C     TEST FOR SIDE BLOCK OVERTURNING

      if (flag3.eq.1) then
          go to 420
      else if (hf1.lt.0.0.and.rf1.gt.0.0.and.abs(hf1/rf1).gt.crit3) then
          time3= dtau*(1-1)

```

```

        flag3=1
    else if (hf2.gt.0.0.and.rf2.gt.0.0.and.abs(hf2/rf2).gt.crit3) then
        time3=dtau*(1-1)
        flag3=1
    endif
    x3=x(mm)
    y3=y(mm)
    t3=t(mm)
420  continue

C      TEST FOR KEEL BLOCK OVERTURNING

    if (flag4.eq.1) then
        go to 430
    else if (rf3.gt.0.0.and.abs(hf3/rf3).gt.crit4) then
        time4=dtau*(1-1)
        flag4=1
    endif
    x4=x(mm)
    y4=y(mm)
    t4=t(mm)
430  continue

C      TEST FOR SIDE BLOCK LIFTOFF

    if (flag5.eq.1) then
        go to 440
    else if (rf1.lt.0.0 .or. rf2.lt.0.0) then
        time5=dtau*(1-1)
        flag5=1
    endif
    x5=x(mm)
    y5=y(mm)
    t5=t(mm)
440  continue

C      TEST FOR KEEL BLOCK LIFTOFF

    if (flag6.eq.1) then
        go to 450
    else if (rf3.lt.0.0) then
        time6=dtau*(1-1)
        flag6=1
    endif
    x6=x(mm)
    y6=y(mm)
    t6=t(mm)
450  continue

C      TEST FOR SIDE BLOCK CRUSHING

    if (flag7.eq.1) then
        go to 460
    else if (rf1.gt.0.0 .and. (rf1/sidearea).gt.plside) then
        flag7=1
        time7=dtau*(1-1)

    else if (rf2.gt.0.0 .and. (rf2/sidearea).gt.plside) then
        flag7=1
        time7=dtau*(1-1)

```

```

endif
x7=x (mm)
y7=y (mm)
t7=t (mm)
460 continue

C TEST FOR KEEL BLOCK CRUSHING

if (flag8.eq.1) then
go to 470
else if (rf3.gt.0.0 .and. (rf3/keelarea).gt.plkeel) then
flag8=1
time8=dtau*(1-1)
endif
x8=x (mm)
y8=y (mm)
t8=t (mm)
470 continue

301 continue

C PLOT RESULTS
go to 999
60000 continue
if(DEC.EQ.'N') THEN
write(6,*) 'I am finishing.'
GO TO 998
endif
write(6,*) 'I am plotting.'
XSCL(1)=0.0
XSCL(2)=30.0
XLABEL='TIME IN SECONDS'
YLABEL='ROTATION IN RADIANS'
YYLABEL='RELATIVE HORIZONTAL DISPLACEMENT IN INCHES'
YYYLABEL='RELATIVE VERTICAL DISPLACEMENT IN INCHES'
CALL QPICTR (X,1,1500,QXSCL(XSCL),QISCL(-2),QXLAB(XLABEL),
+ QYLAB(YYLABEL),QLABEL(4))
CALL QPICTR (T,1,1500,QXSCL(XSCL),QISCL(-2),QXLAB(XLABEL),
+ QYLAB(YLABEL),QLABEL(4))
CALL QPICTR (Y,1,1500,QXSCL(XSCL),QISCL(-2),QXLAB(XLABEL),
+ QYLAB(YYYLABEL),QLABEL(4))
998 go to 20000
999 CONTINUE

if(ampacc.eq.1.0) then

write(46,4000) nsys
4000 format(1x,/,28x,'**** System ',I2,1x,'****')
write(46,4050) hull
4050 format(1x,/,30x,'** Hull ',I3,1x,'**')
write(46,4100)
4100 format(1x,/,28x,'* Ship Parameters *')
write(46,4150)
4150 format(1x,/,5x,'Weight',8x,'Moment of Inertia',9x,'K.G.')
write(46,4200) weight,Ik,h
4200 format(1x,f9.1,1x,'kips',1x,f11.1,1x,'kips-in-sec2',
+3x,f6.1,1x,'ins')
write(46,4250)
4250 format(1x,/,26x,'* Drydock Parameter *')

```

```

write(46,4300)
4300 format(1x,/,1x,'Side Block Height',3x,'Side Block Width',
+3x,'Keel Block Height',3x,'Keel Block Width')
write(46,4350) htside,baseside,htkeel,basekeel
4350 format(2x,f6.1,1x,'ins',11x,f6.1,1x,'ins',11x,f6.1,1x,'ins',
+9x,f6.1,1x,'ins')
write(46,4400)
4400 format(1x,/,1x,'Side-to-Side Pier Distance')
write(46,4450) br
4450 format(1x,t7,f6.1,1x,'ins')
write(46,4470)
4470 format(1x,/, ' Total Side Pier Contact Area'
+,3x,'Total Keel Pier Contact Area')
write(46,4475) sidearea,keelarea
4475 format(1x,8x,f11.1,1x,'in2',14x,f11.1,1x,'in2')
write(46,4500)
4500 format(1x,/,1x,'Block-on-Block Friction Coeff',3x,'Hull-on-Block
+ Friction Coeff')
write(46,4550) u1,u2
4550 format(1x,10x,f7.3,23x,f7.3)
write(46,4600)
4600 format(1x,/,1x,'Side Pier Proportional Limit',3x,'Keel Pier'
+,' Proportional Limit')
write(46,4650) plside,plside
4650 format(1x,10x,f7.3,1x,'kips/in2',15x,f7.3,1x,'kips/in2')
write(46,4700)
4700 format(1x,/,1x,'Side Pier Vertical Stiffness',3x,'Side Pier',
+' Horizontal Stiffness')
write(46,4750) kvs,khs
4750 format(1x,3x,f11.1,1x,'kips/in',11x,f11.1,1x,'kips/in')
write(46,4775)
4775 format(1x,/,1x,'Keel Pier Vertical Stiffness',3x,
+' Keel Pier Horizontal Stiffness')
write(46,4780) kvk,khk
4780 format(1x,3x,f11.1,1x,'kips/in',11x,f11.1,1x,'kips/in')
write(46,4800)
4800 format(1x,/,20x,'* System Parameters and Inputs *')
write(46,4850)
4850 format(1x,/,1x,'Input Forcing Function is Horizontal Component',
+' of the 1946 El Centro')
write(46,4875)
4875 format(1x,20x,' Earthquake Acceleration Time History.')

write(46,4995)
4995 format(1x,/,1x,'Vertical/Horizontal Ground Acceleration Ratio'
+,3x,'Data Time Increment')
write(46,4990) amp,dtau
4990 format(1x,10x,f6.3,t55,f6.3,1x,'sec')
write(46,4900)
4900 format(1x,/,1x,'Gravitational Constant',3x,'Percent System
+ Damping')
write(46,4950) gravity,zeta*100.
4950 format(1x,7x,f6.2,1x,'in/sec2',10x,f6.2,1x,'%')
write(46,5000)
5000 format(1x,/,25x,'Mass Matrix',/)
do 5100 i=1,3
write(46,5050) m(1,1),m(1,2),m(1,3)
5050 format(1x,f15.4,5x,f15.4,5x,f15.4)
5100 continue
write(46,5200)

```

```

5200 format(1x,/,25x,'Damping Matrix',/)
do 5300 i=1,3
write(46,5250) cx(1,1),cx(1,2),cx(1,3)
5250 format(1x,f15.4,5x,f15.4,5x,f15.4)
5300 continue
write(46,5400)
5400 format(1x,/,25x,'Stiffness Matrix',/)
do 5500 i=1,3
write(46,5450) k(1,1),k(1,2),k(1,3)
5450 format(1x,f15.4,5x,f15.4,5x,f15.4)
5500 continue
write(46,5700)
format(1x,/)
WRITE(46,6000)
6000 FORMAT(1X,'Undamped Natural Frequencies',t35,'Mode #1',t50,
+'Mode #2',t65,'Mode #3')
write(46,6001) w1,w2,w3
6001 format(1x,t31,f7.3,1x,'rad/sec',t46,f7.3,1x,'rad/sec',t62,f7.3,
+' rad/sec')
WRITE(46,6002)
6002 FORMAT(1X,'Damped Natural Frequencies',t35,'Mode #1',t50,
+'Mode #2',t65,'Mode #3')
WRITE(46,6500) w1*sqrt(1-zeta**2),w2*sqrt(1-zeta**2),w3*sqrt(1-zeta**2)
6500 format(1x,t31,f7.3,1x,'rad/sec',t46,f7.3,1x,'rad/sec',t62,f7.3,
+' rad/sec')
endif

write(46,10500) ampacc*100
10500 format(1x,///,1x,'For Earthquake Acceleration of ',f6.2,' % '
+', 'of the El Centro',/)

write(46,25000)
25000 format(1x,'Maximums/Failures',t26,'X (ins)',t36,'Y (ins)',t51,
+'Theta (rads)',t65,'Time (sec)')
write(46,25001)
25001 format(1x,'-----',t25,'-----',t35,'-----',t50,
+'-----',t64,'-----')
write(46,310) maxx,timex
310 format(1x,' Maximum X',t25,f9.6,t65,f5.2)
write(46,311) maxy,timey
311 format(1x,' Maximum Y',t35,f9.6,t65,f5.2)
write(46,312) maxt,timet
312 format(1x,' Maximum Rotation',t50,f9.6,t65,f5.2)

if (flag1.eq.1) then
flag10=flag10+1
write(46,313) x1,y1,t1,time1
313 format(1x,'Side block sliding',t25,f9.6,t35,f9.6,t50,f9.6,
+t65,f5.2)

endif

if (flag2.eq.1) then
flag10=flag10+1
write(46,314) x2,y2,t2,time2
314 format(1x,'Keel block sliding',t25,f9.6,t35,f9.6,t50,f9.6,
+t65,f5.2)
endif

if (flag3.eq.1) then

```

```

        flag10=flag10+1
        write (46,315) x3,y3,t3,time3
315   format (1x,'Side block overturning' ,t25,f9.6,t35,f9.6,t50,f9.6,
        +t65,f5.2)
        endif

        if (flag4.eq.1) then
        flag10=flag10+1
        write (46,316) x4,y4,t4,time4
316   format (1x,'Keel block overturning' ,t25,f9.6,t35,f9.6,t50,f9.6,
        +t65,f5.2)
        endif

        if (flag5.eq.1) then
        flag10=flag10+1
        write (46,317) x5,y5,t5,time5
317   format (1x,'Side block liftoff' ,t25,f9.6,t35,f9.6,t50,f9.6,
        +t65,f5.2)
        endif

        if (flag6.eq.1) then
        flag10=flag10+1
        write (46,318) x6,y6,t6,time6
318   format (1x,'Keel block liftoff' ,t25,f9.6,t35,f9.6,t50,f9.6,
        +t65,f5.2)
        endif

        if (flag7.eq.1) then
        flag10=flag10+1
        write (46,319) x7,y7,t7,time7
319   format (1x,'Side block crushing' ,t25,f9.6,t35,f9.6,t50,f9.6,
        +t65,f5.2)
        endif

        if (flag8.eq.1) then
        flag10=flag10+1
        write (46,320) x8,y8,t8,time8
320   format (1x,'Keel block crushing' ,t25,f9.6,t35,f9.6,t50,f9.6,
        +t65,f5.2)
        endif

        if(flag10.le.0) then
        write(46,11000)
11000  format(1x,/,1x,'No failures occurred.')
        if(counter.eq.1.0 .and. flag10.le.0) then
        go to 60000
        endif
        if(counter.eq.0.0) then
        ampacmax=ampacc
        ampacc=ampacc+.1
        counter=1.0
        write(6,*) 'I am in the secondary looping stage.'
        endif
        endif
        if(ampacc.le.ampacmax) go to 20000
        if(counter.eq.1.0) then
        ampacc=ampacc-.01
        else if(counter.eq.0.0) then
        ampacc=ampacc-.1
        endif

```

```

20000 go to 10000
      continue
      stop
      end

      subroutine mult (a,b,cyy)
      real b(6,6)
      complex a(6,6),cyy(6,6),d(6)
      do 100,i=1,6
      do 200,j=1,6
      do 300,k=1,6
      d(k)=a(i,k)*b(k,j)
300   continue
      cyy(i,j)=d(1)+d(2)+d(3)+d(4)+d(5)+d(6)
200   continue
100   continue
      return
      end

      subroutine multc (a,b,cyx)
      complex a(6,6),b(6,6),cyx(6,6),d(6)
      do 100, i=1,6
      do 200, j=1,6
      do 300, k=1,6
      d(k)=a(i,k)*b(k,j)
300   continue
      cyx(i,j)=d(1)+d(2)+d(3)+d(4)+d(5)+d(6)
200   continue
100   continue
      return
      end

```

APPENDIX 2

```

C      NON-LINEAR THREE DEGREE OF FREEDOM SYSTEM RESPONSE
C      USING FOURTH ORDER RUNGE-KUTTA METHOD

integer NN,1,mm,n,hull,nsys,flag10
integer flag1,flag2,flag3,flag4,flag5,flag6,flag7,flag8
real beta,weight,h,Ik,gravity
real m(3,3),cx(3,3),k(3,3),sidearea,keelarea,plside
real baseside,basekeel,htside,htkeel,crit1,crit2,crit3
real ac(6000),dtau,maxx,maxt,maxy,timex,timet
real rfl,rf2,rf3,hf1,hf2,hf3,ampacc,mass,ampacmax
real kvs,kvk,khs,khk,base,ht,counter
real time1,time2,time3,time4,time5,time6,time7,time8
real x(6000),t(6000),y(6000),XSCL(6)
real bbb,ccc,w12,w1,w22,w2,w32,w3,model,mode3,capwidth
real mmx1,mmang1,mmx3,mmang3,br,amp,plkeel,crit4,u1,u2
real timey,mmmm1,mmmm2,mmmm3,mmmm4
real R,S,TAU,A(5),B(5),C(5),D(5),E(5),F(5),G(5),HH(5)
CHARACTER*40 XLABEL,YLABEL,YYLABEL,YYLABEL,DEC

C      READ IN VESSEL AND DRYDOCK DATA; VESSEL WEIGHT,KG,I (ABOUT KEEL),
C      TIME INCREMENT OF DATA POINTS,VERTICAL STIFFNESS OF SIDE AND
C      KEEL PIERS,HORIZONTAL STIFFNESS OF SIDE AND KEEL PIERS,
C      GAVITATIONAL CONSTANT,SIDE BLOCK BASE AND HEIGHT,
C      KEEL BLOCK BASE AND HEIGHT,
C      BLOCK-BLOCK AND BLOCK-HULL FRICTION COEFFICIENTS,
C      SIDE AND KEEL BLOCK'S PROPORTIONAL LIMIT,
C      SIDE PIER-VESSEL CONTACT AREA,KEEL PIER-VESSEL CONTACT AREA,
C      CAP BLOCK INCLINATION ANGLE.

read(44,*) weight,h,Ik,dtau,kvs,kvk,khs,khk,gravity
read(44,*) baseside, basekeel,htside,htkeel,u1,u2
read(44,*) br,amp,plside,plkeel,sidearea,keelarea,zeta
read(44,*) hull,nsys
write(6,*) 'do you want response plots? (y or n)'
read(5,15) dec
15  format (a)
do 12,i=1,3
do 13,j=1,3
m(1,j)=0.0
k(1,j)=0.0
cx(1,j)=0.0
13  continue
12  continue

C      CALCULATE SYSTEM PARAMETERS

mass=weight/gravity

beta=asin(sqrt(br**2/(4*h**2)))

```

```

m(1,1)=mass
m(1,3)=h*mass
m(2,2)=mass
m(3,1)=mass*h
m(3,3)=Ik

k(1,1)=(2*khs+khk)
k(2,2)=(2*kvs+kvk)
k(3,3)=((0.5*kvs*(br**2.0))-(weight*h))
C DETERMINE NATURAL FREQUENCIES OF SYSTEM

bbb=- (m(1,1)*k(3,3)+m(3,3)*k(1,1)-m(1,3)*k(3,1)-m(3,1)*k(1,3))
+ / (m(1,1)*m(3,3)-m(1,3)*m(3,1))
ccc=(k(1,1)*k(3,3)-k(1,3)*k(3,1))/(m(1,1)*m(3,3)-m(1,3)*m(3,1))
C
C NATURAL FREQ. MODE #1

w12=(-bbb-sqrt(bbb**2.0-4*ccc))/2
w1=sqrt(w12)
C NATURAL FREQ. MODE #2

w22=k(2,2)/m(2,2)
w2=sqrt(w22)
C NATURAL FREQ. MODE #3

w32=(-bbb+sqrt(bbb**2.0-4*ccc))/2
w3=sqrt(w32)
C MODE SHAPE #1 & #3

mode1=(m(1,3)*w12-k(1,3))/(-m(1,1)*w12+k(1,1))
mode3=(m(1,3)*w32-k(1,3))/(-m(1,1)*w32+k(1,1))
C DETERMINE C11,C13,C31,C33
mmx1=m(1,1)+m(1,3)/mode1
mmang1=mode1*m(3,1)+m(3,3)
mmx3=m(1,1)+m(1,3)/mode3
mmang3=mode3*m(3,1)+m(3,3)
mmmm1=2*zeta*mmx1*w1
mmmm2=2*zeta*mmx3*w3
mmmm3=2*zeta*mmang1*w1
mmmm4=2*zeta*mmang3*w3

cx(1,3)=(mmmm1-mmmm2)/(1/mode1-1/mode3)
cx(1,1)=mmmm1-(cx(1,3)/mode1)
cx(2,2)=2*zeta*m(2,2)*w2
cx(3,1)=(mmmm3-mmmm4)/(mode1-mode3)
cx(3,3)=mmmm3-(cx(3,1)*mode1)

C READ IN ACCELERATION DATA

do 300,n=1,5001,5

```

```

300      read (45,*) ac(n),ac(n+1),ac(n+2),ac(n+3),ac(n+4)
C      continue
      ESTABLISH FAILURE CRITERIA AND FLAGS

      crit1= min(u1,(u2*cos(beta)+sin(beta))/
+      (cos(beta)-u2*sin(beta)))
      crit2=min (u1,u2)
      crit3= (0.66*baseside-12.0)/htside
      crit4=basekeel/(6*htkeel)
      ampacc=1.0
      counter=0.0
      ampacmax=0.0
10000   continue
      flag1=0
      flag2=0
      flag3=0
      flag4=0
      flag5=0
      flag6=0
      flag7=0
      flag8=0
      flag10=0
      maxx=0.0
      maxt=0.0
      maxy=0.0
      mm=0
      x(1)=0.0
      y(1)=0.0
      t(1)=0.0
      R=0.0
      S=0.0
      TAU=0.0

C      IMPLEMENTATION OF EQUATIONS OF MOTION INTO THE
C      RUNGE-KUTTA FORMULUS

      do 301,1=1,6000
      DO 3000,11=0,4
      A(11)=0.0
      B(11)=0.0
      C(11)=0.0
      D(11)=0.0
      E(11)=0.0
      F(11)=0.0
      G(11)=0.0
      HH(11)=0.0
3000   CONTINUE
      mm=mm+1
      DO 302, NN=1,4
      IF (NN.EQ.1) THEN
      FF=0.0
      ELSE IF (NN.EQ.2 .OR. NN.EQ.3) THEN
      FF=0.5
      ELSE IF (NN.EQ.4) THEN
      FF=1.0
      ENDIF
      A(NN)=dtau*(R+FF*D(NN-1))
      B(NN)=dtau*(S+FF*E(NN-1))

```

```

C(NN)=dtau*(TAU+FF*F(NN-1))
D(NN)=dtau*((-cx(2,2)/m(2,2))*(R+FF*D(NN-1))-(k(2,2)/m(2,2))
** (y(mm)+FF*A(NN-1))-amp*ampacc*ac(1)/2.54)
G(NN)=dtau*((-cx(1,1)/m(1,1))*(S+FF*E(NN-1))-(cx(1,3)/m(1,1))
** (TAU+FF*F(NN-1))-(k(1,1)/m(1,1))*(x(mm)+FF*B(NN-1))-ampacc*ac(1)/
+2.54)
HH(NN)=dtau*((-cx(3,3)/m(3,3))*(TAU+FF*F(NN-1))-(cx(3,1)/m(3,3))
** (S+FF*E(NN-1))-(k(3,3)/m(3,3))*(t(mm)+FF*C(NN-1))+(m(3,1)/m(3,3))
** ((-cx(2,2)/m(2,2))*(R+FF*D(NN-1))-(k(2,2)/m(2,2))*(y(mm)+FF*A(NN-
+1)))*(t(mm)+FF*C(NN-1))-(m(3,1)/m(3,3))*ampacc*ac(1)/2.54)

E(NN)=(m(1,1)*m(3,3)*C(NN)-m(1,3)*m(3,3)*HH(NN))/
+(m(3,3)*m(1,1)-m(1,3)*m(3,1))
F(NN)=(HH(NN)-(m(3,1)/m(3,3))*E(NN))
302 continue

```

C DETERMINING SYSTEM RESPONSE

```

y(mm+1)=y(mm)+(A(1)+2*A(2)+2*A(3)+A(4))/6
x(mm+1)=x(mm)+(B(1)+2*B(2)+2*B(3)+B(4))/6
t(mm+1)=t(mm)+(C(1)+2*C(2)+2*C(3)+C(4))/6
R=R+(D(1)+2*D(2)+2*D(3)+D(4))/6
S=S+(E(1)+2*E(2)+2*E(3)+E(4))/6
TAU=TAU+(F(1)+2*F(2)+2*F(3)+F(4))/6

```

C MAXIMUM VALUES FOR TRANSLATIONS AND ROTATION

```

if (abs(x(mm)).gt.abs(maxx)) then
    timex=dtau*(1-1)
    maxx=x(mm)
endif
if (abs(t(mm)).gt.abs(maxt)) then
    timet=dtau*(1-1)
    maxt=t(mm)
endif
if (abs(y(mm)).gt.abs(maxy)) then
    timey=dtau*(1-1)
    maxy=y(mm)
endif

```

C CALCULATE VERTICAL AND HORIZONTAL FORCES CAUSED BY VESSEL.
C TEST FOR FAILURE

```

C CALCULATE FORCES ON SIDE/KEEL BLOCKS
rf1=kvs*((weight/k(2,2))-y(mm)-(br/2)*t(mm))
rf2=kvs*((weight/k(2,2))-y(mm)+(br/2)*t(mm))
rf3=kvk*((weight/k(2,2))-y(mm))
hf1=khs*(x(mm))
hf2=khs*(x(mm))

```

```

hf3=khk*x(mm)
C TEST FOR SIDE BLOCK SLIDING

if (flag1.eq.1) then
  go to 400
else if (hf1.lt.0.0.and.rf1.gt.0.0.and.abs(hf1/rf1).gt.crit1) then
  time1= dtau*(1-1)
  flag1=1
else if (hf2.gt.0.0.and.rf2.gt.0.0.and.abs(hf2/rf2).gt.crit1) then
  time1=dtau*(1-1)
  flag1=1
endif
x1=x(mm)
y1=y(mm)
t1=t(mm)
400 continue

C TEST FOR KEEL BLOCK SLIDING

if (flag2.eq.1) then
  go to 410
else if (rf3.gt.0.0.and.abs(hf3/rf3).gt.crit2) then
  time2=dtau*(1-1)
  flag2=1
endif
x2=x(mm)
y2=y(mm)
t2=t(mm)
410 continue
C TEST FOR SIDE BLOCK OVERTURNING

if (flag3.eq.1) then
  go to 420
else if (hf1.lt.0.0.and.rf1.gt.0.0.and.abs(hf1/rf1).gt.crit3) then
  time3= dtau*(1-1)
  flag3=1
else if (hf2.gt.0.0.and.rf2.gt.0.0.and.abs(hf2/rf2).gt.crit3) then
  time3=dtau*(1-1)
  flag3=1
endif
x3=x(mm)
y3=y(mm)
t3=t(mm)
420 continue

C TEST FOR KEEL BLOCK OVERTURNING

if (flag4.eq.1) then
  go to 430
else if (rf3.gt.0.0.and.abs(hf3/rf3).gt.crit4) then
  time4=dtau*(1-1)
  flag4=1
endif
x4=x(mm)
y4=y(mm)
t4=t(mm)
430 continue

C TEST FOR SIDE BLOCK LIFTOFF

```

```

    if (flag5.eq.1) then
      go to 440
    else if (rf1.lt.0.0 .or. rf2.lt.0.0) then
      time5=dtau*(1-1)
      flag5=1
    endif
    x5=x(mm)
    y5=y(mm)
    t5=t(mm)
440  continue

C    TEST FOR KEEL BLOCK LIFTOFF

    if (flag6.eq.1) then
      go to 450
    else if (rf3.lt.0.0) then
      time6=dtau*(1-1)
      flag6=1
    endif
    x6=x(mm)
    y6=y(mm)
    t6=t(mm)
450  continue

C    TEST FOR SIDE BLOCK CRUSHING

    if (flag7.eq.1) then
      go to 460
    else if (rf1.gt.0.0 .and. (rf1/sidearea).gt.plside) then
      flag7=1
      time7=dtau*(1-1)

    else if (rf2.gt.0.0 .and. (rf2/sidearea).gt.plside) then
      flag7=1
      time7=dtau*(1-1)

    endif
    x7=x(mm)
    y7=y(mm)
    t7=t(mm)
460  continue

C    TEST FOR KEEL BLOCK CRUSHING

    if (flag8.eq.1) then
      go to 470
    else if (rf3.gt.0.0 .and. (rf3/keelarea).gt.plkeel) then
      flag8=1
      time8=dtau*(1-1)
    endif
    x8=x(mm)
    y8=y(mm)
    t8=t(mm)
470  continue

301  continue

C    PLOT RESULTS
60000 go to 999
      continue

```

```

if(DEC.EQ.'N') THEN
write(6,*) 'I am finishing.'
GO TO 998
endif
write(6,*) 'I am plotting.'
XSCL(1)=0.0
XSCL(2)=30.0
XLABEL='TIME IN SECONDS'
YLABEL='ROTATION IN RADIANS'
YYLABEL='RELATIVE HORIZONTAL DISPLACEMENT IN INCHES'
YYYLABEL='RELATIVE VERTICAL DISPLACEMENT IN INCHES'
CALL QPICTR (X,1,3000,QXSCL(XSCL),QISCL(-2),QXLAB(XLABEL),
+ QYLAB(YYLABEL),QLABEL(4))
CALL QPICTR (T,1,3000,QXSCL(XSCL),QISCL(-2),QXLAB(XLABEL),
+ QYLAB(YLABEL),QLABEL(4))
CALL QPICTR (Y,1,3000,QXSCL(XSCL),QISCL(-2),QXLAB(XLABEL),
+ QYLAB(YYLABEL),QLABEL(4))
998 go to 20000
999 CONTINUE

if(ampacc.eq.1.0) then

write(46,4000) nsys
4000 format(1x,/,28x,'**** System ',I2,1x,'****')
write(46,4050) hull
4050 format(1x,/,30x,'** Hull ',I3,1x,'**')
write(46,4100)
4100 format(1x,/,28x,'* Ship Parameters *')
write(46,4150)
4150 format(1x,/,5x,'Weight',8x,'Moment of Inertia',9x,'K.G.')
write(46,4200) weight,1k,h
4200 format(1x,f9.1,1x,'kips',1x,f11.1,1x,'kips-in-sec2',
+3x,f6.1,1x,'ins')
write(46,4250)
4250 format(1x,/,26x,'* Drydock Parameter *')
write(46,4300)
4300 format(1x,/,1x,'Side Block Height',3x,'Side Block Width',
+3x,'Keel Block Height',3x,'Keel Block Width')
write(46,4350) htside,baseside,htkeel,basekeel
4350 format(2x,f6.1,1x,'ins',11x,f6.1,1x,'ins',11x,f6.1,1x,'ins',
+9x,f6.1,1x,'ins')
write(46,4400)
4400 format(1x,/,1x,'Side-to-Side Pier Distance')
write(46,4450) br
4450 format(1x,t7,f6.1,1x,'ins')
write(46,4470)
4470 format(1x,/, ' Total Side Pier Contact Area'
+,3x,'Total Keel Pier Contact Area')
write(46,4475) sidearea,keelarea
4475 format(1x,8x,f11.1,1x,'in2',14x,f11.1,1x,'in2')
write(46,4500)
4500 format(1x,/,1x,'Block-on-Block Friction Coeff',3x,'Hull-on-Block
+ Friction Coeff')
write(46,4550) u1,u2
4550 format(1x,10x,f7.3,23x,f7.3)
write(46,4600)
4600 format(1x,/,1x,'Side Pier Proportional Limit',3x,'Keel Pier'
+,' Proportional Limit')
write(46,4650) plside,plside
4650 format(1x,10x,f7.3,1x,'kips/in2',15x,f7.3,1x,'kips/in2')

```

```

write(46,4700)
4700 format(1x,/,1x,'Side Pier Vertical Stiffness',3x,'Side Pier',
+' Horizontal Stiffness')
write(46,4750) kvs,khs
4750 format(1x,3x,f11.1,1x,'kips/in',11x,f11.1,1x,'kips/in')
write(46,4775)
4775 format(1x,/,1x,'Keel Pier Vertical Stiffness',3x,
+'Keel Pier Horizontal Stiffness')
write(46,4780) kvk,khk
4780 format(1x,3x,f11.1,1x,'kips/in',11x,f11.1,1x,'kips/in')
write(46,4800)
4800 format(1x,/,20x,'* System Parameters and Inputs *')
write(46,4850)
4850 format(1x,/,1x,'Input Forcing Function is Horizontal Component',
+' of the 1946 El Centro')
write(46,4875)
4875 format(1x,20x,' Earthquake Acceleration Time History.')

write(46,4995)
4995 format(1x,/,1x,'Vertical/Horizontal Ground Acceleration Ratio'
+,3x,'Data Time Increment')
write(46,4990) amp,dtau
4990 format(1x,10x,f6.3,t55,f6.3,1x,'sec')
write(46,4900)
4900 format(1x,/,1x,'Gravitational Constant',3x,'Percent System
+ Damping')
write(46,4950) gravity,zeta*100.
4950 format(1x,7x,f6.2,1x,'in/sec2',10x,f6.2,1x,'%')
write(46,5000)
5000 format(1x,/,25x,'Mass Matrix',/)
do 5100 i=1,3
write(46,5050) m(i,1),m(i,2),m(i,3)
5050 format(1x,f15.4,5x,f15.4,5x,f15.4)
5100 continue
write(46,5200)
5200 format(1x,/,25x,'Damping Matrix',/)
do 5300 i=1,3
write(46,5250) cx(i,1),cx(i,2),cx(i,3)
5250 format(1x,f15.4,5x,f15.4,5x,f15.4)
5300 continue
write(46,5400)
5400 format(1x,/,25x,'Stiffness Matrix',/)
do 5500 i=1,3
write(46,5450) k(i,1),k(i,2),k(i,3)
5450 format(1x,f15.4,5x,f15.4,5x,f15.4)
5500 continue
write(46,5700)
5700 format(1x,/)
WRITE(46,6000)
6000 FORMAT(1X,'Undamped Natural Frequencies',t35,'Mode #1',t50,
+'Mode #2',t65,'Mode #3')
write(46,6001) w1,w2,w3
6001 format(1x,t31,f7.3,1x,'rad/sec',t46,f7.3,1x,'rad/sec',t62,f7.3,
+' rad/sec')
WRITE(46,6002)
6002 FORMAT(1X,'Damped Natural Frequencies',t35,'Mode #1',t50,
+'Mode #2',t65,'Mode #3')
WRITE(46,6500) w1*sqrt(1-zeta**2),w2*sqrt(1-zeta**2),w3*sqrt(1-zeta**2)
6500 format(1x,t31,f7.3,1x,'rad/sec',t46,f7.3,1x,'rad/sec',t62,f7.3,
+' rad/sec')

```

```

endif

write(46,10500) ampacc*100
10500 format(1x,///,1x,'For Earthquake Acceleration of ',f6.2,' % '
+,'of the El Centro',/)

write(46,25000)
25000 format(1x,'Maximums/Failures',t26,'X (ins)',t36,'Y (ins)',t51,
+'Theta (rads)',t65,'Time (sec)')
write(46,25001)
25001 format(1x,'-----',t25,'-----',t35,'-----',t50,
+'-----',t64,'-----')
write(46,310) maxx,timex
310 format(1x,' Maximum X',t25,f9.6,t65,f5.2)
write(46,311) maxy,timey
311 format(1x,' Maximum Y',t35,f9.6,t65,f5.2)
write(46,312) maxt,timet
312 format(1x,' Maximum Rotation',t50,f9.6,t65,f5.2)

if (flag1.eq.1) then
flagl0=flagl0+1
write(46,313) x1,y1,t1,time1
313 format(1x,'Side block sliding' ,t25,f9.6,t35,f9.6,t50,f9.6,
+t65,f5.2)
endif

if (flag2.eq.1) then
flagl0=flagl0+1
write(46,314) x2,y2,t2,time2
314 format(1x,'Keel block sliding' ,t25,f9.6,t35,f9.6,t50,f9.6,
+t65,f5.2)
endif

if (flag3.eq.1) then
flagl0=flagl0+1
write(46,315) x3,y3,t3,time3
315 format(1x,'Side block overturning' ,t25,f9.6,t35,f9.6,t50,f9.6,
+t65,f5.2)
endif

if (flag4.eq.1) then
flagl0=flagl0+1
write(46,316) x4,y4,t4,time4
316 format(1x,'Keel block overturning' ,t25,f9.6,t35,f9.6,t50,f9.6,
+t65,f5.2)
endif

if (flag5.eq.1) then
flagl0=flagl0+1
write(46,317) x5,y5,t5,time5
317 format(1x,'Side block liftoff' ,t25,f9.6,t35,f9.6,t50,f9.6,
+t65,f5.2)
endif

if (flag6.eq.1) then
flagl0=flagl0+1
write(46,318) x6,y6,t6,time6
318 format(1x,'Keel block liftoff' ,t25,f9.6,t35,f9.6,t50,f9.6,
+t65,f5.2)

```

```

endif

if (flag7.eq.1) then
flag10=flag10+1
write (46.319) x7,y7,t7,time7
319 format (1x,'Side block crushing' ,t25,f9.6,t35,f9.6,t50,f9.6,
+t65,f5.2)
endif

if (flag8.eq.1) then
flag10=flag10+1
write (46.320) x8,y8,t8,time8
320 format (1x,'Keel block crushing' ,t25,f9.6,t35,f9.6,t50,f9.6,
+t65,f5.2)
endif

if(flag10.le.0) then
write(46.11000)
11000 format(1x,/,1x,'No failures occurred.')
if(counter.eq.1.0 .and. flag10.le.0) then
go to 60000
endif
if(counter.eq.0.0) then
ampacmax=ampacc
ampacc=ampacc+.1
counter=1.0
write(6,*) 'I am in the secondary looping stage.'
endif
endif
if(ampacc.le.ampacmax) go to 20000
if(counter.eq.1.0) then
ampacc=ampacc-.01
else if(counter.eq.0.0) then
ampacc=ampacc-.1
endif
go to 10000
20000 continue
stop
end

```

APPENDIX 3

MODAL ANALYSIS OF THE TWO AND THREE DEGREE OF FREEDOM SYSTEMS

Since the vertical equation of motion is uncoupled from the other equations, the three degree of freedom system need only to be analyzed to obtain damping coefficients for both degree of freedom mathematical models. Also, the maximum response of the two systems will be determined using response spectrum analysis with participation factors described in Section 6.4.

The three degree of freedom equations of motions, undamped, as shown in Equations 4.4.11a, b and c are

$$m_{11} \ddot{x} + m_{13} \ddot{\theta} + k_{11} x = -m_{11} \ddot{x}_g$$

$$m_{22} \ddot{y} + k_{22} y = -m_{22} \ddot{y}_g$$

and

$$m_{33} \ddot{\theta} + m_{31} \ddot{x} + k_{33} \theta = -m_{31} \ddot{x}_g$$

where $m_{11} = m_{22} = M$

$$m_{13} = m_{31} = MKG$$

$$m_{33} = I_k$$

$$k_{11} = 2K_{sh} + K_{kh}$$

$$k_{22} = 2K_{sv} + K_{kv}$$

$$k_{33} = (B^2/2) K_{sv} - W \overline{KG}.$$

To perform modal analysis, consider the free vibration system

$$m_{11} \ddot{x} + m_{13} \ddot{\theta} + k_{11} x = 0$$

$$m_{22} \ddot{y} + k_{22} y = 0$$

and

$$m_{33} \ddot{\theta} + m_{31} \ddot{x} + k_{33} \theta = 0.$$

Assume the system response is in the form

$$x = \phi_1 \sin(\omega t + \rho)$$

$$y = \phi_2 \sin(\omega t + \rho)$$

$$\text{and } \theta = \phi_3 \sin(\omega t + \rho).$$

Now, the equations of motion are

$$m_{11}(-\phi_1 \omega^2 \sin(\omega t + \rho)) + m_{13}(-\phi_3 \omega^2 \sin(\omega t + \rho)) + k_{11}(\phi_1 \sin(\omega t + \rho)) = 0$$

$$m_{22}(-\phi_2 \omega^2 \sin(\omega t + \rho)) + k_{22}(\phi_2 \sin(\omega t + \rho)) = 0$$

and

$$m_{33}(-\phi_3 \omega^2 \sin(\omega t + \rho)) + m_{31}(-\phi_1 \omega^2 \sin(\omega t + \rho)) + k_{33}(\phi_3 \sin(\omega t + \rho)) = 0.$$

The trivial solution to the above set of equations is

$\sin(\omega t + \rho) = 0$. Assuming $\sin(\omega t + \rho) = 0$, then

$$\begin{bmatrix} k_{11} - m_{11}\omega^2 & 0 & -m_{13}\omega^2 \\ 0 & k_{22} - m_{22}\omega^2 & 0 \\ -m_{31}\omega^2 & 0 & k_{33} - m_{33}\omega^2 \end{bmatrix} \begin{bmatrix} \phi_1 \\ \phi_2 \\ \phi_3 \end{bmatrix} = \begin{bmatrix} 0 \\ 0 \\ 0 \end{bmatrix}. \quad (\text{A.3.1})$$

These equations are solved for ω by setting the determinant of the first matrix equal to 0. However, the second row of the matrix is uncoupled. Thus one solution for ω is

$$\omega^2 = k_{22}/m_{22}.$$

Now, the determinant equation reduces to

$$\omega^4 - \omega^2 \left(\frac{m_{11}k_{11} + m_{33}k_{33}}{m_{11}m_{33} - m_{31}m_{31}} \right) + \frac{k_{11}k_{33}}{m_{11}m_{33} - m_{13}m_{31}} = 0.$$

Using the quadratic formula, the other values of ω^2 are

$$\omega^2 = \frac{-b \pm \sqrt{b^2 - 4c}}{2} \quad (\text{A.3.2})$$

where
$$b = - \left(\frac{m_{11}k_{11} + m_{33}k_{33}}{m_{11}m_{33} - m_{13}m_{31}} \right)$$

and
$$c = \frac{k_{11}k_{33}}{m_{11}m_{33} - m_{13}m_{31}} .$$

Using parameters found in Section 5 for the eleven representative vessel-drydock systems, the natural frequencies ω_1 , ω_2 , and ω_3 for each system is calculated and listed in Table A3.1.

The mode shapes are determined with the relationship

$$(k_{11} - m_{11}\omega^2)\phi_1 - m_{13}\omega^2\phi_3 = 0$$

or
$$\frac{\phi_1}{\phi_3} = \frac{m_{13}\omega^2}{k_{11} - m_{11}\omega^2} , \quad \omega = \omega_1, \omega_3 .$$

With mode shapes determined, the equation of motion can be rewritten, including coupled damping

$$m_{11}\ddot{x} + m_{13}\ddot{\theta} + c_{11}\dot{x} + c_{13}\dot{\theta} + k_{11}x = 0$$

$$m_{22}\ddot{y} + c_{22}\dot{y} + k_{22}y = 0$$

and

$$m_{33}\ddot{\theta} + m_{31}\ddot{x} + c_{33}\dot{\theta} + c_{31}\dot{x} + k_{33}\theta = 0 .$$

At natural frequencies ω_1 , ω_2 and ω_3 the coupled three degree of freedom system acts as a single degree of freedom system with the following relationship:

$$(\phi_1/\phi_3)x = \theta$$

$$(\phi_1/\phi_3)\dot{x} = \dot{\theta}$$

and $(\phi_1/\phi_3)\ddot{x} = \ddot{\theta} .$

Using these relationships, the three degree of freedom equations of motion at the three system natural frequencies are

$$[m_{11} + (\phi_3/\phi_1)m_{13}] \ddot{x} + [c_{11} + (\phi_3/\phi_1)c_{31}] \dot{x} + k_{11} x = 0$$

$$m_{22} \ddot{y} + c_{22} \dot{y} + k_{22} y = 0$$

and

$$[(\phi_1/\phi_3)m_{31} + m_{33}] \ddot{\theta} + [(\phi_1/\phi_3)c_{31} + c_{33}] \dot{\theta} + k_{33} \theta = 0.$$

The damping coefficients for the problem are 5% of the critical damping for each mode,

$$[c_{11} + (\phi_3/\phi_1)c_{13}] = 2 \xi M_1 \omega_n, \omega_n = 1, 3 \quad (\text{A3.3a})$$

$$c_{22} = 2 \xi m_{22} \omega_2 \quad (\text{A3.3b})$$

and

$$[(\phi_1/\phi_3)_n c_{31} + c_{33}] = 2 \xi M_3 \omega_n, \omega_n = 1, 3 \quad (\text{A3.3c})$$

where ξ = percentage of critical damping, 0.05

$$M_1 = m_{11} + (\phi_3/\phi_1)_n m_{13}$$

$$\text{and } M_3 = m_{33} + (\phi_1/\phi_3)_n m_{31}.$$

Substituting known values and rearranging Equations A3.3a and A3.3c yields the following four equations:

$$\text{Mode 1, } c_{11} + (\phi_3/\phi_1)_1 c_{13} = 2 \xi M_1 \omega_1$$

$$(\phi_1/\phi_3)_1 c_{31} + c_{33} = 2 \xi M_3 \omega_1$$

$$\text{Mode 2, } c_{11} + (\phi_3/\phi_1)_3 c_{13} = 2 \xi M_1 \omega_3$$

$$(\phi_1/\phi_3)_3 c_{31} + c_{33} = 2 \xi M_3 \omega_3$$

$$\text{or } c_{11} + (\phi_3/\phi_1)_1 c_{13} = 2 \xi M_1 \omega_1$$

$$c_{11} + (\phi_3/\phi_1)_3 c_{13} = 2 \xi M_1 \omega_3$$

$$\text{and } (\phi_1/\phi_3)_1 c_{31} + c_{33} = 2 \xi M_3 \omega_1$$

$$(\phi_1/\phi_3)_3 c_{31} + c_{33} = 2 \xi M_3 \omega_3$$

Using the above set of equations and equation A3.3b, damping coefficients c_{11} , c_{13} , c_{22} , c_{31} , and c_{33} are determined and listed in Table A3.2 for the eleven vessel-drydock configurations. Note that c_{13} equals to c_{31} . In the two degree of freedom case, the damping coefficients c_{11} , c_{12} , c_{21} , and c_{22}

are equal to those in the three degree problem, i.e.

Two Degree Case

Three Degree Case

c_{11}

c_{11}

c_{12}

c_{13}

c_{21}

c_{31}

c_{22}

c_{33}

Using the response spectrum method and modal participation factors, the maximum response of the two and three degrees of freedom systems can be calculated. Starting with the forced vibration equation

$$[m_{11} + (\phi_3/\phi_1)_n m_{13}] \ddot{x} + c_1 \dot{x} + k_{11} x = -m_{11} \ddot{x}_g$$

or

$$\ddot{x} + \frac{c_1 \dot{x} + k_{11} x}{[m_{11} + (\phi_3/\phi_1)_n m_{13}]} = \frac{-m_{11}}{[m_{11} + (\phi_3/\phi_1)_n m_{13}]} \ddot{x}_g$$

Equations 6.3.1, 6.3.2 and 6.3.3 predict a maximum response for a 5% critically damped system for a given mode as

$$(x_{\max})_n = 11.62 * \frac{m_{11}}{[m_{11} + (\phi_3/\phi_1)_n m_{13}]} \text{ for } \omega_1, \omega_3 < 2.24$$

$$\text{or } (x_{\max})_n = \frac{26.03}{\omega} * \frac{m_{11}}{[m_{11} + (\phi_3/\phi_1)_n m_{13}]} \text{ for } 2.24 < \omega_1, \omega_3 < 12.74$$

$$\text{else } (x_{\max})_n = \frac{331.53}{\omega^2} * \frac{m_{11}}{[m_{11} + (\phi_3/\phi_1)_n m_{13}]} \text{ for } \omega_1, \omega_3 > 12.74$$

Similarly for rotational response, the equation of motion is

$$[m_{33} + (\phi_1/\phi_3)_n m_{31}] \ddot{\theta} + c_3 \dot{\theta} + k_{33} \theta = -m_{31} \ddot{x}_g$$

or

$$\ddot{\theta} + \frac{c_3 \dot{\theta} + k_{33} \theta}{[m_{33} + (\phi_1/\phi_3)_n m_{31}]} = \frac{-m_{31}}{[m_{33} + (\phi_1/\phi_3)_n m_{31}]} \ddot{x}_g$$

and the maximum response for given mode is

$$(\theta_{\max})_n = 11.62 \frac{m_{31}}{[m_{33} + (\frac{1}{3})_n m_{31}]} \text{ for } \omega_1, \omega_3 < 2.24$$

$$\text{or } (\theta_{\max})_n = \frac{26.03}{\omega} * \frac{m_{31}}{[m_{33} + (\frac{\phi_1}{\phi_3})_n m_{31}]} \text{ for } 2.24 < \omega_1, \omega_3 < 12.74$$

$$\text{else } (\theta_{\max})_n = \frac{331.53}{\omega^2} * \frac{m_{31}}{[m_{33} + (\frac{\phi_1}{\phi_3})_n m_{31}]} \text{ for } \omega_1, \omega_3 > 12.74$$

Since being uncoupled, the vertical equation of motion is

$$m_{22} \ddot{Y} + c_2 \dot{Y} + k_{22} Y = -m_{22} \ddot{Y}_g$$

$$\text{or } \ddot{Y} + \frac{c_2 \dot{Y} + k_{22} Y}{m_{22}} = -\ddot{Y}_g = -AMP \ddot{x}_g$$

where AMP = ratio of vertical/horizontal El Centro earthquake accelerations.

The maximum vertical response is

$$(Y_{\max})_2 = 11.62 * AMP \text{ for } \omega_2 < 2/24$$

or

$$(Y_{\max})_2 = \frac{26.03}{\omega} * AMP \text{ for } 2.24 < \omega_2 < 12.74$$

else

$$(Y_{\max})_2 = \frac{331.53}{\omega^2} * AMP \text{ for } \omega_2 > 12.74.$$

Now, the maximum response for each mode of the x and θ equations and for the uncoupled y equation are calculated.

The configuration of the three degree of freedom system at any time is a superposition of the two coupled natural mode shapes along with the independent vertical maximum response. The absolute maximum response to a given earthquake is the numerical summation of the maximum response of each mode shape times its respective participation factor. The general

formula for each modal participation factor is

$$\Gamma_n = \sum M_r \phi_{rn} / M_r \phi_{rn}^2$$

where Γ_n = modal participation factor for the n^{th} mode
 r refers to which equation of motion is being considered. In the three degree of freedom case, $r = 1$ or 3 .

Using these participation factors, the maximum response of the three degree of freedom system should be no greater than

$$x_{\max} = (x_{\max})_1 \Gamma_1 + (x_{\max})_3 \Gamma_3,$$

$$y_{\max} = (y_{\max})_2$$

$$\text{and } \theta_{\max} = (\theta_{\max})_1 \Gamma_1 + (\theta_{\max})_3 \Gamma_3.$$

These maximum response are determined and listed in Table A3.3 for the eleven vessel-drydock configurations. Once again due to the uncoupled vertical response, the maximum response of x and θ in the two degree of freedom is identical to that of the three degree of freedom case.

TABLE A3.1

Three Degree of Freedom Vessel-Drydock System
Natural Frequencies
(rad/sec)

<u>SYSTEM</u>	ω_1	ω_2	ω_3
1	5.454	39.071	37.230
2	3.883	36.823	34.367
3	4.013	29.468	23.791
4	2.819	27.773	21.511
5	2.848	35.737	32.742
6	9.690	45.450	40.863
7	7.953	41.322	36.351
8	6.976	39.247	34.045
9	5.863	32.829	29.060
10	6.857	34.832	29.921
11	6.177	33.293	28.010

NOTE: Two Degree of Freedom System Natural Frequencies correspond to ω_1 and ω_3 .

TABLE A3.2

Three Degree of Freedom Vessel-Drydock System
Damping Coefficients
(kim-sec/inch)

SYSTEM	C ₁₁	C ₂₂	C ₃₃	C ₁₃ , C ₃₁
1	65.398	166.826	1322882.125	3920.416
2	58.612	157.226	938583.250	2874.701
3	42.452	125.824	976657.438	2829.964
4	37.308	118.583	682485.813	2053.786
5	54.303	152.588	687504.500	2159.187
6	188.657	445.695	7879946.000	17130.227
7	167.100	405.212	6430934.500	14269.135
8	155.786	384.866	5622059.000	12660.506
9	43.963	116.475	1196244.250	3340.509
10	33.833	86.437	836179.438	2408.758
11	31.639	82.618	751062.813	2185.568

NOTE: Two Degree of Freedom System Damping Coefficients correspond to C₁₁, C₁₃, C₃₁ and C₃₃.

TABLE A3.3

Three Degree of Freedom Vessel-Drydock System
 Maximum Response Using Response Spectrum Analysis

<u>SYSTEM</u>	<u>(ins.)^x</u>	<u>(ins.)^y</u>	<u>(rads.)^θ</u>
1	0.33275	0.10859	0.01646
2	0.27141	0.12225	0.02348
3	0.65142	0.19089	0.02350
4	0.53788	0.21491	0.02350
5	0.21468	0.12980	0.03202
6	0.45271	0.08025	0.00683
7	0.46833	0.09708	0.00866
8	0.46597	0.10762	0.01009
9	0.64366	0.15381	0.01525
10	0.65864	0.13662	0.01342
11	0.67467	0.14955	0.01522

NOTE: Two Degree of Freedom System Maximum Response correspond to x and θ .

END

12-86

DTIC